THE FUNDAMENTAL PHYSICS EXPLORER

TECHNOLOGY REFERENCE STUDY
FINAL REPORT

A. Special & General Relativity

B. The Equivalence Principle

C. Bose Einstein Condensation

David Binns
December 2007
SCI-PA/2007.025/FPE/DB

document title/ *titre du document*

THE FUNDAMENTAL PHYSICS EXPLORER

TECHNOLOGY REFERENCE STUDY

FINAL REPORT

FPE YGT Final Report v9 FINAL

A P P R O V A L

Title titre	THE FUNDAMENTAL PHYSICS EXPLORER TECHNOLOGY REFERENCE STUDY	issue issue	1	revision revision	0
author auteur	David Binns	date date	12/12/2007		
approved by approuvé by	Nicola Rando	date date	12/12/2007		

C H A N G E   L O G

reason for change /raison du changement	issue/*issue*	revision/*revision*	date/*date*

C H A N G E   R E C O R D

Issue: 1 Revision: 0

reason for change/*raison du changement*	page(s)/*page(s)*	paragraph(s)/*paragraph(s)*

TABLE OF CONTENTS

Acknowledgements

List of Figures

List of Tables

List of Acronyms

ADC	Analogue to Digital Converter
AIF	Atomic Interferometry
AIV&T	Assembly, Integration, Verification and Test
AOCS	Attitude and Orbit Control System
AOM	Acoustic Optical Modulator
AoP	Argument of Perigee
ASU	Atomic Sensor Unit (Hyper terminology)
BEE	Back End Electronics
BoL	Beginning of Life
BPSK	Binary Phase Shift Keying
BTP	BEC Trap Package
CACS	Composite Attitude Control System (LPF terminology)
CCU	Caging Control Unit (LPF terminology)
CFRP	Carbon Fibre Reinforced Plastic (LPF Terminology)
CL	Cavity Laser
CMB	Cosmic Microwave Background
CMRR	Common Mode Rejection Ratio
CoM	Centre of Mass
CoP	Centre of Pressure
CPU	Central Processing Unit
DA	Differential Accelerometer
DAC	Digital to Analogue Converter
DAS	Differential Accelerometer Suite
DFACS	Drag Free Attitude Control System
DHS	Data Handling Sub-System
DMA	Differential Mode Acceleration
DoF	Degree of Freedom
DPU	Data Processing Unit
DRS	Disturbance Reduction System (LPF terminology)
DSP	Digital Signal Processor
ECU	Electronic Control Unit
EoL	End of Life
EOM	Electric Optical Modulator
EP	Equivalence Principle
EPDP	Electric Propulsion Diagnostic Package (LPF terminology)
EPI	Equivalence Principle Instrument

EPS	Electrostatic Positioning System
ERP	Earth Radiation Pressure
ESA	European Space Agency
FC	Frequency Comb
FD	Fundamental Constants
FDIR	Failure Detection Isolation and Recovery
FEE	Front End Electronics
FEEP	Field Emission Electric Propulsion
FPE	Fundamental Physics Explorer
GG	Galileo Galilei (a spacecraft)
GR	General Relativity
GRS	Gravitational Red-Shift
GYP	Gyro Package (LPF terminology)
IS	Inertial Sensor
LB	Laser Bench
LEO	Low Earth Orbit
LEOP	Launch and Early Orbit Phase
LGA	Low Gain Antenna
LMU	Laser Metrology Unit (LPF terminology)
LO	Local Oscillator (Probe Laser)
LPF	LISA Pathfinder
LTP	LISA Technology Package
MGA	Medium Gain Antenna
MOT	Magneto-Optical-Trap
MPACS	Micro Propulsion Attitude Control System (LPF terminology)
MWL	Microwave Link
NASA	National Aeronautics and Space Administration
OAC	Optical Atomic Clock
OBC	Onboard Computer
OBDH	On-Board Data Handling
OR	Optical Resonator
ORB	Optical Resonator Bench
P/L	Payload
PCDU	Power and Control Distribution Unit
PCU	Power Control Unit (specifically for Payload sub-systems)
PDH	Pound-Drever-Hall
PEPR	Proportional Electronic Pressure Regulator (LPF terminology)
PLM	Payload Module

PLSC	Probe Laser Stabilisation Cavity
PMU	Phasemeter Unit (LPF terminology)
PSD	Power Spectral Density
RAAN	Right Ascension of the Ascending Node
RLU	Reference Laser Unit (LPF terminology)
RMS	Robertson-Mansouri-Sexl
S/C	Spacecraft
SAA	South Atlantic Anomaly
SAU	Sensing and Actuation Unit (LPF terminology)
SCMB	Super-Conducting Magnetic Bearing
SHM	Space Hydrogen Maser
SNR	Signal to Noise Ratio
SQUID	Superconducting QUantum Interference Device
SR	Special Relativity
SRP	Solar Radiation Pressure
SSO	Sun-Synchronous Orbit
SSPA	Solid State Power Amplifier
T/F	Time and Frequency
TBC	To Be Confirmed
TBD	To Be Determined
TC	Telecommand
TCS	Thermal Control System
TIC	Time Interval Counter
TLM	Telemetry
TM	Test Mass
TRS	Technology Reference Study
TTC	Telemetry Tracking and Control
TWTA	Travelling Wave Tube Amplifier
TWTFT	Two Way Time and Frequency Transfer
UHV	Ultra-High Vacuum
UHVIC	Ultra High Vacuum Interrogation Chamber
ULU	Ultraviolet Lamp Unit (LPF terminology)
UV	Ultra Violet
VDA	Vacuum Deposited Aluminium (LPF Terminology)
w.r.t.	with respect to
WEP	Weak Equivalence Principle

PART 1

INTRODUCTION

1   Introduction

Our understanding of the Universe has come under increased scrutiny over the last 25 years. New instruments have opened fascinating perspectives for testing General Relativity, alternative theories of gravitation, as well as studying quantum mechanics and exploring the boundaries of quantum gravity. Violations of the principle laws of the currently underlying theories can give clues to aid the unification of the four physical forces, or lead the way for the discovery of new interactions and particles.

The aim of the Fundamental Physics Explorer (FPE) is to provide the means to test the the foundations of modern physics in a cost effective and efficient manner. The FPE programme could consist of up to three spacecrafts, each re-using a small platform, accessing space to take advantage of an almost constantly unperturbed environment, thus improving the precision of current measurements. More specifically, the FPE Technology Reference Study (TRS) aims to identify the key technologies required and the technical challenges associated with fundamental physics missions. The areas of investigation can be broken down into three areas:

The areas of investigation can be broken down into three areas:
*   Tests of Special and General Relativity (FPE-A)
*   Tests of the Equivalence Principle (FPE-B)
*   The Behaviour of Bose Einstein Condensates (FPE-C)

The re-use of LISA Pathfinder's (LPF) science module is being considered here for use with FPE, together with a small launcher (VEGA, with Rockot as an option). This will allow easy procurement and heritage from a mission for which main goal is to study fundamental physics under drag-free control. FPE's science goals are different from LPF but in a similar mould. In fact, LISA is supposed to detect gravitational waves from distant sources/objects in the universe. This requires stringent attitude control which will be provided by a Drag Free Attitude Control System (DFACS), so that the spacecraft is only disturbed by gravitational effects. Similarly, FPE is supposed to make sensitive measurements for fundamental physics experiments, which also require an extremely still environment, clearly implying a spacecraft similar to LPF.

This report summarise the work performed on the payload definition, the orbit and the required adaptations of LISA Pathfinder, considering all three mission scenarios (FPE-A/B/C), although the case of FPC-A and FPE-B have been analysed in more detail. It also is the culmination of the work completed during the author's YGT period.

Part One serves as an introduction to the field of fundamental physics and the approach taken for measurement. This section includes an overview of the Special and General Relativity (SR and GR), the equivalence principle and Bose Einstein Condensates. The basic principles of drag free control are introduced as they apply to any measurements of the geodesic (i.e. the trajectory followed by an object in a purely gravitational field, not subject to any disturbances). A definition of terms is provided as theoretical background.

Part Two describes the reference payload determined to achieve the scientific objectives. FPE-A's payload is designed to measure the speed of light and compare atomic clocks in space and on ground. FPE-B's payload is required to test the Weak Equivalence Principle (WEP) using cryogenics and accelerometers. Finally, FPE-C tests Quantum Gases, specifically Bose Einstein Condensates (BECs), in microgravity.

Part Three deals with mission analysis aspects, including a discussion of Low Earth Orbit (LEO) perturbations and radiation. The chapter includes a trade-off, for both an elliptical orbit (FPE-A) and a circular orbit (FPE-B and C). The launcher performances for both cases are considered.

Issues related to the adaptation of Lisa Pathfinder to FPE are presented in Part Four. The required changes to LPF due to the payloads are described and the implications of this for re-use.

Finally, in Part Five, the conclusions are presented, also with reference to the relevance of FPE to the Cosmic Vision 2015-2025 programme.

2   Fundamental Physics in Space

In preparation for the next generation of science missions to be flown within the Cosmic Vision 2015-2025 framework, the scientific priorities and areas of most interest were defined (see [1] and [2]). A review of fundamental physic in space can also be found in [14].

One of the questions asked by Cosmic Vision is [2]:
"What are the fundamental laws of the universe?"

To answer this question we must explore [2]:

- "The limits of contemporary physics" – using weightlessness to study deviations from the standard model (the theory that encompasses the four forces of particles and interactions)
- "The gravitational wave universe" – the detection of gravitational 'foot print' of the big band an other large objects
- "Matter under extreme conditions" – a study of gravity within very strong field environment of compact objects and the state of matter within neutron stars.

The Fundamental Physics Explorer (FPE) Programme would focus on the fundamental laws of the universe and address questions such as: How light really behaves? Does it really depend on the conditions of the experiment (the speed you are travelling)? Is the observed Gravitational Red-Shift (GRS) the same for all clocks? Do objects fall at the same rate? Finally, how do microscopic pieces of matter behave when cooled to such a degree, that the constituents revert to the same quantum state and can be described by a single wave function?

2.1   Theoretical Background

This section serves as a reference to some of the concepts that will be employed throughout this report.

2.1.1   Power Spectral Density (PSD, $S_y(f)$)

This describes how the energy (Energy s^{-1} or power) is distributed by frequency. In other terms the PSD can be used to determine at what frequencies the signal is small and /or large. The units of a PSD are usually given as Energy (or Volts, Current, Acceleration, Force etc) $Hz^{-1/2}$ (or bandwidth). PSD plays an important role in any physical measurement process and can be determined by measuring a particular parameter with the time series data converted to a PSD using the auto correlation function and then into Fourier space.

Mathematically [16],

$$S_y(f) = \sum_{\alpha=-2}^{2} h_\alpha f^\alpha$$

2.1

Where f is the Fourier frequency (measurement frequency) and h_α is a constant dependant on the physics of the instrument or clock. Also, α, is a term which describes the type of noise. It

encapsulates the behaviour of noise as a function of frequency. There are five types in total. The terms used to describe them are shown in Table 2.1. Another convention of describing the noise is simply by stating the function ('1/f noise' etc). Figure 2.1 shows an example of a PSD and the five types of noise. The sum of which would show the PSD (Equation 2.1)

α	Noise Source	Function
2	White Phase Noise	f^2
1	Flicker Phase Noise	f
0	White Frequency Noise	1
-1	Flicker Frequency Noise	$1/f$
-2	Random Walk Frequency Noise	$1/f^2$

Table 2.1 – Terms used to describe the five types of Noise [16]
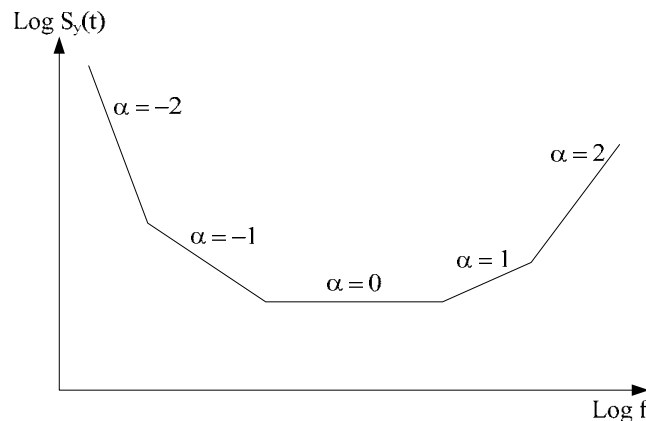
Figure 2.1 – General PSD Example Showing Each Noise Trend [16]|

Take for example a glass beaker in a room with a window. Placed in the glass beaker is a thermometer. A Bunsen burner heats the water automatically every few minutes. The system is left to evolve for a few days. The time series of the data is then plotted showing sinusoid varying a low frequency with small fluctuations along the data. The temperature of the room is driven by the visibility of the sun, i.e. cooler at night and warmer during the day. This of course also affects the temperature of the water. Heating up during the day and cooling it during the night. There are smaller fluctuations due to the periodic operation of the Bunsen burner. If this is converted to frequency space, what will be seen is a feature at low frequencies and one at high frequencies. Other intermediate fluctuations may also appear, such as the opening and closing of a door shaking the system. If one needs to determine the temperature at a frequency comparable to a day the environment must be controlled such that day and night do not affect the water masking the measurement (perhaps by closing the curtains?). However one does not need to control the Bunsen Burner as this feature in frequency space will be visible in another part of the spectrum to the daily measure of temperature.

A further example would be to measure sea level over a period of time. The time series would be a dataset were minute changes occur over fast timescales giving a feature at high frequencies. In another case there maybe large variations over longer timescales at or at low frequencies. The difference between the two here is the small waves on the surface and tidal behaviour respectively. From a time series it may be difficult to determine the periodicity of the variations. However, in the

frequency domain they will appear as features at the order of 1 Hz (1 sec - wave) or 20 µHz (12 hours – tide). A good discussion can be found in [15].

What must not be forgotten, in both examples, is the noise of the sensor, and how that can impact the PSD.

2.1.2   The Allen Variance ($\sigma_y(\tau)$)

The Allen variance is to the time domain what a PSD is to the frequency domain. It stems from statistics and is similar to the standard deviation. The Allen Deviation shows the average variation from the mean. For clocks and oscillators it is a measure of stability and accuracy and for inertial sensors a measure of accuracy. It provides an instantaneous measure of stability, rather than calculating the average over a longer period. For this reason it is also known as the two sample variance.

The Allen deviation in a more formal way; is the half of the square of the difference between one measurement error and the previous measurement error. This is expressed as,

$$\sigma_y^2(\tau) = \frac{1}{2}\left\langle \left(y_n - y_{n+1}\right)^2 \right\rangle$$

2.2

Where τ is the integration time or length of time that you will/or have been measuring and,

$$y_n = \left\langle \frac{dv}{v} \right\rangle$$

2.3

The quantity v could refer to the frequency of a clock measured by a counter and the measured error, dv, between that and the nominal frequency. This can also be called the **'fractional frequency instability'** of clocks or oscillators (more detail can be found in Refs [16], [17] and [23]).

The required Allen Deviation can be specified by stating the expected value that is desired, in other words the mathematical expectation value. For example, the desired frequency stability over a given time is the expectation ('requirement'), and hence will demand a given Allen Deviation. For another experiment such as a measure of angular acceleration in a gyroscope for example, the expectation value ('required level of accuracy') would provide the Allen Deviation.

For both the above examples, the Allen Variation would describe the average instantaneous deviation from the mean value that is acceptable in the time domain.

2.1.3   Conversion Between the Allen Deviation and PSD

As it has been mentioned before, time series is used in the time domain, while its counterpart, PSD, is used in the frequency domain.

The noise or stability is usually described as a PSD. This quantity provides information regarding performance at a given frequency. This parameter can then be compared to the desired measurement requirement, to determine performance compliance of key units, such as thruster or DFACS performance. A detailed discussion can be found in [16 and 17].

The PSD of the instrument can be determined by computation from the time series data, from which the Allen Deviation can also be calculated. In engineering terms, the noise requirement (e.g. the performance of a sensor or of a clock) needs to be compared with the relevant science requirements, and the residual sensor noise would have to below the science parameter measurement at that same frequency. For instance, thruster noise would have to be kept below the sensitivity of the sensor, not to degrade the actual science measurements. To these ends it is sometimes useful to convert from the desired measurement accuracy (statistical expectation) to the PSD so to allow a comparison of desired science requirements with the performance of available hardware.

The Allen Deviation is calculated based upon the required science accuracy. Depending on the integration time and measurement frequency (sample taking interval), the required PSD can be determined. Table 2.2 shows the relationship between PSD and the Allen Variance for each of the five noise types. The expressions do simplify as $\tau^0 = 1$ and $\tau^1 = \tau$. All are shown to illustrate the role of α.

Noise Type (f^α)	$S_y(\tau)$ (PSD)
f^2	$\dfrac{(2\pi)^2}{3f_h}\left[\tau^2\sigma_y^2(\tau)\right]f^2$
f^1	$\dfrac{(2\pi)^2}{(1.04+3\ln(2\pi f_h\tau))}\left[\tau^2\sigma_y^2(\tau)\right]f^1$
1	$2\left[\tau^1\sigma_y^2(\tau)\right]f^0$
$1/f$	$\dfrac{1}{2\ln 2}\left[\tau^0\sigma_y^2(\tau)\right]f^{-1}$
$1/f^2$	$\dfrac{6}{(2\pi)^2}\left[\tau^{-1}\sigma_y^2(\tau)\right]f^{-2}$

Table 2.2 – PSD as a Function Allen Deviation, integration time and measurement frequency [17]

In later sections (FPE-B, Section (4.6.5)) this approach will be used to show the instrument and thruster requirements. It should also be mentioned that there are additional factors that can attenuate noise and other residual disturbances, for instance the control loop gain.

2.2 Special and General Relativity

In preparation for the statement of the science requirements [TN1], some background is now provided to Special and General Relativity and why we would want to test them so rigorously.

2.2.1 Special Relativity (SR)

Length Contraction and Time Dilation

An observer viewing an object in a frame moving relative will view its length differently to its 'proper' (actual) length. Lorentz contraction is given by [18],

·eesa

$$L = \frac{1}{\sqrt{1 - v^2/c^2}} L'$$

2.4

A primed quantity represents how it appears to the observer. The length of an object moving past an observer appears shorter than if measured in the moving frame, length L, its proper length.

The phenomenon of Time Dilation is similar. Two events occurring in a moving frame when observed from another relative frame appear longer. Essentially, the time between the ticks of a clock in the moving frame measured in the observer (relative) frame is longer than the proper actual time. In this case the primed value is the time between events in the moving frame. The non-primed quantity represents the time in the observer frame between ticks [18],

$$T = \frac{1}{\sqrt{1 - v^2/c^2}} T'$$

2.5

Note that v corresponds to the velocity of the frame and c is the speed of light.

Local Lorentz Invariance (LLI)
"In a freely falling frame the outcome of a non-gravitational test experiment is independent of the velocity of the frame."

No matter what velocity the laboratory is moving at (a constant v, as if v is not constant we begin to move into the realms of General Relativity) a fire would burn or a clock would tick at the same rate, whether or not the experiment was performed at 10 ms^{-1} or 100 000 ms^{-1}.

Local Position Invariance (LPI)
"In local freely falling frames, the outcome of any test experiment is independent of where and when in the universe it is performed."

A piece of magnesium will burn with the same colour if lit, either in Earth orbit today or at the end of the universe a million years from now, although, the conditions of the experiment would have to be constant. This also implies that c does not change if the laboratory is moved such that is has a different attitude, or the light is travelling in a new direction.

Modifications to SR
The above assumes that c is constant, but from the following discussion, there are theories which counter this.

The following equation is taken from [13] and it describes the relationship of the speed of light between the orientation and velocity an adjustment to SR.

$$\frac{c}{c_0} = 1 + A\frac{v^2}{c_0^2} + B\frac{v^2}{c_0^2}\sin^2\theta$$

2.6

c_0 is the speed of light in the preferred reference frame usually taken to be the Cosmic Microwave Background (CMB). v is the velocity of the frame and has components of the Sun (amongst others) through the galaxy, Earth around the sun and the orbital velocity. The angle w.r.t. the frame velocity vector is θ. The parameters A and B relate to the augmentation of Lorentz transforms to describe a variation of the light velocity. If A and B are zero special relativity reverts to normal. The goal of the experiment is to measure A and B. They are functions of the parameters α, β and δ ($A = \alpha - \beta + 1$ and $B = \beta - \delta - 1/2$) the augment special relativity. Any experiment has two goals, each made up of two parts, the first to measure changes (velocity) in the speed of light and also to determine, to a better precision, these parameters.

2.2.2   General Relativity (GR)

Einstein's theories of GR take into account acceleration. In addition to this the theory describes the curvature of space. FPEs interests are the Gravitational Red-Shift (GRS) and its universality.

This effect was measured using aircraft and GP-A. Comparisons with ground based clocks will ascertain frequency differentials. A time and frequency link is required as the proper time of a clock as measured from where the clock is will not change. The following equation describes this effect [14],

$$v(x_1) = \left(1 - \frac{U(x_1) - U(x_0)}{c^2}\right)v(x_0)$$

2.7

Where U is the Newtonian potential (*GM/r*) at a given position (*x*) and v is the frequency. The objective of the experiment is to measure the red-shift at different altitudes. So the clock onboard the spacecraft would transfer the signal to ground and they would be compared. As $U(x)$ decreases the frequency reduces (or the clock slows) at x_1 compared with x_0. Clearly to reduce the gravitational potential the variable is the distance from the CoM a central body (the Earth). As r increases, $U(x)$ decreases.

Einstein also postulated that the outcome should be independent of the clock type. If the frequency is independent of velocity (LLI) and location (LPI) and combining this with the fact that all frames move in the same way along a geodesic, the shift in clock rate should be the same. In other words, $v(x_1)/v(x_0)$ is the same for all clocks or $\Delta v_{clock1} = \Delta v_{clock2}$. To show this, Equation 2.7 can be extended to include a term that takes into account the clock type.

$$\frac{v_{clock1}(x_1)}{v_{clock2}(x_1)} = \left[1 - (\alpha_{clock1} - \alpha_{clock2})\frac{U(x_1) - U(x_0)}{c^2}\right]\frac{v_{clock1}(x_0)}{v_{clock2}(x_0)}$$

2.8

If the α_{clock} quantities (note α is different in Sections 2.2.1 and 2.2.3) are the same Equation 2.8 will revert to Equation 2.7.

2.2.3   Fundamental Constants (FD)

The fine structure constant relates directly to the hyper-fine transitions between atomic energy levels (see [18]). As space-time is expanding over time it is thought that the fine structure constant may also be changing. A comparison between clocks in space, as well as ground clocks, will attempt to identify any time dependence on α. Clocks of differing types result in different transitions. Frequency is related to the fine structure constant as follows (there may be alternatives),

In [19] it is described how Dirac postulated the age of the universe was comparable to ratio of the electrostatic and gravitational forces between the electron and proton (when expressed units of light travel time across the electron radius). Dirac suggested that this ratio was proportional to the age of universe, calculating that $dG/G \approx$ -5 x 10^{-11}/yr. Further to this Teller (described in [19]) postulated that the fine structure constant, $d\alpha/\alpha \approx \alpha(dG/G) \approx$ -3.6 x 10^{-13}/yr. A recent experiment is described in [27].

The measurement could be made by taking the difference between clocks at a time t_0 and comparing it with a difference between frequencies at t_1 a certain time later. If the difference between the two Δv is not the same then the fine structure constant must have changed over time. If the frequencies are compared at intervals during this period the rate of the relative frequency shift can be determined. If there was a shift outside the bounds of the known errors, it could be attributed to $d\alpha/\alpha$. High accuracy clocks would further improve the degree of certainty that this variation was zero.

2.3   The Equivalence Principle

In preparation for the statement of the science requirements that would be taken from [TN1], the Sci-RD, some background is now provided relating to the theory of equivalence and why we would want to test it so rigorously.

The Equivalence Principle (EP)
The gravitational mass of an object is equivalent to the inertial mass. The force due to the gravity of a body (the Earth for example) is indistinguishable from an acceleration of the same magnitude. This simply means that an acceleration of equal magnitude against the force of gravity will result in a motionless test mass.

Weak Equivalence Principle (WEP)
"The trajectories of freely falling test bodies are independent of their structure and composition."

No matter what the object 'is', if released, it will fall with the same acceleration as a completely independent object of different structure, density, mass etc. E.g., from the same height, a golf and bowling ball will hit the ground at the same time, over the same amount of time.

Measurement and Quantification
Certain theories predict that the WEP could be violated, particularly ones aiming to unify the four forces. The aim is to detect extremely small differences in the acceleration in two dissimilar proof masses, and thus a violation in the WEP.

We can also consider the Eötvös parameter given by,

$$\eta = 2 \frac{(m_g / m_i)_A - (m_g / m_i)_B}{(m_g / m_i)_A + (m_g / m_i)_B}$$

2.9

The subscripts g and a represent the gravitational mass and inertial mass respectively. A and B represent the two test masses. This represents the differential acceleration between the two test masses A and B expressed as a fraction of the common mode acceleration between the two (the average). For the WEP to be true the ratio has to be zero (as $(m_g / m_i)_A - (m_g / m_i)_B = 0$), and also indicates that gravitational and inertial mass are equivalent.

By testing the WEP and EP we can test the foundations of GR and prove whether or not 'inaccuracies or flaws really do exist. Ground based tests in vacuum tubes are estimated to measure effects on a free falling body to a level of $\eta = 10^{-16}$ over 30 s [TN1]. The best drop tower experiment confirmed the WEP to $\eta = 3 \times 10^{-10}$ [2]. A further experiment is planned in Bremen [33]. Of course the free fall time, the window of opportunity for measurement, is limited by the length of the vacuum tube. An Earth-Moon experiment based upon laser ranging provided η to 5×10^{-13} [20] and [34]. Another form of the test is the use of torsion balances. The most accurate of which from reviewed literature is η to 5×10^{-13} [20].

To measure these effects, a differential accelerometer(s) (DA) will be used, allowing the detection of minute differences in displacement due to the Earth's gravitational field. Any detected differences in the motion of two test masses will result in a signal that shows the violation of the WEP.

2.4   Unification Theory

Violations in the postulates described above are evidence for the validation of theories that could relate the four forces [14]. The electromagnetic, strong and weak forces are discretely quantised within the laws of quantum mechanics. However, gravity is a continuous quantity that is incompatible with quantum mechanics. A diagram of the relation between these four forces is shown in Figure 2.2.

String theory and canonical quantisation of gravity (loop gravity) are presently being considered. Below the level of protons, neutrons and electrons there is a phenomena that exists in ten dimensions known as a 'string'. The vibrating resonances of these loops determine a corresponding particle. Interactions between particles have to be different depending on type. According to these theories, new field interactions are introduced, which are dependant on the type of matter. Therefore there would be a phenomenon that the gravitational, electromagnetic, strong and weak are all functions of. FPE would also focus on the aspects of Special and General Relativity that could prove or disprove the proposed unifying theories.
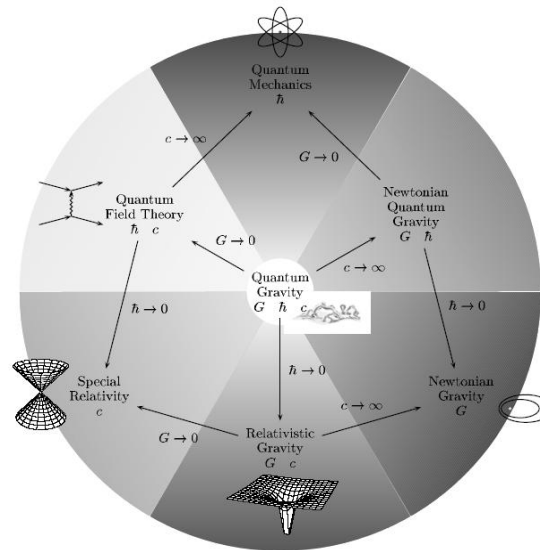
Figure 2.2 – Illustration of the links Between Gravity and Quantum Mechanics [20]

To achieve the level of accuracies required (in the case of the WEP the relative displacement of two Test Masses of order the diameter of an atom) an extremely stable measurement environment is required. For this reason we need to go to space. A free floating laboratory allows microgravity (FPE-C – BECs), in theory perpetual free fall conditions (FPE-C BECS and FPE-B WEP) and of course the opportunity to measure light and red-shift in a variable gravitational field.

2.5   *Bose Einstein Condensates (BEC)*

All particles can be described as a wave. The wave-function depends on the spin, the velocity and energy, amongst other things. In a given cloud of atoms, there are a number of atoms each in differing discrete energy levels. Cool atoms tend to occupy the lower energy states. A gas will have a distribution of atoms/particles mainly in higher energy states than a liquid. The same is true for a solid. Even less atoms are sitting at lower energy levels than that of a liquid. If the cloud of atoms was to be cooled to very low temperatures a strange phenomenon occurs. The number of atoms at this low energy level (as temperature is proportional to energy) increases rapidly.

Recall that the momentum of a particle is related to its wavelength by $p = h/\lambda$. The de Broglie wavelength is a characteristic of a given atom and at a given thermal momentum distribution, can be given as [52],

$$\lambda_{dB} = \frac{h}{\sqrt{2\pi m k T}}$$

2.10

Where h is Planck's constant, m is the atomic mass, k is Stefan-Boltzmann's constant and T the temperature.

As the energy decreases the wavelength must increase. At the point where all the atoms exist in the same low energy level, they all have equally long wavelengths. As a critical temperature approaches, the de Broglie wavelength becomes comparable to the average distance (*d*) between

atoms and the wave-functions begin to overlap. The peculiar situation each of these now finds themselves in is that they all have the same wave-function and become indistinguishable. Each quantum state is the same and this gas is otherwise known as Bose Einstein Condensation. Figure 2.3 illustrates this. In other words we have a quantum gas in which all atoms behave in the same way.
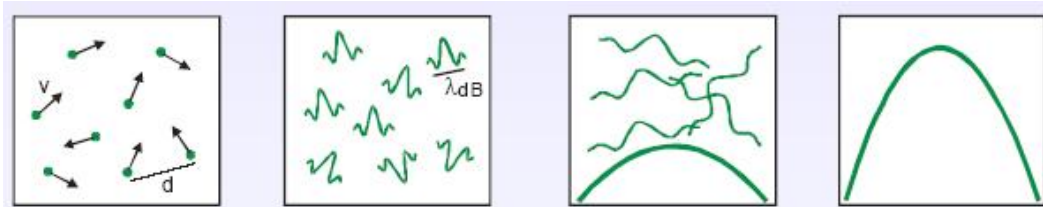
Figure 2.3 – Illustration of the Formation of a BEC [53]

The condition of BEC can be expressed as, for a given gas density, ρ,

$$\rho \lambda_{dB}^3 = 2.612...$$

2.11

The goal is therefore to attempt to cool a gas down into the hundreds nK regime. In 1995 this was successfully done for the first time using laser and evaporative cooling [55]. In space it is suggested that the fK regime can be reached [TN1].

The next stage is to study its characteristics by exciting it, shining light on it and squeezing it (the magnetic field containing it can be used for this).

2.6   Drag-Free Control

One of the key areas of technology required for providing the disturbance free environment, in addition to a spacecraft which is near vibration free and thermally stable, is a Drag Free Attitude Control System (DFACS). This is the ability to follow the natural geodesic in space. This is more important for tests of the WEP as any disturbance could affect the position of the test masses.

The DFACS can be split into the following units:
- The inertial sensor
- Control law or feedback loop (which would be computational)
- Actuators or thrusters

The basic concept is that the position of a test mass within the spacecraft is measured. If an external disturbance, such as residual atmospheric drag, moves the spacecraft, its position will change relative to the test mass (unaffected by drag as kept inside the S/C). Figure 2.4 illustrates this concept. A sensor would then detect this relative motion and provide a signal for actuation of the thrusters to re-centre the test mass or move it back to a reference point. In other words the force that moved the spacecraft away from the geodesic would be balanced out.

There are two drag free control scenario's to be considered: the accelerometer mode and the free floating mode.

- **Accelerometer mode** – The Test Mass is held in position by an electrostatic field. Any motion of the test mass due to the spacecraft moving around it is resisted by a counter force. The applied force provides the signal of acceleration to the control system. The principle is the same as a force feedback accelerometer. The advantage is a direct measurement of acceleration.
- **Free-Floating** – In this case the Test Mass is not held but the changes in a sensor (an electrode for example) are detected as it moves. This provides a signal for the actuators or thrusters to move the spacecraft such that there is no signal. In principle the spacecraft simply follows the test mass.
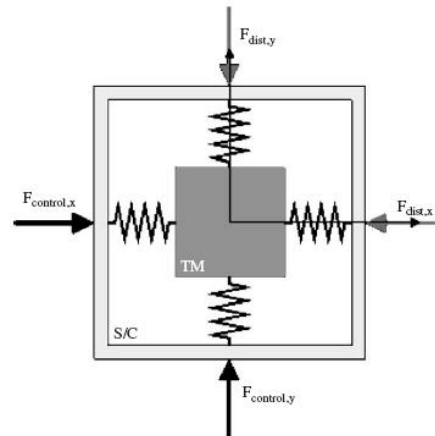
Figure 2.4 – Schematic of the Principle of Drag Free Control [21]

The key difficulties and aspects which require consideration are:

- **Charging of the Test Masses** – Charge effects from cosmic rays or the Earths local trapped particles could induce un-wanted motion, thus creating an error.
- **Radiometer effect** – Particles with higher momentum striking the surface of the test mass due to higher temperature than compared with a lower temperature on the other, create a residual force.
- **Radiation Pressure** – The exchange of momentum between Test Mass and particle.
- **Brownian Motion –** Residual forces due to impacts of particles in an imperfect vacuum.

Some of Lisa Pathfinder's science goals are to characterise these effects. The next part of a DFACS is the control system which takes as input the signal from the inertial sensor (including the Test Mass) and computes the acceleration on the spacecraft. This is then converted to the thrust vector which is required to counter it. Finally the level of thrust required of each actuator (thruster) on-board the spacecraft is determined. The appropriate signal is then given to each thruster (some could be zero).
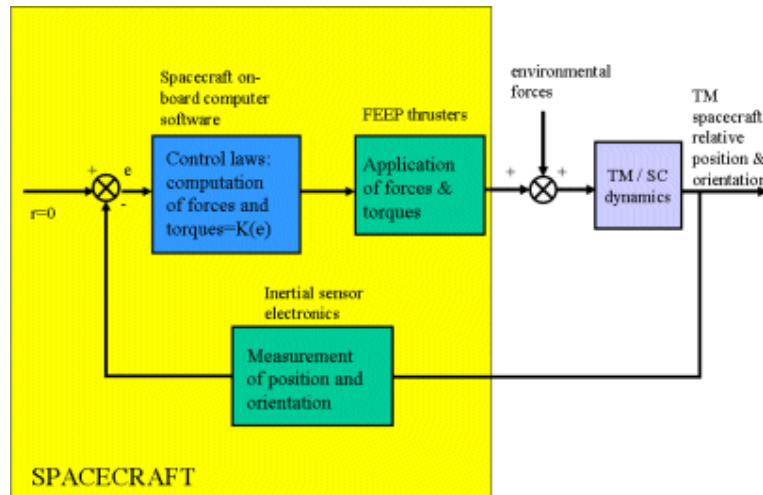
(Credit: ESA)
Figure 2.5 – Example DFACS Control Law
(Credit: ESA - LISA Pathfinder)

The final element to the DFACS sub-system is the thrusters (actuators). A cold gas system was employed on GP-B (Section (2.7.2)). LISA Pathfinder and Microscope plan to take advantage of FEEPs (Section (2.7.6) and (8) respectively). FEEPs were also assessed for Hyper (Section (2.7.3)).

2.7   Previous Missions

2.7.1   GP-A (Gravity Probe A)

This spacecraft was launched in 1976 by NASA with the intention of measuring general relativistic effects using an H-Maser atomic clock. GP-A weighed 60 kg and was in flight for 1 hour 51 minutes reaching an altitude of 10224 km. Scout was used as the launch vehicle inserting the spacecraft into a sub-orbital ballistic trajectory. The main goal of this mission was to verify the effects of Gravitational Red-Shift predicted by Einstein.

The basic principle of measurement was the comparison of clock frequencies with the spacecrafts clock and a ground clock to determine gravitational red-shift measurements and to detect the slowing of the space borne clock. To separate the two effects, first the phase change over the distance between spacecraft and ground was compared. This gives the red-shift as the phase change would be expected to shift towards the red end of the spectrum. The second comparison detected the change in the frequency between clocks, hence detecting a change in the passage of 'time'. Clearly corrections were made for the atmosphere.

The payload had a mass of 43 kg and required 22 W of power. The clock uses a Caesium atom. achieving a frequency accuracy then of 10^{-16}.

2.7.2 GP-B

A recent follow-on from GP-A is GP-B, again by NASA [12], launched 20th April 2004 on a Delta II rocket. This spacecraft differs from the first in that it achieved a full orbit and measured the Lense-Thirring effect. As a reminder, this effect is the dragging of the local Lorentz frame due to the Earth's gravitational field warping local space and time. It was designed for a 60 day check-out period followed by a 13 month data collection mission and a two month data calibration phase. The mission was capable of measuring 0.014 arcsec of rotation.
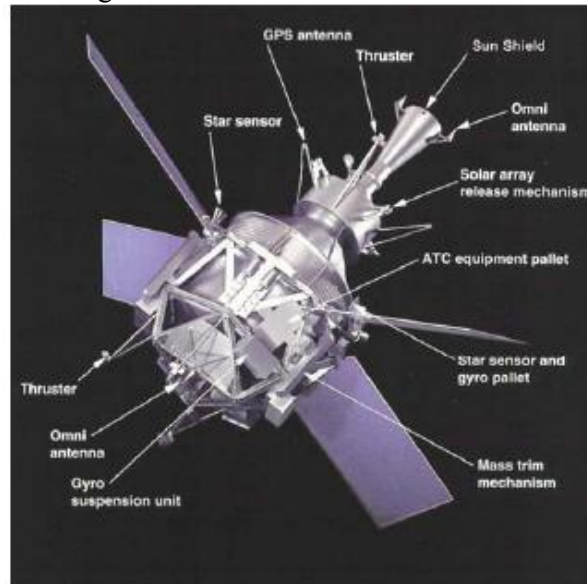
Figure 2.6- The GP-B Spacecraft [12]

Aligned with the spin axis, the telescope maintains a lock on a reference star. the system was designed to measure an angle change of 6.6 arcsec per year. Also co-aligned with this axis are four near-perfect spherical gyroscopes (3.8 cm in diameter). The gyroscopes are inside a helium filled Dewar cylinder to maintain 1.8 K of size 3.0 m and 2.2 m diameter containing 2,441 litres (338 kg) super fluid helium with an entire cryogenic dry structure has a mass of 810 kg [3]. 12.3 kg of hydrogen is used to prevent helium boil off during pre-launch.

The objective is to detect the Lense-Thirring effect by monitoring the change in the rotation rate of the gyroscope. Unperturbed the spin-axis of the gyroscope should not change w.r.t. the Earth. However, if the Lense-Thirring does exist the rate of spin will change. The gyroscopes are shown in Figure 2.7.

The gyros spheres themselves have a diameter of 3.81 cm placed in fused quartz. The gyroscope package is stored in a probe which is inserted into the Dewar (Figure 2.8). It is of length 2.74 m and contains eighty-one electrical cables, 85 instrumentation wires and 15 plumbing lines. The quartz block was of weight 34 kg and length 0.56 m, diameter 0.18 m. The required accuracy was 0.5 milliarcsec.

Clearly drag-free control is required. The measurement of disturbance is provided by electrostatic sensing of the position of one of the gyroscopes. A specific type of cold gas thruster is used as an

actuator. The propellant is taken from the venting helium from the cryostat. A pressure regulator provides constant thrust in a balance, only to be changed to counter a signal of an external disturbance from the gyroscope serving inertial sensor, enabling the spacecraft to follow the geodesic. A heater ensures that the mass flow rate to the thruster remains above a pre-determined minimum by heating the helium to increase the pressure in the tank

Photo Credit: GP-B Photo Archive, Stanford University

Photo Credit: Don Harley
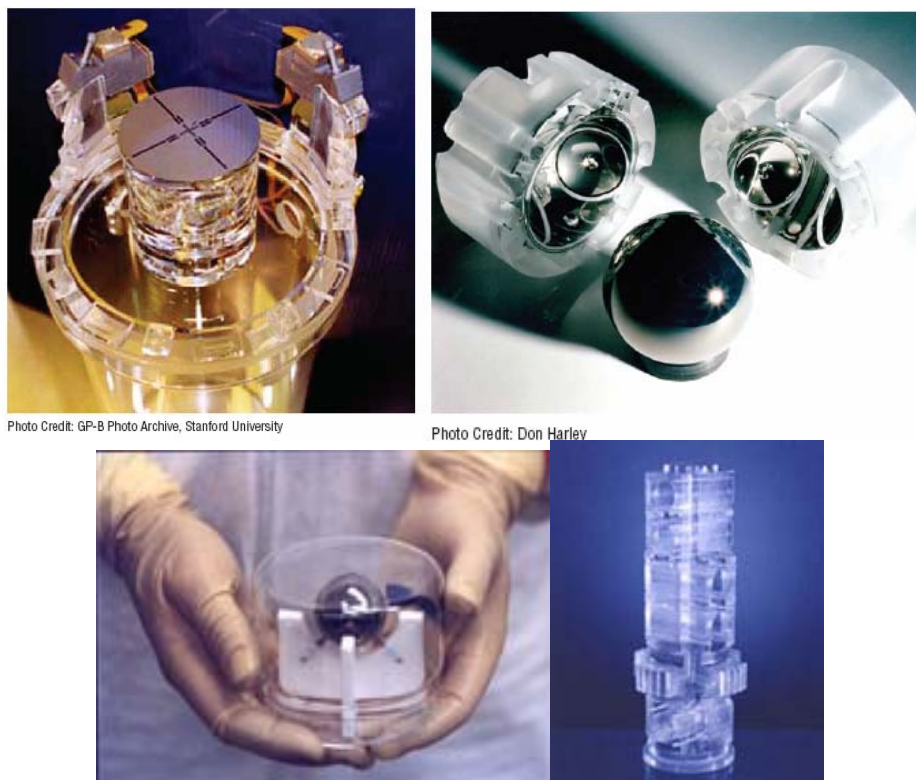
Figure 2.7 – Elements of the GP-B Payload
(Credit: Stanford University)
Telescope (top left), Gyroscopes (top right), gyroscope relative size (bottom left) and the Quartz block (bottom right)

A 650 km polar-orbit was used which was in-plane with the reference star. 60 days were spent verifying and checking systems before pre-science calibration begins. After calibration, the spacecraft spent 10 months taking measurements.

GP-B weighs 3100 kg. The spacecraft generates 293 W of power and the payload 313 W. Its dimensions are 6.4 x 2.6 m [12]. The Gas Management Assembly provided the means to spin the gyroscopes up to operating speeds. The antennas are omni-directional with the primary one located on the bottom truss segment. The secondary antenna is located on the mounted sun-shade. The solar array is 3.5 m by 1.3 m providing primary power. Two star trackers are present consulting of one wide field and one narrow field. Possibly to acquire the general direction of the chosen guide star and then fully more finely focus in on it and maintain the reference. There are 8 pairs of thrusters to provide attitude control.

Credit: Stanford University (left) and EOPortal.org (right)
Figure 2.8 – The GP-B Flight Dewar

The data is still being analysed at the time of writing for GP-B and the results from GP-A were not forth coming after a search.

2.7.3   Hyper

Hyper is a mission that would aim to test and measure the Lense-Thirring effect in Earth orbit. As a reminder, this effect is the dragging of the local Lorentz frame due to the Earth's gravitational pull. This mission follows on from GP-B. This mission was not selected during ESA's Horizon 2000 program, but the initial study work done can provide useful information for the FPE. The mission concept can be seen in Figure 2.9.

The difference between this approach and GP-B is the use of atomic interferometry to measure the angular rates caused by frame dragging (for a better resolution) (see Figure 2.9). Two interferometers are used measuring the path of the atomic wave packet in two opposite directions. The Sagnac effect can then be observed, completing the measurement of rotation, by comparing the fringe pattern of two interferometers which are aligned to the sensitive axis, will remove common motion. These instruments are better known as Atomic Sagnac Units (ASUs). The relative phase shift forms the rotation rate measurement.

A precision star tracker (PST) is used to provide a reference. The star is chosen depending on its magnitude, right ascension and declination w.r.t the orbit plane. The PST measures attitude and angle w.r.t. the reference star and this value is subtracted from the ASU rotation to remove common spacecraft motion. After accounting for errors such as, component alignment and instrument noise (low due to atomic interferometry), the remaining value is the Lense-Thirring effect. Measurements over an entire orbit will show the effect repeating over an orbit building a dataset which varies at double the frequency of the orbit. An optical bench (in addition to the Atom Preparation Bench) is surrounded by thermal control to maintain the temperatures and stability needed in the interferometer. The mass of the entire payload suite is estimated to be 275 kg excluding the atomic bench. The aim is to achieve an accuracy of 10^{-15} rads^{-1}. For these accuracies drag-free control is once again required to provide the stable platform.

The requirements of the mission can be expressed as a split of the Lense-Thirring measurement between the ASU, PST-ASU alignment and PST accuracies. In terms of the ASU, gravity, radiation, magnetic fields and timing must be accounted for. According to [4] the requirement accuracy is 5×10^{-12} rads^{-1}. External and internal and low and high frequency errors drive the accuracy of the PST. It needs to be kept extremely still to give a desired accuracy of 1.2×10^{-8} rad. In terms of interferometer performance, within 1/10 of the central fringe the rates must appear. Further accuracy requirements can be found in [4].
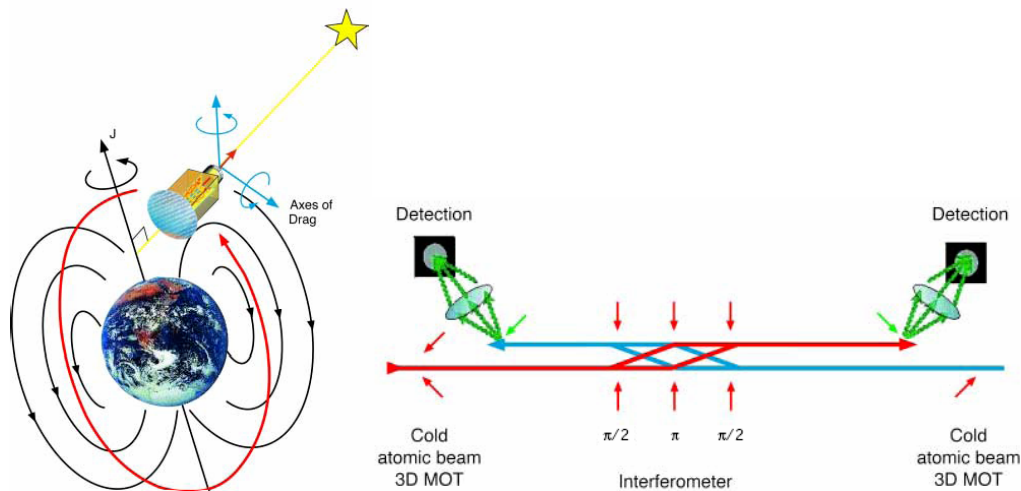
Figure 2.9 – The Hyper mission concept (left) and the principle of the ASU (right)

The orbit is chosen as a trade between atmospheric drag and the strength of the local gravitational field. For this mission a circular orbit is required at an altitude of 1000 km. Higher altitudes result in an increase in the intensity of radiation, a reduction in the gravitational field and increases launcher costs. Lower altitude reduces launch costs and increases gravitational effects but also causes an increase in drag. A sun-synchronous orbit was chosen to simplify thermal control.

The drag-free control sensors (two) lie either side of the centre of mass along the alignment axis of the ASU and the PST providing disturbance measurements for control thrusts to remove external forces and torques. A GRADIO accelerometer, to be used on GOCE, was considered to be a possibility.

To summarise Hyper; it would have a total mass of 1061 kg and have cubic shape, with a solar panel mounted on one side. For Hyper, the intention is to launch aboard a cheaper Rockot launcher (1000 kg max). The configuration is compatible, but the mass is over budget. The value for mass includes a margin of 20% at the system level. For a comparison, initial thoughts for the FPE indicate a 1500 kg mass limit. From discussions concerning the top-down and bottom-up requirements, 1000 kg is a target for the FPE. In both cases there is the option of using an ESA Vega rocket (in development), providing a capability of around 1500 kg.

The total power requirements of the solar array is 714 W. A payload shut down during an eclipse period would save 240 W nearly half the demand. There will be a long period between eclipses as the declination of the Sun is the major factor.

2.7.4   STEP

Again this is a study for a mission that was not taken forward, although useful calculations and study options can be considered. The mission, instrument and spacecraft concept are shown in Figure 2.10.

The orbit selected is a 400-500 km orbit [1] with the sensitive axis of the accelerometer constant. The orbit will be sun-synchronous for the same reasons as Hyper. At 400 km 97° is required and is eclipse free for eight months until the Sun's declination motion takes the northern most points of the orbit into shadow.
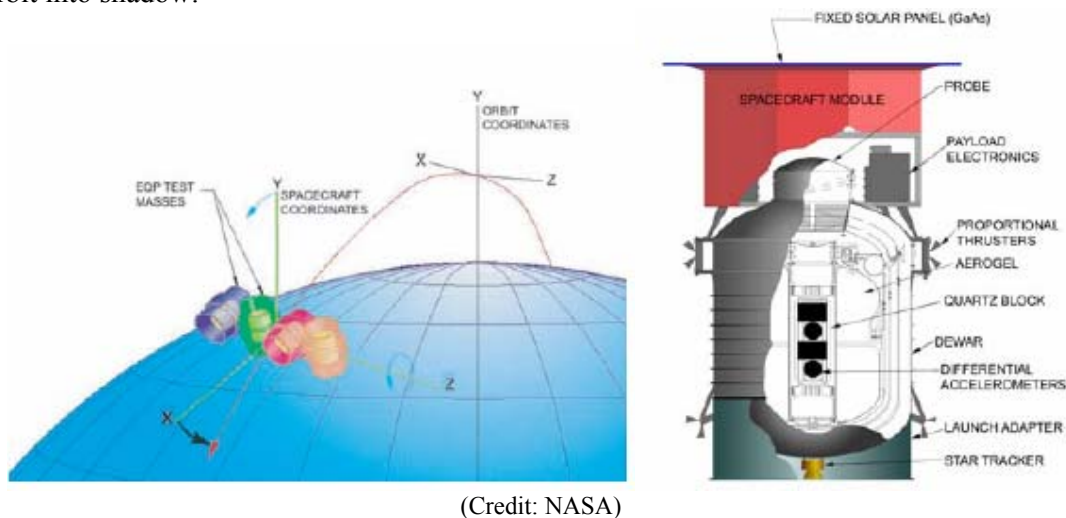
(Credit: NASA)
Figure 2.10 – The STEP Orbital Concept (left) and the Current Spacecraft Configuration (right)

It is assumed that the instrument is aligned along the Earth radius vector. The gravity gradient and spacecraft perturbations are removed using models and drag free control respectively allowing the measurement of acceleration towards the Earth. The instrument would consist of four Differential Accelerometers (DA) with two test masses (TM), each differing materials to test the WEP. The change in acceleration between each will show violations in the WEP. This small acceleration is detected by a SQUID. In principle, a small current is generated by each TM as it moves towards a coil of wire. The difference in these currents is detected by the SQUID (see Section (4.4) for more details). The Equivalence Principle measurement is at its maximum when the accelerometer sensitive axis is nadir pointing. This would happen twice per orbit if the spacecraft was three-axis stabilised.

In addition to the four accelerometers, there are two cross track gradiometers and a mass-s/c coupling differential accelerometer. The first is to test the interaction between matter and the spin of particles. The second additional experiment is to measure the Earths gravitational field. This will highlight features using a gradiometer aligned with the spin axis.

The tests will be conducted under differing conditions such as spacecraft roll and temperature variations.

Clearly the choice of test mass will be important. The basic considerations highlighted by the STEP team were; the number of materials against the possibility of spurious measurements due property differences. They favoured certainty rather than a thorough test. To avoid mass coupling with the spacecraft, cylinders were chosen as the desired shape for the test masses. This is close to a symmetric sphere as you can get. A sphere of two test mass one inside the other is not possible to construct. The inner mass is Pt-Ir of a high density common to all accelerometers. The outer masses (for comparison) are Ti, Be, and Si. One of these materials will be used twice to vary both the shape and mass to fairly measure systematic errors.

Thermal control, with the payload in a Dewar Helium filled container (built by Lockheed), will keep the temperature, approximately, at a required 1.8K varying by no more than 0.5 mK per orbit [6], using liquid helium. A single cavity, helium filled for insulation, was not desirable due to tidal effects of helium bubbles. A new design known as a Claudet bath, with two cavities, was proposed for STEP. More detail can be found in [5].

The boiled off helium would provide the propellant for the micro thrusters. Surrounding the quartz mounted accelerometers is a super-conducting lead shield to eliminate stray magnetic fields. Also a tungsten shield is used to prevent radiation from infiltrating the experiment. An Electrostatic Positioning System (EPS) surrounding each TM can be used for the residual acceleration signal.

The accuracy of STEP was estimated to be near 3×10^{-19} ms^{-2} g over 20 orbits [6]. Verification of results can be done by comparing the differential measurement of three accelerometers. The cryogenic payload could have a mass of 202.4 kg and power of 3 W, the warm payload is 56.5 kg and consumes 84.4 W. The cryostat could have a mass of 345 kg (50.2 kg of Helium, 9 kg of electronics and 286.5 kg dry) and consume 32.2 W. Total STEP payload could be 645.3 kg 119.6 W nominal (figure taken from [5]).

The spacecraft consists of a Service Module (SM) and the cryostat containing the sensitive equipment. Two panels are mounted around the cryostat and the lower serves as platform for the electronic equipment. This also houses the GPS system with the antenna mounted on the solar array and the lower platform. Two star trackers are attached to the upper platform. A radiator for the cryostat protrudes from the bottom of the spacecraft.

Power is derived from a single solar panel mounted in the top of the cryostat. Its specifications are 474 W and 78 V [5].

A distributed system handles data processing and communications is handled using the S-Band with to 0.7 W transponder systems able to handle a data rate of 1 Mbps. There is a capability for 24 hour storage [5].

Thermal control is passive and handled by paint, insulation and radiators (with the exception of the cryostat). Operating range is 190 K to 205 K.

Total spacecraft mass is estimated to be 973 kg, adding 53 kg of fairing and the margin 20%the launcher requirement is 1220 kg [5].

2.7.5   ACES

This mission is to be attached to the Columbus module's payload adapter on the International Space Station. The main scientific objectives are split into two categories. The first is the testing of the space clocks and telemetry links with the ground. Measurements of the gravitational red-shift, Lorentz violations (light anisotropies) and time dependence of the fine structure constant were to be made. However, it appears that ACES will not go ahead.

The operation is split into phases. The first is the attachment to the ISS if it were to be delivered by the space shuttle. The second is on-orbit verification and check-out which will last six months. Finally, the experiments will begin with the clocks in optimal mode. The permanency of the set up means there can be extensive comparison with ground clocks testing Einstein's theories. The last two stages will take approximately 18 months and PHARAO was scheduled for launch in 2010.

The clock is based upon the Caesium ion and is compared with another on-board clock, a Space Hydrogen Maser (SHM). The distribution and comparison is handled by the Frequency Comparison and Distribution Package. This comparison is done by a Microwave link (MWL) with the ground specifically designed for the task.
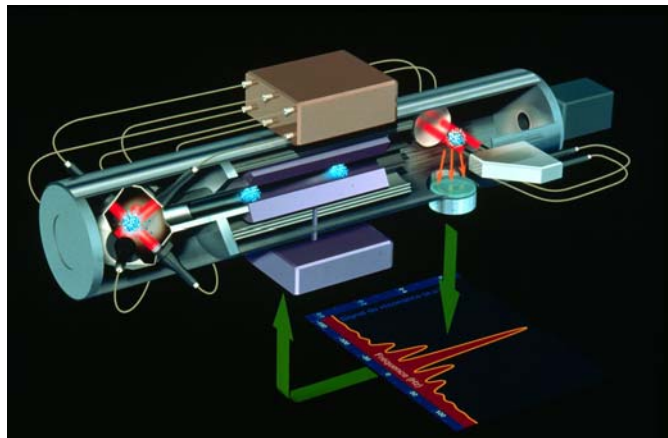
Figure 2.11 – Concept of the Micro Gravity Atomic Clock PHARAO [7]

In the case of the SHM a microwave cavity is tuned based upon the sapphire bulb loaded with the resonance of a Hydrogen atomic transition. The purposes of flying this clock may be to space qualify it and also verify the accuracy of the Caesium clock. The FCDP provides a mechanism to lock the clocks and measure stability as well as comparing the timing signals from both.

The clock operated on the following principle. A given amount of Cs atoms are cooled then pushed gently down a tube (known as the Cs tube in [7]). A microwave cavity excites them as they pass. The fluorescence is then measured by a detector. This is one cycle of the clock. Another mass of Cs is then injected. The microwave cavity frequency is adjusted until the Cs fluorescence that is being monitored is at a maximum. The microwave frequency is then maintained based on the fluorescence in a feedback loop constantly correcting the cavity. The microwave signal can be then counted. The resonant frequency for Cs is 9.2 GHz. The reciprocal of which is one second.

In terms of hardware, the ACES experiment consists of the following;
   • External Payload Computer

- Power Distribution Unit
- Frequency Comparison and Distribution Package
- MWL antennas
- Heat Pipes
- Microwave Link
- SHM Assembly
- PHARAO Caesium Tube
- PHARAO Laser Source
- PHARAO Accelerometer and coils Control Unit

2.7.6   Microscope

The principle of MICROSCOPE is the same as STEP. In this case the cryogenic aspects are removed by using an electro-static accelerometer. The experiment hopes to achieve an accuracy of nearly $\eta = 10^{-15}$, at room temperature [8]. An orbital altitude of 700 km was chosen in a trade, again between drag and field strength. The eccentricity must be such that the orbit follows one major spectral line of the Earths gravitational field.

The payload contains two accelerometers. One contains two similar masses and the second different units. Properties to considered for MICROSOPE [8] were; geometry, thermal stability, ageing, magnetic stability, electrical properties and out-gassing. Titanium and platinum (forming the three 'similar' masses) were chosen.

The data downlink will need to be able to support the 480 MBit per day data rate. After launch the spacecraft is checked in a safe-mode. The payload is calibrated and then tests of the drag-free control system are performed. Measurements are taken from each accelerometer one after the other, using the non-experimental accelerometer for attitude and disturbance rejection.
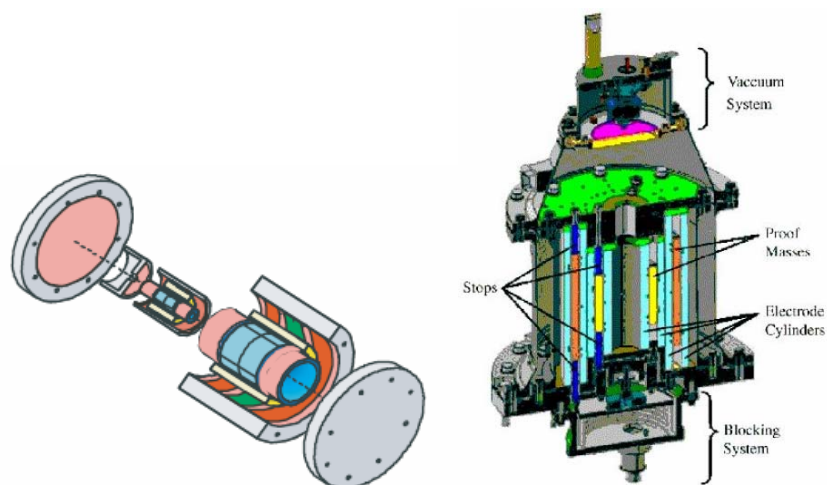
Figure 2.12 – Exploded View of the Microscope Accelerometer (left) and an Internal Schematic (right)

A representation of the DA is shown in Figure 2.12. A set of electrodes provide a radial and axial symmetry all around the test masses. Motion is sensed by capacitance. Applying a voltage to the

electrodes maintains the test mass at null (in an accelerometer mode). Mass movement will change the field and a different voltage will need to be applied to maintain the null position. The voltage is linked to the electrostatic field, giving a measure of force. The differences in these accelerations (or the electrostatic forces) of the two accelerometers may show an WEP violation. The sum of the acceleration in all degrees of freedom will provide the necessary signal for the AOCS sub-system. The electronic architecture for one Degree of Freedom (DoF) is shown in Figure 2.13. MICROSCOPE differs from STEP in that the differential measurement is determined through post-processing rather than directly by the SQUIDs.
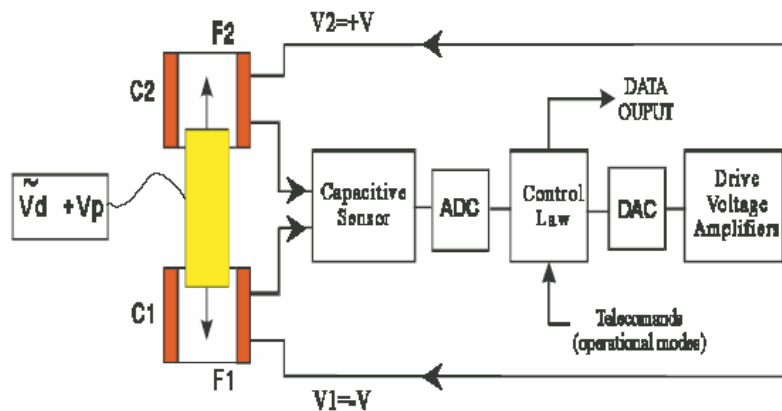
Figure 2.13 – Functional Block Diagram for One DoF of Microscopes Differential Accelerometer (DA)

The spacecraft itself is a small satellite that is envisioned to be launched on an Ariane V accompanying another satellite. In the case of [8] the launch of Helios 2 was targeted. The dimensions are 0.9 m x 0.9 m x 1.3 m and the spacecraft weighs 200 kg. The payload weighs 50 kg and consumes 40 W of power. The fixed solar arrays provide 200W maximum shared with other sub-systems. The data rate is estimated at 1 kbit/s. There are twelve thrusters of which eight are required. The axis of rotation has to be aligned with the sensitive axis of the accelerometers better than 10^{-3} rad [8]. The spacecraft is based on the Myriade line of re-usable spacecraft buses and is shown below.

Figure 2.14 – 3D (left) and Exploded 3D View of the Microscope Spacecraft

2.7.7 LISA Pathfinder

A review of LISA Pathfinder, its science objectives, mission profile, payload and spacecraft are considered in much more detail in Section (8).

2.7.8 OPTIS

OPTIS aims to test SR and GR using optical cavities and an H-Maser atomic clock as a frequency standard. This concept was a mission proposal by Lammerzahl, Dittus, Peters and Schiller [9].

The isotropy of light was tested in the famous Michelson Morley experiment. The OPTIS mission aims to test to verify if light propagates in an identical way when oriented orthogonal. The payload is based on two orthogonal cavity resonators, to which two lasers are locked by the Pound-Drever-Hall (PDH) method.

In addition to the optical resonators a further component is an atomic clock based on Hydrogen transitions to provide an alternative source of frequency. The principle is the same as for the PHARAO clock.
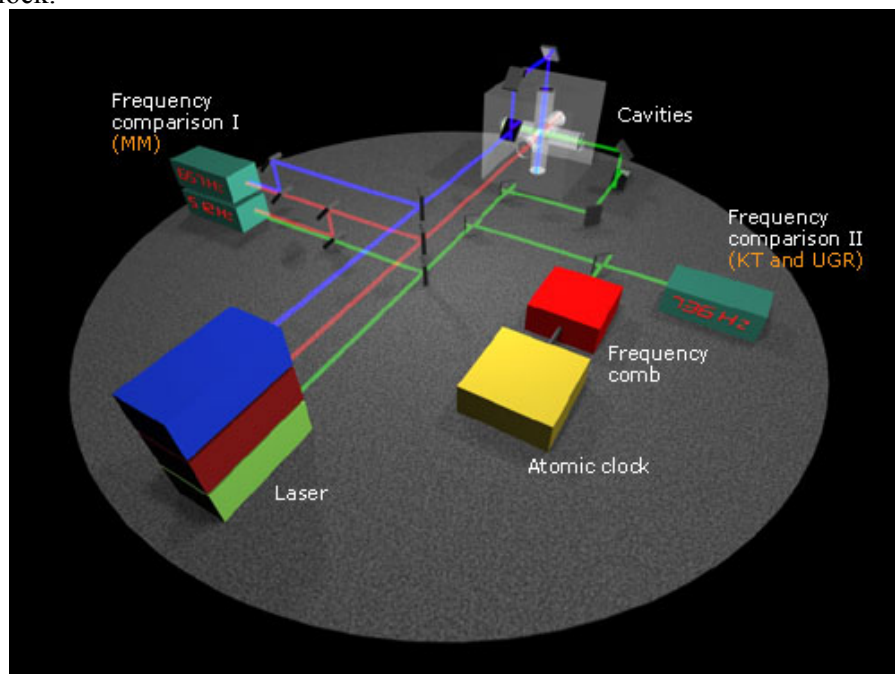
Figure 2.15 – The OPTIS Experiment Concept

The experimental goals are to test the isotropy of light, constancy of the speed of light and the universality of GRS.

- Isotropy (Michelson-Morley (MM) experiment) – Detected by monitoring the speed of light as spacecraft rotates. When one is aligned with the velocity vector there should be no shift. Conversely when perpendicular to the velocity vector there could be a shift. So the light from the cavities is combined there should be a beat. Projected accuracy ($\Delta c/c$) ~ 3 x 10^{-18}.

- Constancy (Kennedy-Thorndike (KT) experiment) – The laser frequency is measured using the comb, which is locked by the hydrogen maser. Projected accuracy ($\Delta c/c$) ~ 10^{-15}.
- Universality if GRS – The hydrogen frequency is compared with the cavity referenced laser using the frequency comb. Projected accuracy ($\Delta c/c$) ~ 10^{-4}.

Frequency combs are explained in more detail in Section (3.4.3).

The spacecraft itself would contain three optical cavities and an H-Maser atomic clock and is of cylindrical shape. Sun pointing is maintained throughout the orbit and thermal protection is provided by a shield. The orbit is highly elliptical and achieved using an Ariane 5 to insert the spacecraft into a GTO of 35 800/280 km apogee/perigee. An on-board small propulsion system would raise the perigee to 10 000km. At the time of the study, which this description follows [9], FEEPS were assumed to be capable of provided drag free attitude control at a minimum height of 10 000 km. The spacecraft would have a mass of 250 kg, the payload 90 kg and consumes 250 W of power [9].

AOCS is consists of FEEP micro thrusters to provide drag free control during experimental periods. Coarse attitude determination is done using gyros and cold gas thrusters in addition to a sun sensor and star tracker. A MICROSCOPE like inertial sensor was to be used for drag free control based upon capacitive sensing to allow the spacecraft to follow its natural traditional path around the Earth, by removing the effects of aerodynamic drag and solar radiation pressure, all in a similar vain to other fundamental physics missions.

2.7.9   Galileo Galilei

Galileo Galilei (GG) is a mission proposed for the verification of the WEP. The specific feature of GG is the measurement approach proposed, with a high spin rate of the spacecraft. The spin rate would modulate the EP violation signal, providing more frequently science data [36].

If the spacecraft is inertial pointing and three-axis stabilised the WEP violation appears modulated to the orbital rate to an order of 10^{-4} Hz. In the case of GG, this force rotates at 2 Hz. The advantage of this is that low frequency noise is reduced significantly from both mechanical and electrical sources. Thermal noise is reduced by making the test masses larger than STEP (0.244 kg the largest) weighing 10 kg. This is from the proportionality $(T/m)^{1/2}$, where T is temperature in K and m is the mass of the test mass. The same thermal noise results for a test mass of 10 kg at 300 K as for a 0.1 kg mass at 3K. The test masses are cylindrical consisting of one inside an outer test mass.

FEEPS are used for Drag Free Attitude Control System (DFACS) as the order of local aerodynamic drag at the altitude of the GG spacecraft (low Earth equatorial) is 8 orders of magnitude larger than the expected WEP violation signal, although this is from the Phase A study [10]. The present status is to have a Sun-Synchronous Orbit (SSO) with a LISA PF like 'hat' solar array [11]. This should be considered as an option.
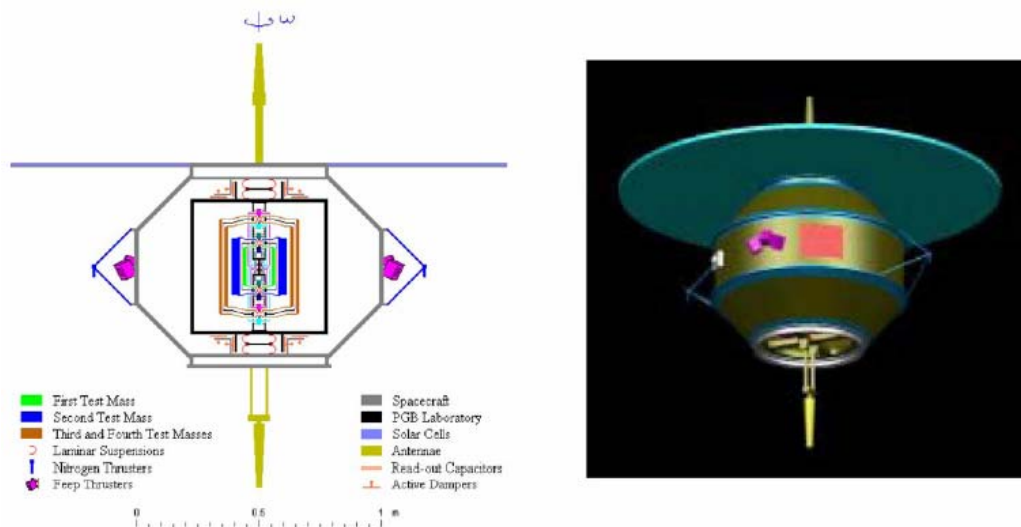
Figure 2.16 – The GG Mission Concept

A capacitive plate is placed between the two concentric cylinders. Motion towards one and away from another, causes a change in voltage across the capacitor. As the spacecraft spins perpendicular to the orbit plane one test mass will be displaced relative to the other if the WEP is violated. The displacement is detected by a change in the common capacitive plate. The signal detection and measurement is similar to the technique employed by MICROSCOPE.

The challenge of GG is the maintenance of drag-free control while spinning at 2 Hz. This is implemented by monitoring the spin rate of the spacecraft using an Earth sensor. Each thruster is timed to fire at the appropriate time to remove residual accelerations. Communications will be implemented using two omni-directional antennas directed as shown in Figure 2.16. The thrusters used for attitude control could be FEEPs for science operations and there is an additional cold gas system for spinning the spacecraft in preparation for these science ops. Power is provided by the solar array and in addition to this, there is a battery capable of providing power for one hour.

The payload has a mass of 105 kg [10] although this may have changed due to newer literature being available. Reference [10] is shown as this provided the most detailed information. The service module has a mass of 146 kg of which 2.2 kg is allocated for propellant for cold gas thrusters. A system margin is added bringing the total mass to be launched as 301.8 kg. This reference is dated 1998, but provides the most detailed information.

PART 2

PAYLOAD DEFINITION AND

REQUIREMENTS

3   FPE-A Tests of Special Relativity

3.1   Science Requirements

The science goals for FPE-A are listed in Table 3.1. The detailed requirements and further references can be found in the Sci-RD [TN1].

The goals are combined into three areas, the SR experiments (A1, A2), the GR experiments (A3, A4, A5) and the space to ground tests (A6, A7). The Sci-RD [TN1] should be used as the main science requirements definition in conjunction with this report.

Code	Experiment	Area	Requirements
A1	Light Isotropy	SR	- Two On-Board Clocks (based on cavity resonators) $\Delta v/v \sim 10^{-16} - 10^{-17}$ - System for On-Board Comparison - Allen Variance/time of 10% for integration times (τ) of 1 to 1000s - Satellite spinning w.r.t. its velocity vector
A2	Constant Light Velocity	SR	- One On-Board Clock (based on cavity resonators) $\Delta v/v \sim 10^{-16} - 10^{-17}$ - System for On-Board Measurement - Allen Variance/time of 10% for integration times of 1 to 10000s or comparison
A3	Absolute Gravitational Red-Shift	GR	- One On-Board Optical Atomic Clock $\Delta v/v \sim 10^{-15} \tau^{-1/2}$ for τ of 1s to 10^5s - Accuracy of 10^{-18} - Space to ground link not degrading the space clock's performance - Space-ground clock comparison not de-grading the space clock performance - Ground clocks performance comparable to the space clock - Allen Variance/time of 20% for relativistic corrections from orbit determination, of τ 1 to 10^5s - Bias of clock position determination should be better than $\sqrt{20\%(clockaccuracy)^2}$ for relativistic corrections - Bias of g-potential and velocity determination should be lower than $\sqrt{10\%(clockaccuracy)^2}$ for relativistic corrections - Ground clock monitored by another ultra-stable clock for common view comparisons. This number should be maximised 10 measurement sessions of 10 days are required

A4	Universality of the Gravitational Red-Shift	GR	• Two On-Board Optical Atomic Clock • $\Delta v/v \sim 10^{-15} \tau^{-1/2}$ for τ of 1s to 10^5s • Accuracy of 10^{-18} • System for On-Board Comparison • Allen Variance/time of 10% for integration times of 1 to 10000s for comparison • 10 measurement sessions of 10 days are required
A5	α time dependence	FDC	• One On-Board Optical Atomic Clock • $\Delta v/v \sim 10^{-15} \tau^{-1/2}$ for τ of 1s to 10 days • Accuracy of 10^{-18} • Space to ground link not degrading the space clock's performance • Space-ground clock comparison not de-grading the space clock performance • Ground clocks performance comparable to the space clock • Allen Variance/time of 20% for relativistic corrections from orbit determination, of τ 1 to 10 days • Bias of clock position determination should be better than $\sqrt{20\%(clockaccuracy)^2}$ for relativistic corrections • Bias of g-potential and velocity determination should be lower than $\sqrt{10\%(clockaccuracy)^2}$ for relativistic corrections • Four ground clocks for comparisons. This number should be maximised, two simultaneously • 10 measurement sessions of 10 days are required
A6	Ground Link Light Velocity	SR	• One On-Board Optical Atomic Clock • $\Delta v/v \sim 10^{-15} \tau^{-1/2}$ for τ of 1s to 10^5s • Space to ground link not degrading the space clock's performance • Ground clocks performance comparable to the space clock • Allen Variance/time of 20% for relativistic corrections from orbit determination, of τ 1 to 10^5s • Ground clock monitored by another ultra-stable clock for common view comparisons. This number should be maximised
A7	Ground Link Time Dilation	GR	• One On-Board Optical Atomic Clock • $\Delta v/v \sim 10^{-15} \tau^{-1/2}$ for τ of 1s to 10 days • Space to ground link not degrading the space clock's performance • Ground clocks performance comparable to the space clock • Allen Variance/time of 20% for relativistic corrections from orbit determination, of τ 1 to 10 days • Ground clock monitored by another ultra-stable clock for common view comparisons. This number should be maximised • 10 measurement sessions of 10 days are required

Table 3.1 – Science Requirements for FPE-A
Note: $\Delta v/v$ is the fractional frequency instability and τ is the integration time.

Clearly there are some different configurations that would achieve the scientific goals. The options are discussed in the next section.

The key aspects of a potential payload are:
- High accuracy clock, one that is based upon an atomic transition at optical frequencies.
- Frequency comb for measuring optical frequency
- Highly stable cavity resonator serving as a method of stabilising a laser.
- Comparison system, either by beating cavity and clock lasers together directly or using a frequency comb.
- Highly stable Microwave Link for space to ground clock comparison
- Appropriate Front End Electronics (FEE) and Back End Electronics (BEE)

3.2   Key Payload Elements

3.2.1   Introduction

The basic hardware forming the 'building blocks' of a payload to test SR and GR, is discussed including the physical principles. Particular emphasis is given to Fabry-Perot Optical Resonators (ORs), Optical Atomic Clocks (OAC) and the frequency comb necessary to measure frequencies in the 100 THz range. A trade to decide the best configuration of these can be found in Section (3.3).

3.2.2   Cavity Resonators

A standing wave can be formed between two dielectric coated mirrors with a very high finesse (~100000) achieving near perfect reflection. This forms the basis of an Optical Cavity or Optical Resonator (OR). One specific type of cavity is the Fabry-Perot. Only a finite number of wavelengths can exist within the cavity. A possible implementation is shown using a functional diagram in Figure 3.1.

The principle of a Fabry-Perot can be described as a beam of light that is sent into the space between mirrors. The light inside the cavity is reflected back from one mirror to the other and back again. As the waves travel along the cavity they are subject to interference by the counter propagating radiation or light in this case. When any wave interferes it is subject to destructive and constructive interference. When constructive interference is at its maximum, resonance occurs. If part of the light beam is then allowed to pass into a detector (a photo diode for example), the intensity can be monitored. Clearly the maximum intensity corresponds to when all waves within the cavity are in phase and constructively interfering. This point is also known as the resonance of the cavity. Therefore there is a corresponding characteristic wavelength for length of cavity and thus frequency from $\upsilon = c / \lambda$. The Pound-Drever-Hall (PDH) method is used to stabilise the laser on the cavity [22].
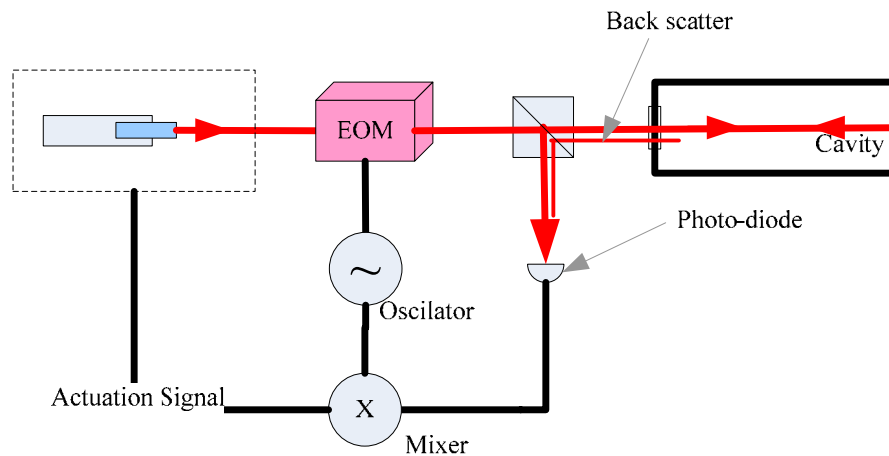
Figure 3.1 – Pound-Drever-Hall method of locking a laser to an Optical Cavity (Fabry-Perot)

A drift away from the resonance frequency of the laser light can be caused by many external effects. The construction of components the motion of optics due to thermal and vibrational variations electrical noise from the laser's power supply or a violation of special relativity which we want to detect.

An important factor to consider is the effect of the environment of the cavity. Noise on the cavity can come from many sources. These drifts will cause the error signal for the feedback loop controller. Areas of particular concern are thermal variations in the local environment which occur over low frequencies. The laser will only be as stable as the cavity's fractional frequency instability.

3.2.3   Optical Atomic Clocks

The principle of an Optical Atomic Clock (OAC) is similar to the principle of the OR or any clock for that matter. The frequency of a laser is locked/stabilised to a physical phenomenon that is unique and regular. Like in the case of a standard H-Maser or Caesium fountain an atomic transition can be probed. An introductory article can be found in [39] and an excellent review is presented in [23].

An optical clock aims to provide a frequency standard at a much greater level of accuracy compared with a microwave clock (Caesium, H-Maser). The increase in accuracy is gained by going to a much higher frequency band, the 400-700 THz band. If the frequency standard is say, for argument, 1 GHz, we would make a count after 10^9 cycles are detected adding a second to our count register. If 10 errors are made every second, i.e. 10 cycles are missed, the clock will begin to drift and 10^{-8} seconds will be lost every second. If the same number errors are made in the THz domain, in this case defining one second as 1 THz, 10^{-11} seconds are lost each second. Therefore if we increase the frequency band to a higher one, we improve the stability of our clock. Microwave clocks are in the 10^9 Hz frequency band, when we shift up to 10^{15} Hz (100s of THz) we arrive in the optical band, pushing towards the Ultra Violet (UV).

A description of the concept of an optical clock follows below. A schematic of a possible implementation is shown in Figure 3.2. The key components are an oven and atomic source, an Ultra High Vacuum (UHV) chamber, laser system and control electronics.

An atomic source is cooled so it is extremely stable with only small amounts of kinetic energy. The atom (s) or ion can then be trapped. The manipulation of the atoms/ion is very dependant on the species and transition chosen (further detail in Section (3.4.2)).
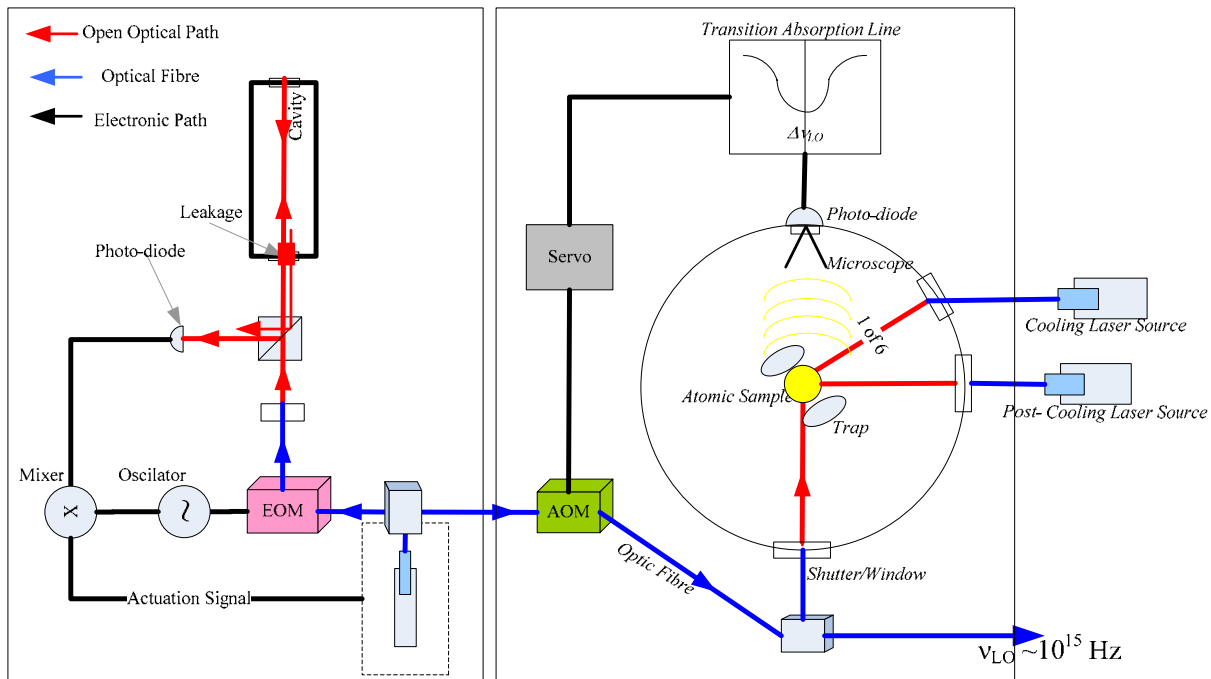
Figure 3.2– Concept of an Optical Atomic Clock

A probe laser with a very narrow line width is shone on the atomic sample. When an incident photon is absorbed the ion or atom moves up to a higher hyper-fine energy level. If the laser is tuned to a specific frequency the ion can be exited to the level of the clock transition, v_{cl}. This maximum corresponds to a corresponding maximum absorption. If the probe laser is periodically shone on the ion or atomic cloud its fluorescence can be monitored. If this is not at optimum levels (in the case of a single ion when at a minimum), the laser frequency has drifted. This error forms the feedback signal in the control loop which acts on the probe laser frequency by means of a servo driven Acoustic Optical Modulator (AOM). The probe laser can then be thought of as a Local Oscillator (LO), which is used as a reference of time.

Hence, we are locking the laser to an extremely stable reference. The laser frequency is then measured or cycles counted to give a time reference. The optical frequencies are modified as a result of the error signal driven for example.

In addition to the feedback loop controlling the frequency of the laser, there is another loop which locks the laser to a cavity providing a stable enough laser to begin the probing. These transitions

occur over a very small bandwidth, so the laser must be of a similar line width. The method of stabilisation to the cavity is the same mould as described in Section (3.2.2) for the Fabry-Perot locked laser using PDH stabilisation and provides short term stability for the laser while the atomic transition provides the long term.

The challenge of this system is in counting the cycles of locked laser light of the Local Oscillator/Probe Laser. For this a frequency comb is used. Early work is presented in [24] with one of the latest experiments describing an Hg^+ OAC in [25].

3.2.4   The Frequency Comb

Standard electronic hardware is incapable of measuring the frequency of EM radiation much beyond a GHz. A method has been devised with which to 'down convert' the THz optical frequencies for counting in regular electronics and absolute measurement of an optical frequency reference. A comb forms an important part of modern optical metrology, especially in optical clocks, so a brief explanation is repeated here and can also be found extensively in literature. A good introduction can be reviewed in [26].

The frequency comb makes use of a pulsed laser.
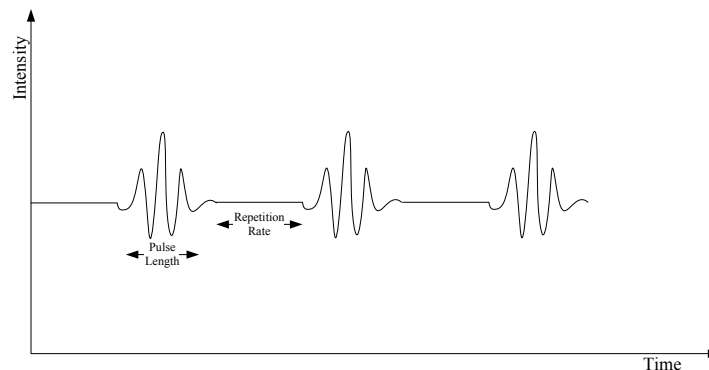
Figure 3.3 – Example of a mode-locked laser wave train
Note that the pulse and repetition rate are not to scale

The length of the pulse is in the femto-second domain and the repetition rate v_{rep} can be in the GHz domain. If we now look at the pulse in the frequency domain, the result would be like Figure 3.4. It can be seen that the components of the pulse form evenly spaced lines which are commonly called the teeth of the comb. The spacing between each tooth is equal to the repetition rate of the pulsed laser, v_{rep}. The faster the repetition rate of the pulsed laser the closer the teeth are together. Also, the smaller the pulse width itself, the larger the frequency band the entire comb encompasses ($f = 1/T$).
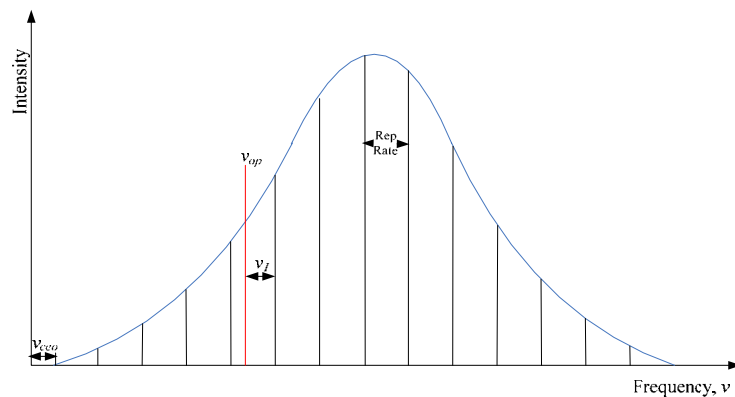
Figure 3.4 – Mode-Locked Pulsed Laser as Seen in the Frequency Domain (adapted from [26])

Although the spacing between comb lines is the same, the spacing between the hypothetical origin and the first tooth can be slightly off-set, not the same as the comb spacing v_{rep}. This is known as the Carrier Envelope Offset (CEO) or v_{ceo}. Keeping this constant prevents the entire comb from moving laterally in frequency space.

The key to the frequency comb is to stabilise both the repetition rate v_{rep} and offset v_{ceo} by maintaining the spacing between combs and anchoring the distance of the first tooth from the origin.

In terms of a clock
The repetition rate is controlled such that the interference between a tooth of the comb and the optical reference from the atomic transition line is constructive and maximum in intensity. A deviation from this maximum reduces intensity measured in the photo-diode and forms an error signal. To change the repetition rate so that constructive interference is at a maximum a mirror is moved using a piezoelectric actuator altering the delay between pulses. The adjustment in delay changes the repetition rate which would change the spacing of the teeth expanding or contracting the comb. The adjustment would be continual so that a tooth coincides with the very stable optical reference line and is now locked. The repetition rate can then be counted as it is in the GHz domain.

In terms of absolute frequency measurement
Another important process is the one that actually measures or determines the optical frequency of some source. In this case the goal is not to move the comb so it locks to the stable optical frequency but to use the comb as a ruler. This of course means that the comb must be stabilised independently of the optical frequency to be measured. The repetition rate can be locked to a highly stable oscillator, perhaps a cavity, H-Maser or in the case of [25] the NIST Caesium standard.

The unknown optical frequency reference is:

$$v_{op} = v_{ceo} + n v_{rep} + v_b$$

3.1

Where v_{op} is the optical frequency to be measured, v_{rep} is the pulse laser repetition rate and v_b is the beat between v_{op} and a tooth of the comb. The value n can be determined by a wavemeter. The second unknown that remains is the off-set, v_{ceo}. The solution to determine this off-set is to combine

a spectrally broadened version and a frequency doubled version of the comb. This was the breakthrough that drove forward the implementation of a comb as a tool for frequency measurement. The pulsed laser is broadened by using a micro fibre structure. This is then compared with the doubled frequency by generating a beat frequency. Figure 3.4 shows v_{ceo}.

Consider v_n as the frequency of an nth tooth of the comb, following Figure 3.4, it can be said to be,

$$v_n = n v_{rep} + v_{ceo}$$

3.2

Where v_{rep} is the repetition rate of the comb pulses. The broadened comb would be (in the micro fibre),

$$v_{2n} = 2n v_{rep} + v_{ceo}$$

3.3

If then Equation 3.3 is frequency doubled comb (multiplied by two) would be,

$$2v_n = 2n v_{rep} + 2v_{ceo}$$

3.4

Clearly if we combined Equations 3.3 and 3.4 we have an expression for v_{ceo},

$$v_{ceo} = 2v_n - v_{2n}$$

3.5

This is the beat between the broadened and frequency doubled comb, which is detectable with a fast photodiode.

The accuracy of the absolute frequency measurement is dependant on the stability of the repetition rate and v_{ceo}. Both values are monitored and the feedback system maintains a level of stability hence the need for some reference.

Possible FPE-A Payload Frequency Comb Concept
Shown in Figure 3.5 is a possible functional design of a comb that can be locked to the OAC. Both CEO v_{ceo} and repetition rate v_{rep} need to be stabilised. Rather than using an independent reference (e.g., an H-Maser) the LO of the OAC can be used. Recall that the goal is not necessarily a measurement of the transition line in the clock, but a stable GHz frequency which can be achieved by locking the comb to the LO.

The movable mirror adjusts the repetition rate based upon the beat between a tooth and the optical reference line. The CEO is maintained adjusting the power of the pump laser based upon beat between the doubled and broadened comb light.

$$\nu_{LO} \sim 10^{15}\,\text{Hz}$$

Optic Fibre

Movable Mirror

Mode-Locked fs Laser

PZT

Fibre couplers

Servo

Pump Laser

x 2

Broadening Microfibre

Servo

$$\nu_{rep} \sim 10^{12}\,\text{Hz}$$

Servo

$$\nu_{CEO}$$
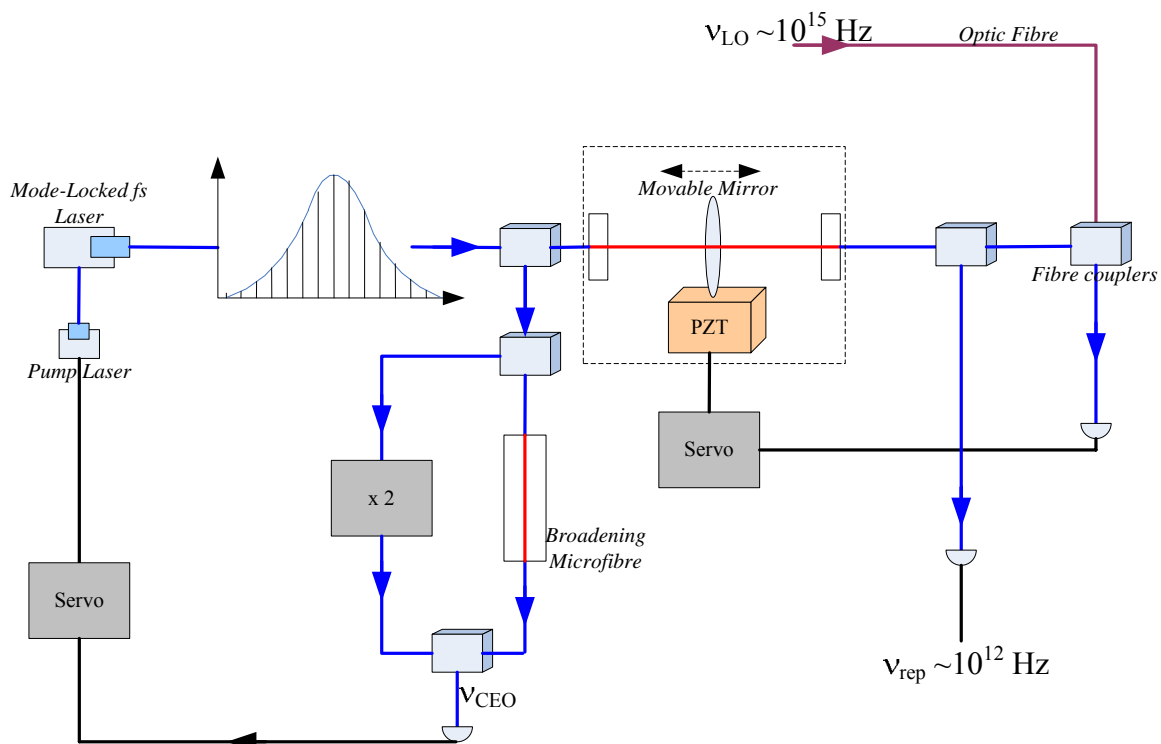
Figure 3.5 – Frequency Comb functional diagram for FPE-A (based upon [23])

3.3 Payload Concept Trade Study

The purpose of this Section is to serve as a reference regarding the selection of possible instrument elements discussed in Section (3.2). A final choice is made, which will form the base of the instrument description allowing the estimate of payload mass, power, data and envelope requirements from these elements. The basis of the trade is between the science requirements and the resulting complexity.

Measure of achievable science:
- The instrument achieves a science objective fully, (1) point
- The instrument partially achieves a science goal, (½) points
- The instrument provides a poor return which is not worthwhile pursuing (¼) points,

It should be noted that the science return is better the more stable the frequency reference is. OACs will naturally have better stability over longer time intervals.

Measure of hardware complexity:
- OAC is given 2 points for complexity (more complex sub-system compared with an OR).
- OR is given 1 point for complexity
- Frequency Comb is given 1 point for complexity

- Independent frequency reference is given ½ a point, which is not of an optical nature a H-Maser for example.

T/F link score is given as the total number of experiments requiring a Time/Frequency (T/F) link. As in the case of the achievable science, the better results (based on a better frequency standard) are given 1 point and the more average data 0.5 points, lower accuracy science measurements relaxing the link requirements (less demands on hardware design and resource requirements).

The combined hardware complexity and T/F are considered implementation penalties.

A ratio is given to compare the achieved science goals with the complexity of implementation which is quoted as **Science Achievable to Implementation Penalties Ratio (SA/IP).** Clearly greater complexity reduces the ratio and larger science return increases the ratio. The smaller the ratio the more optimal the instrument is considered to be.

The results of the trade are shown in Table 3.2. Drag free control requirements are stated. In most cases the level of vibrational control is required to be quasi-still. Each concept is measured against the other using a science goal/Implementation (SA/PI) ratio. The larger numbers serve as a better optimised science to complexity trade.

Any choice not including an OAC is not desirable. It is impossible to justify a flight of solely ORs. One notable benefit of a single clock is the increased science return compared with implementation, although any measurements relating to special relativity are not possible. The clock must be characterised using a ground link. The number of achievable science goals is increased at a cost of further instrument complexity. Two OAC's should not be ruled out as this combination could be accommodated in further iterations, as all science goals can be achieved.

Two ORs can be configured orthogonally. This will allow instantaneous measurements of the isotropy of light rather than relying on the spacecraft to rotate to create angle between the velocity vector and the direction of propagation. The potential anisotropy would vary at the frequency of the orbit period requiring the cavity to be stable for that length of time.

The choice is option 6 consisting of one OAC and two orthogonal OR's. Although a single OR and OAC achieve a better ratio, there is more flexibility with Option 6. More science is performed spanning both SR and GR. Two OAC's may be over complex and the additional OAC could be introduced if there are enough margins on the payload.

Important note:
It should be noted that Option 6, chosen in order to assess the payload resources, does not represent a final selected configuration, but rather an assumption to conduct a sizing exercise. Option 6 is good from this stand point, also as it includes all the main components. If a different concept were selected, an extrapolation based on this configuration would allow an assessment of new payload concepts.

	Option	Achievable Science (AS)	Space to Ground T/F Synchronisation Required	IP	AS/IP	P/L vs Orbit Orientation	Preferred Orbit	Drag Free Control
4	1 x OAC 1 x OR 1 x Frequency Comb	A1- c-Isotropy (0.5) A2 - c-Constancy (1) A3 - Absolute G-RS (1) A4 – Universality of G-RS (0.5) A5 - Time Dependence of $\alpha^\#$ (1) A6 - Space-to-Ground (S-G) c (1) A7 - S-G Time Dilation (P_{KT}/P_{MM}) (1) **Total : 6**	A3 A5 A6 A7 **Total: 4**	8.0	0.75	Not specific other than to control thermal variations and maintain power	Elliptical for G-RS Others have no dependence.	Yes - - Stability of OR structure - Reduce atomic vibrations which would lead to kinetic energy.
6	1 x OAC 2 x OR 1 x Frequency Comb	A1- c-Isotropy (1) A2 - c-Constancy (1) A3 - Absolute G-RS (1) A4 – Universality of G-RS (0.5) A5 - Time Dependence of $\alpha^\#$ (1) A6 - Space-to-Ground (S-G) c (1) A7 - S-G Time Dilation (P_{KT}/P_{MM}) (1) **Total : 6.5**	A3 A5 A6 A7 **Total :4**	9.0	0.72	Not specific other than to control thermal variations and maintain power	Elliptical for G-RS Others have no dependence.	Yes - - Stability of OR structure - Reduce atomic vibrations which would lead to kinetic energy.
7	2 x OAC 2 x OR 2 x Frequency Comb	A1- c-Isotropy (1) A2 - c-Constancy (1) A3 - Absolute G-RS (1) A4 – Universality of G-RS (1) A5 - Time Dependence of $\alpha^\#$ (1) A6 - Space-to-Ground (S-G) c (1) A7 - S-G Time Dilation (P_{KT}/P_{MM}) (1) **Total : 7**	A3 A5 A6 A7 **Total: 4**	12.0	0.58	Not specific other than to control thermal variations and maintain power	Elliptical for G-RS Others have no dependence.	Yes - - Stability of OR structure - Reduce atomic vibrations which would lead to kinetic energy.
3	1 x Optical Atomic Clock 1 x Frequency Comb	A3 - Absolute G-RS (1) A5 - Time Dependence of $\alpha^\#$ (1) A6 - Space-to-Ground (S-G) c (1) A7 - S-G Time Dilation (P_{KT}/P_{MM}) (1) **Total : 4**	A3 A5 A6 A7 **Total :4**	7.0	0.57	Not specific other than to control thermal variations and maintain power	Elliptical – G-RS Others have no dependence.	Yes – Reduce atomic vibrations which would lead to kinetic energy.

				IP	SA			
5	2 x OAC 2 x Frequency Comb	A3 - Absolute G-RS (1) A4 – Universality of G-RS (1) A5 - Time Dependence of $\alpha^{\#}$ (1) A6 - Space-to-Ground (S-G) c (1) A7 - S-G Time Dilation (P_{KT}/P_{MM}) (1) **Total : 5**	A3 A5 A6 A7 **Total: 4**	10.0	0.50	Not specific other than to control thermal variations and maintain power	Elliptical for G-RS Others have no dependence.	Yes - - Reduce atomic vibrations which would lead to kinetic energy.
2	2 x Orthogonal ORs 1 x Frequency Comb 1 x Freq. Ref	A1- c-Isotropy (1) A2 - c-Constancy (0.5) A3 - Absolute Red-Shift (G-RS) (0.25) **Total : 1.75**	A3 **Total: 0.5**	4.0	0.44	Not specific other than to control thermal variations and maintain power	Elliptical for G-RS Others have no dependence.	Yes – stability of OR structure
1	1 x Optical Resonator (OR) 1 x Frequency Comb 1 x Freq. Ref	A1- c-Isotropy (0.5) A2 - c-Constancy (0.5) A3 - Absolute Red-Shift (G-RS) (0.25) **Total : 1.25**	A3 **Total: 0.5**	3.0	0.42	Not specific other than to control thermal variations and maintain power	Elliptical for G-RS	Yes – stability of OR structure

Table 3.2 - Summary of the concept trade-off
Note that IP = Implementation Penalty and SA is Achievable Science. The shaded row is the chosen payload.

3.4 Payload Definition

3.4.1 Functional Architecture
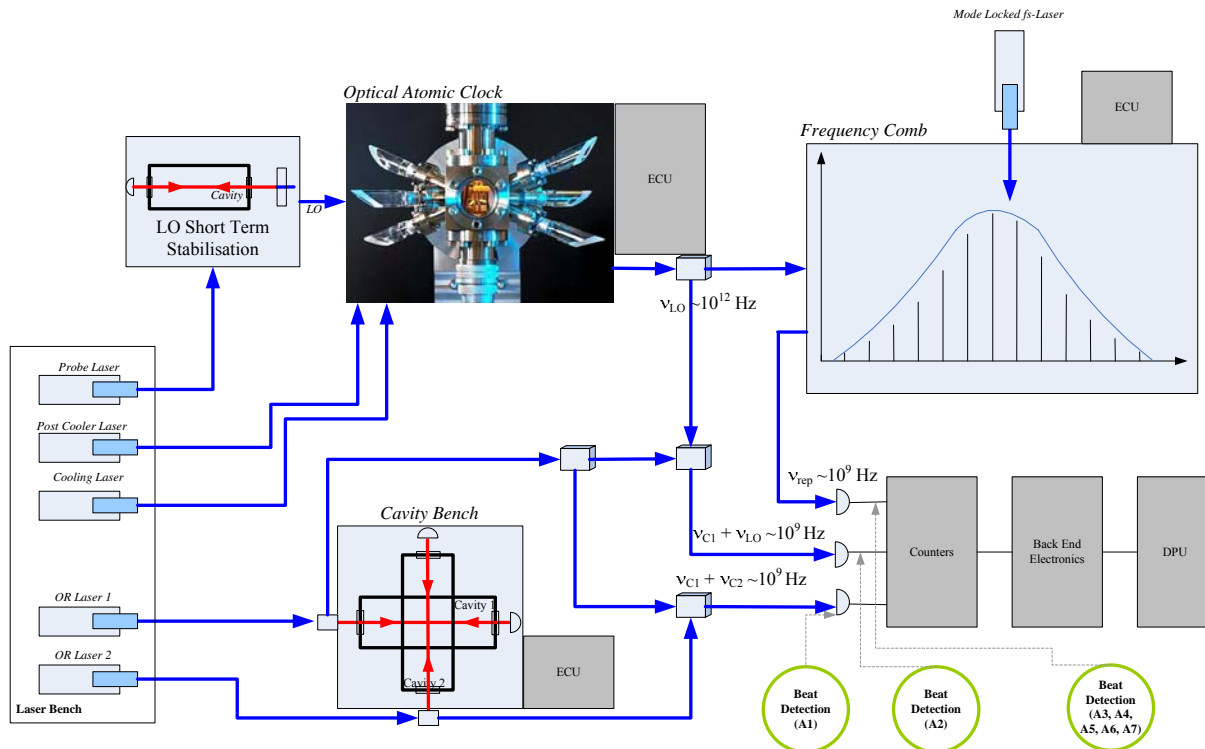
Figure 3.6 – FPE-A Payload Functional Block Diagram
Consisting of a Optical Atomic Clock (OAC), two crosses Optical Resonators (OR), Electronic Control Units (ECU),
Counters, a Laser Bench and a Data Processing Unit (DPU)

As seen in Section (3.3) the concept for the FPE-A Payload (P/L) has been selected to be a single Optical Atomic Clock and two orthogonal cavity resonators. The payload concept functional diagram is shown in Figure 3.6. The P/L can be considered to be five sub-systems:

1) The Optical Atomic Clock (OAC), Section (3.4.2)
2) The Optical Resonator Bench (ORB) and associated lasers, Section (3.4.4)
3) The Frequency Comb (FC), Section (3.4.3)
4) A Laser Bench (LB), Section (3.4.5)
5) Global components for comparison of the frequencies, read-out electronics and DPU.

Each has a local Electronic Control Unit (ECU), Power Control and Distribution Unit (PCDU) and Front End Electronics (FEE) (for the analogue aspects of the feedback loops). The P/L DPU and P/L PCDU control each local ECU and each PCDU centrally respectively. The LB does not require control electronics as actuation signals would come from the locking feedback electronics or clock cycle control.

An alternative design could allow the comb to act as the frequency comparator for the cavities.

3.4.2   The Optical Atomic Clock

The Atomic Reference Transition (s)

The clock will use a single ion transition in an end cap Trap or Magneto Optical Trap. The choice can be left open until the detailed design is considered.

A single ion is selected as the implementation of a neutral atom trap is more complex and less mature in its design. The Signal to Noise Ratio (SNR) may be better, as more atoms are available for probing, but containing them requires an optical lattice. This would require a more complex laser bench. These differences are discussed by [TN1] and [23]. [TN1] states that 10^{-18} fractional frequency instability and 10^{-16} for the single ion and neutrals respectively.

Single ions suggested by [TN1] and [23] are Hg^+, Yb^+, In^+, Sr^+, Ca^+ and Al^+. A final choice is required to determine the laser's to be used and hence the optical architecture. However this is not a trivial matter. Recall that the ion is required to cooled and contained in the trap using an optical molass created by the Cooling Lasers. Figure 3.7 illustrate a transition scheme. (1) shows the cooling transition and (2) the clock transition. The ion may fall into a metastable energy level between the initial state and the clock transition state. This is shown at (3). The ion is then re-pumped to another energy level and then decays to the initial level. The re-pumping requires a different frequency and hence another laser. Also what can happen is the ion may fall below the initial state also requiring yet another re-pumping laser and frequency ((4)).
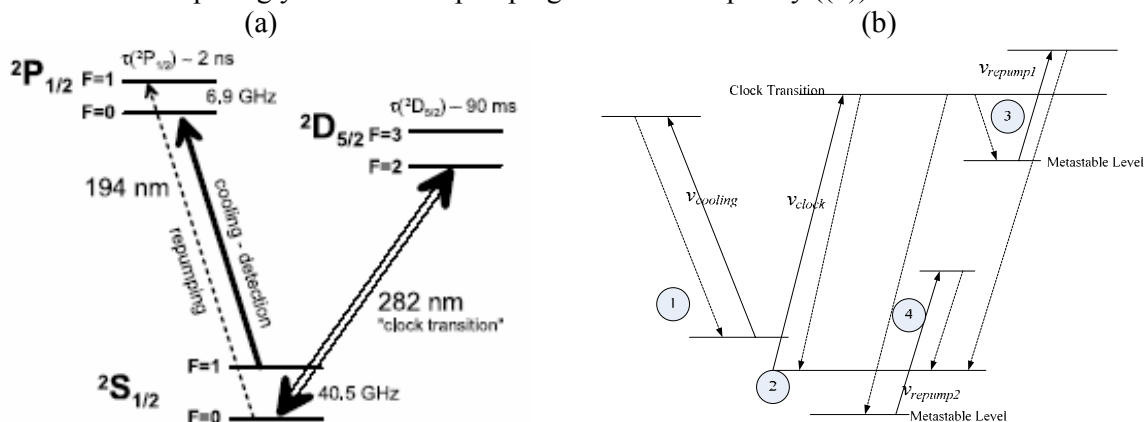
Figure 3.7 - Illustration of a Transition Scheme
(a) Shows the partial scheme of a Mercury Ion (Hg^+) [27] and (b) a schematic representation of the key lasers required

A detailed trade is required weighing the complexity of the transition scheme against the accuracy of the clock and required laser frequency. The choice would be a transition that results in no re-pumping requirements with a wavelength that can be used in fibres while achieving high stabilities. The final selection may be a compromise between these aspects, sacrificing accuracy for the sake of a simpler clock design.

One suggestion would be the Sr^+ ion for its larger wavelength allowing the use of fibres. Hg^+, In^+ and Yb^+ transitions require wavelength of order 236-282 nm. This puts them in the UV. Further consideration has to take into account the laser technology required.
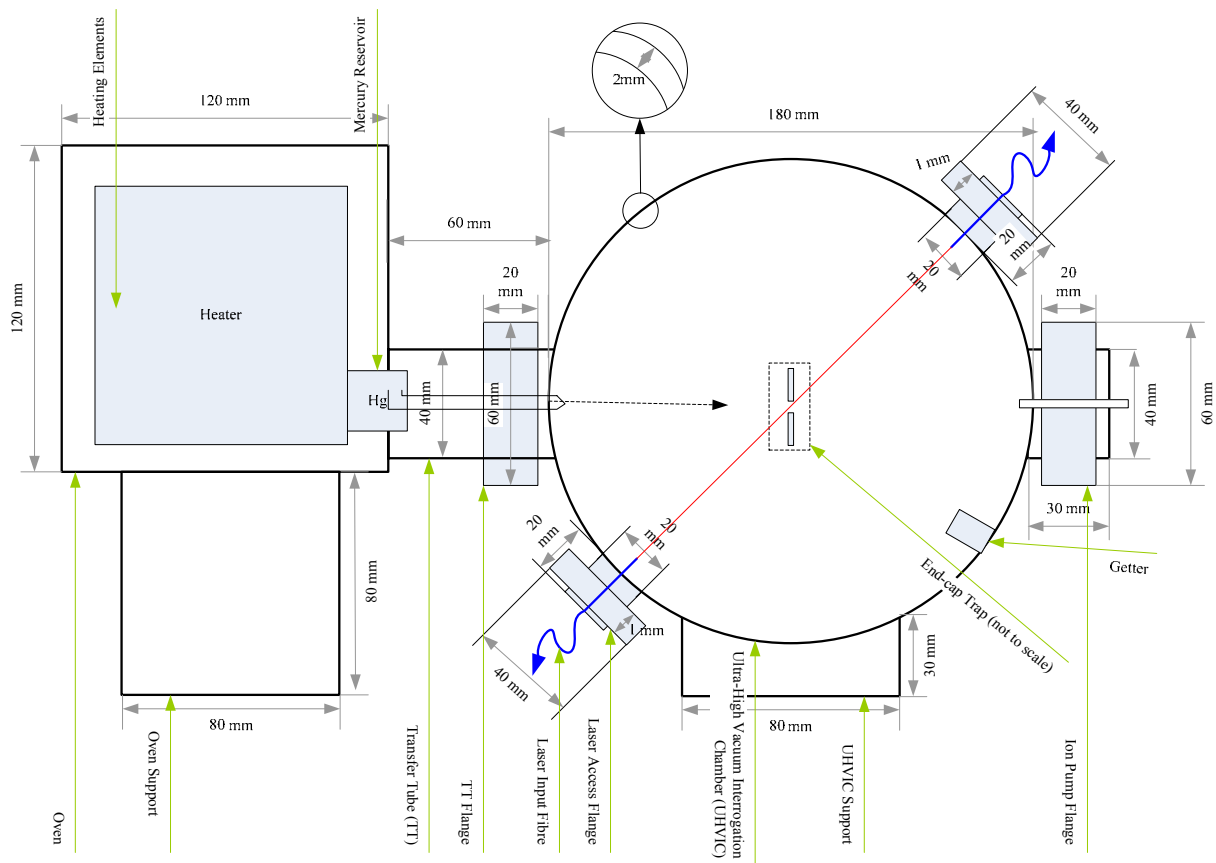
Figure 3.8 – A Schematic for a Possible Implementation of a OAC UHVIC

Ultra High Vacuum Interrogation Chamber (UHVIC) and Oven
Getters and an ion pump provide the required vacuum. The chamber is envisaged to be 2 mm thick stainless steel sphere. Flanges will be positioned allowing the entry of fibres/wires, the microscope/photodiode aperture and the transfer tube into the chamber. Optical fibre is required to transfer the laser light from the cooling laser source, the Local Oscillator (LO) and the Post-Cooler (s) (PC) into the UHVIC. A system of six fibre output emitters will provide each DoF cooling. The LO and PC will have their own emitters.

Any smearing on the windows providing the laser access to the centre of the trap should be minimised preventing attenuation.

Electronics
A photodiode monitors the florescence of the ion for the feedback loop. The ECU also controls the clock cycle. The ECU is in constant contact with the Payload Data Processing Unit (DPU).

Local Oscillator (LO or Probe Laser)
The laser source is stabilised on the short term by a cavity (see Section (3.2.2)). The need for the short term stability is driven by the narrow beam width required to excite the narrow fine energy levels of the ion.

Cooling Lasers
They provide the laser source for reducing the kinetic energy of the atoms ready for probing. The beam is transferred by optical fibre from the source to the flange described above. The beam is split by a 1:6 fibre splitter into 6 parts allowing the control of six degrees of freedom. The source is contained within the LB.

3.4.3   Frequency Comb

The LO of the OAC is used as the reference for the Frequency Comb (FC).

Femtosecond Laser
The stabilised fs-laser is transferred to a fused coupler to be beat with the OAC LO by means of an optical fibre also. The inputs required for self-referencing of the comb are also provided by optical fibre.

Comb Optics
This encompasses the micro fibre and frequency doubling required for the stabilisation of the CEO (Carrier Envelope Offset) and repetition rate using the LO. The micro-fibre structure is mounted on a separate Zerodur bench. The comb optics also include mountings, fixings for the mirrors and fibres. The comb will output a stabilised fs-laser beam that can be used for counting the repetition rate.

Frequency Comb ECU
The feedback electronics are contained within this box to control the frequency comb and provide the actuation signals. A simple low intelligence embedded system is assumed to provide a state of operation to the P/L DPU.

3.4.4   Orthogonal Optical Resonator Bench (ORB)

The cavities and bench are contained within a vacuum chamber (stainless steel) which is surrounded by MLI. An ion pump and getter provide the vacuum. The bench could be made of Zerodur as used by the Lisa Pathfinder due to its excellent thermal stability. The cavities are fused into the bench. This is shown in Figure 3.9

Flanges provide access for the laser and photodiodes. Before entering the ORB, the laser beam is split and sent to be compared. The photodiodes are linked with the ORB ECU to control the feedback loop which actuates the laser (see Section (3.2.2)).
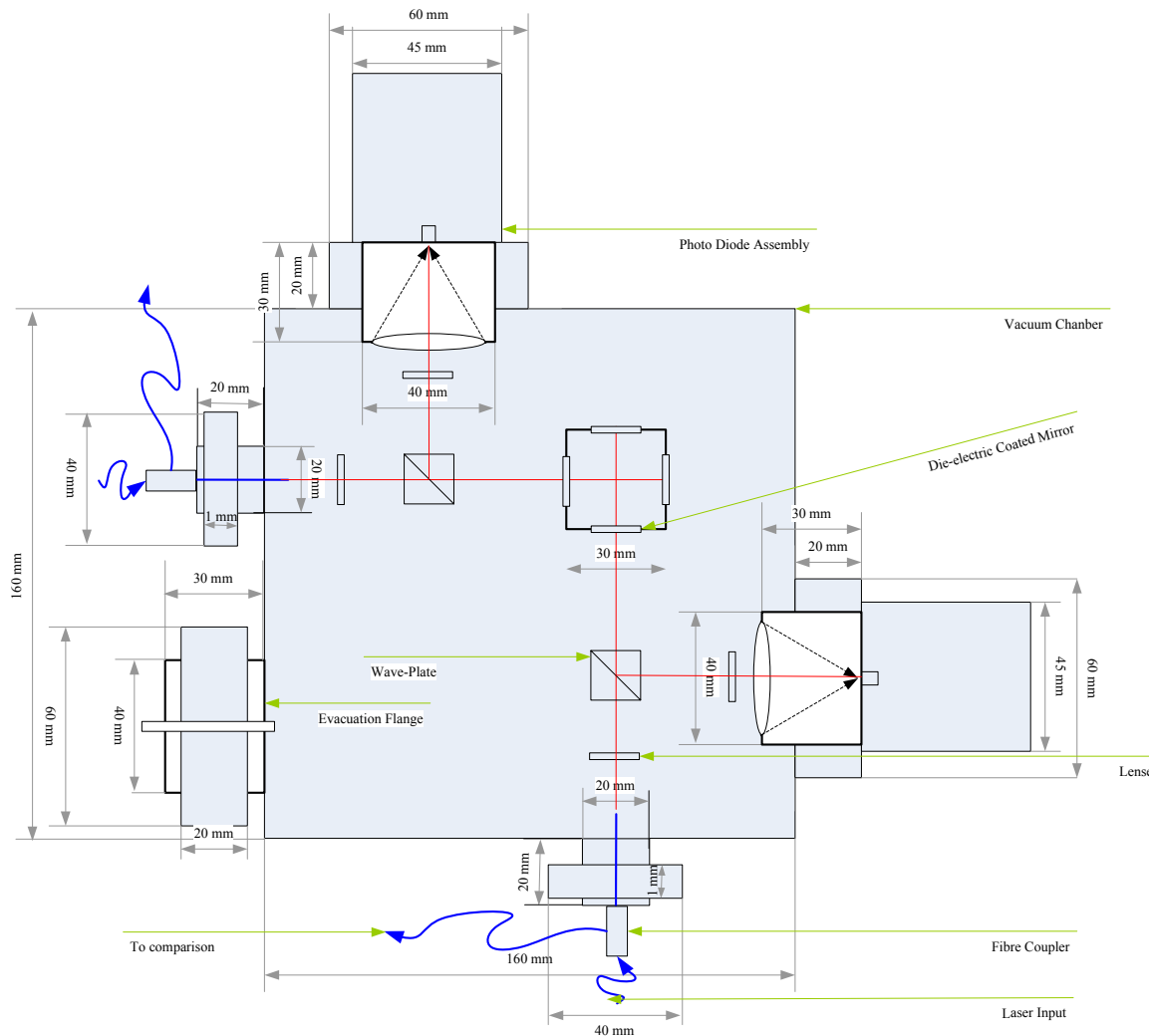
Figure 3.9 – A Schematic for a Possible Optical Resonator Bench Implementation

3.4.5   Laser Bench

The laser bench consists of five lasers. The probe laser (which becomes the LO after stabilisation on the atomic transition), the post cooler unit, cooling laser source and two laser for stabilising on the cavities. The sixth laser is the femtosecond laser for the frequency comb. This comes as part of the comb package as direct actuation of the pump laser power is required, so should be treated as part of the Frequency Comb.

At this point the laser frequency and type has not yet been selected. This depends on the choice of transition in the OAC. This will drive the choice of the cavity and probe laser as they want to be of similar frequency allowing the beat between them two to be within the GHz domain. Without confirmation of the wavelength required the type and mass of the lasers is still open, therefore an appropriate margin is applied.

3.4.6 Payload Control Electronics

Data handling and control is implemented using a central Payload Data Processing Unit (DPU) and its subsidiaries the ECUs. The DPU controls the ECUs in a hierarchal manner enabling it to command and control each individual instrument. The ECUs are control units of limited intelligence that manage the feedback loops, control instrument components and provide status signals for the DPU. The DPU would command the start of operations and the ECU would implement its built in routines to deliver this. This allows a high degree of modularity as each ECU operates independently of another and is commanded centrally. Figure 3.10 shows the interface between the P/L DPU and the ECUs.
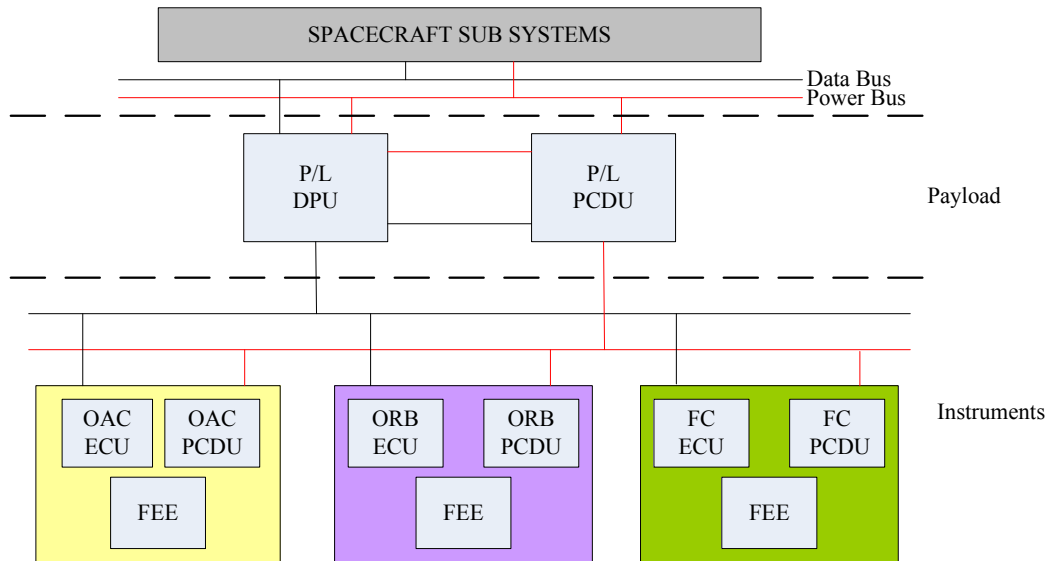
Figure 3.10 – Functional Control and Data Handling Architecture
DPU = Data Processing Unit, OAC = Optical Atomic Clock, ORB = Optical Resonator Bench, FC = Frequency Comb, PCDU = Power and Control Distribution Unit, ECU = Electronic Control Unit, FEE = Front End Electronics

The Data Processing Unit controls the payload in its entirety. It will perform monitoring of the control electronics and status sensors. The DPU will process incoming measurements and transmit them to the OBDH. The DPU also includes and controls the PCDU for the payload, which provides power to the individual instrument PCDUs (Figure 3.10). Also, commanding for start-up will be required from the DPU.

3.5 Space to Ground Requirements

There is the requirement that the OAC in space is compared with one or many ground clocks.

There are two competing methods of direct/real-time comparison of clocks in different positions. The first is Microwave link (MWL) that is baselined for ACES. The other is a laser link (T2L2). The MWL has the advantage of not being affected by weather and attenuation by water or other particles in the atmosphere like the laser link. A further disadvantage of the T2L2 is pointing. The spacecraft must be pointed in the field of view of the receiver within much more stringent requirements than with the MWL. Power amplification would be required bringing heat dissipation requirements into the spacecraft design. The advantage of the T2L2 is that if the laser frequency

were received by the ground directly from the locked Local Oscillator of the Optical Atomic Clock then a direct comparison would be possible. The MWL would first require a down-grading of the optical frequency to Microwave frequencies for transmission. The MWL is chosen for FPE because it is to be implemented on ACES and has less stringent hardware requirements and provide design heritage. Also there is hardware on-board LPF which would be easier to adapt for the MWL frequencies. The architecture of a possible link is outlined in the remaining parts of this section.

The architecture for the ground is a set of local receivers near highly accurate clocks that would (at NIST for example) access the satellite when it came within view. A main ESA ground station would still be used to command the satellite. Svalbard is baselined due to its high altitude. The system would make use of the plans already in place for the ACES mission.

The following issues are key:
- Hardware quality to ensure noise levels not degrading the clock performances (accuracy and stability)
- Reduction of stochastic errors so to recover the clock accuracies and stability
- Thermal noise on receivers and transmitters
- Ground tracking of spacecraft to allow remote station acquisition
- Coordination of ground segment over a large geographical area
- Multipath effects (identified by ACES)
- Near 100 % FoV. The antennas are likely to be fixed and the spacecraft three axis stabilised so, the aspect to the Earth will change.

ACES baselined a K-Band system for clock comparisons. An S-Band system is required to correct for delays in the ionosphere.

It is unlikely that the SNR will be a driver due to the FPE-A orbit being LEO and the data rate being low.

Three scenarios could be considered but are not analysed further:
1. Atomic clocks local to ESA ground stations with experimental results transmitted to the Mission Control Centre (MCC), which maintains full control of the spacecraft.
2. A distributed approach where an institution acquires a ground receiver to compare its own clock with the spacecraft and scheduling is co-ordinated by the MCC, which maintains full control of the spacecraft.
3. A scenario including both 1 and 2 where the first measurements and experiments implemented by ESA institutions and then the system is released to institutional users as an extended mission, still coordinated by ESA.

Note that only Cebreros and Redu-2 provide K-Band receivers. Each individual ground terminal would require its own K-Band receiver [28].

3.6 Payload System Requirements

3.6.1 Accommodation

The envelope of each instrument is shown in Table 3.3.

Item	Envelope (Approx. Cuboid) mm
Optical Atomic Clock (OAC)	410 x 220 x 220
Optical Resonator Bench (ORB)	280 x 280 x 150
Laser Bench (LB)	550 x 330 x 220
Frequency Comb (FC)	600 x 600 x 100
LO Stabilisation Cavity (LOSC)	160 x 100 x 100
Local Control Electronics	TBD
P/L Control Electronics	TBD
P/L Support Structure	n/a
MWL Link	TBD

Table 3.3 – Payload subsystem Envelope requirements

The Configuration of the payload has the following requirements:

- The Laser Bench should be thermally isolated from the other components
- The UHV chambers for the OAC, LO SC and ORB should be mounted vibration free using dampers.
- The thermal transfer to the UHV chambers should not have a thermal instability degrading performance.
- The FC comb laser must also be thermally isolated from the other components of the payload although this should be considered in the flight unit design itself. It will also require vibration free mounts.
- Fibre optics should be free from dimensional changes
- All payload optics require vibrational damping during launch to prevent the movement of aligned optical components
- Any electronics should be thermally isolated from the optic fibres, OAC, LO SC and ORB

The spacecrafts number of moving parts should be minimised, for example, fixed solar arrays, non reaction wheel AOCS system, propellant sloshing in tanks and no slewing antennas. However, these conditions are only required during calibration and experimental phases.

At a high level the thermal expansion (ΔL) of a material (L) caused by a given change in temperature ΔT is,

$$\Delta L = \alpha L \Delta T$$

3.6

where α is the coefficient of linear expansion. α is dependant on temperature in some cases.

The temperature stability over the short term is much more important than the long term. The long term stability is controlled by the ion probing feedback loop. The short term is to provide a stable enough laser for this probing. Therefore the timescale for the Probe Laser is quite short.

In the case of the ORB cavities, a data point is assumed to be taken every 10 minutes so the timescale over which the temperature stability requirements are important is this time (~1.6 mHz).

The value α is dependant on the material selected for the cavities. As an early baseline Zerodur ($\alpha = 0.02$ x10^{-6} K^{-1}) was chosen. This is also the choice of LISA Pathfinder's optical bench.

From Equation 3.6 the **temperature stability requirements** are (assuming $\Delta\nu/\nu = \Delta L/L$):
- Optical Resonator Bench (Experiments A1, A2)
  - $\Delta T = 5 \times 10^{-10}$ **K** 100 Hz ($\Delta\nu/\nu = 10^{-17}$). The frequency is stated so to emphasise that such stability is difficult on the long term. The data-point will be an average of these samples over ten minutes.
- Probe Laser Stabilisation Cavity (PLSC) (Experiments A3-A7)
  - $\Delta T = 5 \times 10^{-8}$ **K** ($\Delta\nu/\nu = 10^{-15}\tau^{-1/2}$ assuming τ as 1 sec for short term instability)

Room temperature (20^0C) is assumed to the ambient temperature hence variations in $\alpha(T)$ are very small.

It should be noted that these requirements are extremely challenging, emphasising the need for measuring at higher frequencies as discussed in Section (3.3).

3.6.2   Mass Budget

Item	Mass w/o Margin (kg)	Margin	Mass w/Margin (kg)
Optical Atomic Clock (OAC)	15.5	20	18.6
LO Stabilisation Cavity	5.4	20	6.4
Optical Resonator Bench (ORB)	10.1	20	12.1
Frequency Comb (FC)	22.4	50	33.6
Laser Bench (LB)	15.0	50	22.5
P/L Control Electronics	10.0	20	12.0
P/L Support Structure	11.6	20	14.1
Environmental Sensors	2.3	20	2.8
MWL Link	8.0	20	9.6
Total	**99.5**		**130.6**

Table 3.4 – Mass Budget for the FPE-A Payload

A more detailed mass budget can be found in the payload description of [TN2].

3.6.3   Power Budget

Item	Average w/o Margin (W)	Margin (%)	Average w/Margin (W)
OAC	64.3	20	77.1
Probe Laser Stabilisation Cavity	1.2	20	1.4
Optical Resonator Bench	8.4	20	10.1
Frequency Comb	14.8	20	17.7
Laser Bench	10.2	20	12.2
Environment Sensors	3.0	20	3.6
P/L Control	34.4	20	41.3
Total	169.3		203.1

Table 3.5 – Power Budget for the FPE-A Payload

A more detailed power budget can be found in the payload description of [TN2].

3.6.4   Data Budget

Data Budget	Size	Units	Sample Rate (Hz)	Rate (bps)	Remarks	
Measurement						
C1-C2 Beat Frequency	44.0	1	0.002	0.1	One measurement every 10mins	
C1-LO Beat Frequency	44.0	1	0.002	0.1	One measurement every 10mins	
TIC Data	44.0	1	1.000	44.0	Continuous transmission of frequency over duration of link	
FC Rep. Rate (Time Record)	44.0	1	0.002	44.0	One measurement every 10mins	
Sub-Total	**176.0**	**4.0**		**88.1**		
Instrument Sensors						
OAC Temp	19.0	5	0.1	9.5	Monitoring, Continuous	
OAC Pressure	33.0	5	0.1	16.5	Monitoring, Continuous	
ORB Temp	19.0	5	0.1	9.5	Monitoring, Continuous	
ORB Pressure	33.0	5	0.1	16.5	Monitoring, Continuous	
LO Stabilisation Cavity Temp	19.0	5	0.1	9.5	Monitoring, Continuous	
LO SC Pressure	33.0	5	0.1	16.5	Monitoring, Continuous	
FC Temp	19.0	5	0.1	9.5	Monitoring, Continuous	
Sub-Total	**175.0**	**35.0**		**87.5**		
Housekeeping Allocation						
20% of Total Data				35.1		
Total w/o Margin				**210.8**		
TOTAL with Margin	**20**	**%**		**252.9**		

Table 3.6 – Data Rate Budget

3.6.5 Drag Free Control Requirements

The main driver of disturbances on the payload is dimensional changes in the cavities that the lasers are locked to. This can be caused by external disturbances.

To quantify the effect on a cavity the following relation relates a residual acceleration, a, to $\Delta L/L$, for a cavity length L,

$$\frac{\Delta L}{L} = \frac{\rho L a}{E}$$

3.7

Where ρ and E are the material density and Young's Modulus respectively. For FPE-A a Zerodur cavity of 3 cm in length is assumed.

The requirements are;
- Minimum thrust 1.1×10^{-9} ms^{-2}, 5.5×10^{-7} N, which has a margin of one order of magnitude. This is justified in the following paragraphs
- Maximum thrust needed is **1.0×10^{-7} ms^{-2}** (which is 6.9×10^{-8} ms^{-2} with a 50% margin); **7.7×10^{-5} N** (which is 5.1×10^{-5} N with a 50% margin). *This requirement is determined by the orbital environment conditions for a 700/3599 km orbit at 105^{0} inclination selected in Section (6.5)*

It should be noted that the requirements of FPE-A are much less stringent than the FPE-B requirements, which require $<10^{-14}$ ms^{-2} Hz$^{-1/2}$. However the effect of the external disturbances in terms of Allen Deviation would require estimation to confirm the level of instability in the clock it would cause. This would also determine if the disturbances need to be compensated for or if FEEP's are required.

4 FPE-B Tests of the Equivalence Principle

4.1 Science Requirements

The principle goals for FPE-B are:
- To measure the Eötvös parameter to the order $\eta = 10^{-17}$.
- Compare at least two free-falling bodies of different material, density and shape to an accuracy of $\eta = 10^{-17}$. More test body variations are desirable to augment the baseline test, but scope will be limited by available spacecraft and/or technical readiness.

4.2 Payload Summary

The FPE-B payload can be split into four parts. The first contains two Differential Accelerometers (DA). The second part is the cryostat, which contains them and their casing. The third includes the electronics, which are not situated in the cryostat and finally the fourth segment, which is the drag free, calibration positioning system, and charge management control units.

The use of a common platform has been explored leading to a LISA Pathfinder baseline to serve as the service module / platform. Within the Service Module (SVM) the Payload Module (PLM) will be fitted. The available volume was determined to be 0.85m x Ø 0.79m.

4.3 Payload Concept Trade Study

There are several technologies that offer the opportunities to test the WEP. For this reason the mission design is based upon previous studies. The literature on the subject is quite extensive. The design consideration in terms of FPE-B is what approach to take. The key considerations are the accuracy that it provides (the chance of detecting the WEP).

Briefly (a more detailed description can be found in [TN3]):
- SQUID Sensing – As used by STEP the relative motion of to concentric cylindrical Test Masses (TMs) is detected by determining the difference in current induced by each. (see Section (4.4.2))
- Electrostatic – As uses by Microscope. The difference in the motion of the TMs is determined by comparing acceleration detected by capacitive sensing.
- Atomic Interferometry (AIF) – Two matter waves are compared by monitoring the relative changes in their interference patterns when combined after they have travelled a given distance.
- High Mechanical Spin – Capacitive sensing is used. But the WEP is generated by spinning the TMs, thusly moving the WEP signal to higher frequencies away from common systematic errors.

The status of the concepts and the advantages and disadvantages are given by Table 4.1 and Table 4.2 respectively.

Concept	Mission	Predicted Accuracy	Reference
SQUID Sensing	STEP	$\sim 10^{-17} - 10^{-18}$	[5], [6] and [30]
Electrostatic	Microscope	$\sim 10^{-15}$	[8] and [31]
Atom Interferometry	n/a	Unclear	[32]
High Mechanical Spin	GG	$\sim 6 \times 10^{-17}$	[10],[11] and [36]

Table 4.1 – Comparison of systems for Measuring Possible Violations of the WEP

Concept	Advantages	Disadvantages
SQUID Sensing	• Best predicted accuracy ($\eta = 10^{-17}$), the order at which WEP violations are thought to exist • Extensive theoretical work performed • Simple measurement based upon single sensitive axis accelerometer • Some breadboarding in progress	• Cryogenic requirement (<1.8 K) • No differential accelerometer working prototype • Provides only linear acceleration measurements along a single axis • Larger spacecraft possibly required
Electrostatic	• Relatively simpler implementation • High design maturity (accelerometers built, spacecraft to be launched 2009-10) • Less stringent environmental constraints • Cryogenics not required • Longer mission scenario not constrained by cryogens	• Predicted accuracy two orders (10^{-15}) worse than SQUID sensing (10^{-17}). • To be flown in the near future
Atom Interferometry	• Less stringent environmental requirements (no cryostat) • Payload technology similarities with other missions in the FPE programme, allowing common platform possibilities • Described as potentially better in performance, but to what degree is unclear	• Least mature technology • Measurement accuracy unclear at this stage • Development timescales are considered to be longer • Least amount of work performed for space applications • Unclear as to how two species would be tested sharing a common centre of mass. Errors would be introduced due to slightly differing geodesics.
High Mechanical Spin	• Room temperature implementation • Mission spacecraft small (GG – 301 kg [10]) • Good amount of theoretical work performed • Ground based experiment (breadboard) implemented similar to payload concept	• SQUID sensing still an improvement in accuracy, although GG is a close second. • Mechanically complex • Test masses are not free-floating • High spin rate of spacecraft required • The performance of the instrument is undecided within the community • Unclear as to how DFACS will be implemented on a fast spinning spacecraft.

Table 4.2 – Advantages and Disadvantages of Differential Accelerometer Concepts

In general the atom interferometer performance is unclear as it is more theoretical. There were plans for drop tower tests such experiments. However it is sensible to assume, due to greater predicted accuracy, the STEP like SQUID design to take advantage of the studies already completed.

4.4 Payload Definition

4.4.1 Functional Architecture

A baseline of two DAs is chosen to provide the minimum science return matching the objectives (this is a similar approach to Mini-STEP [29] and [35]). Figure 4.1 shows the mission concept of FPE-B. A DA will provide a measurement of both a possible differential acceleration and common accelerations due to external forces. The whole package of the DAs and the casing is called the Equivalence Principle Instrument (EPI).

The spacecraft moves in its orbit with a rotation of $\omega_{S/C} = 0$ or greater (three axis stabilised) as and is considered to be the baseline. Removing external forces the instruments frame becomes fully inertial. The rotation is feasible in principle as it was to be used in the STEP study [5] and will be used for the MICROSCOPE mission ([8] and [31]), and GG [36].
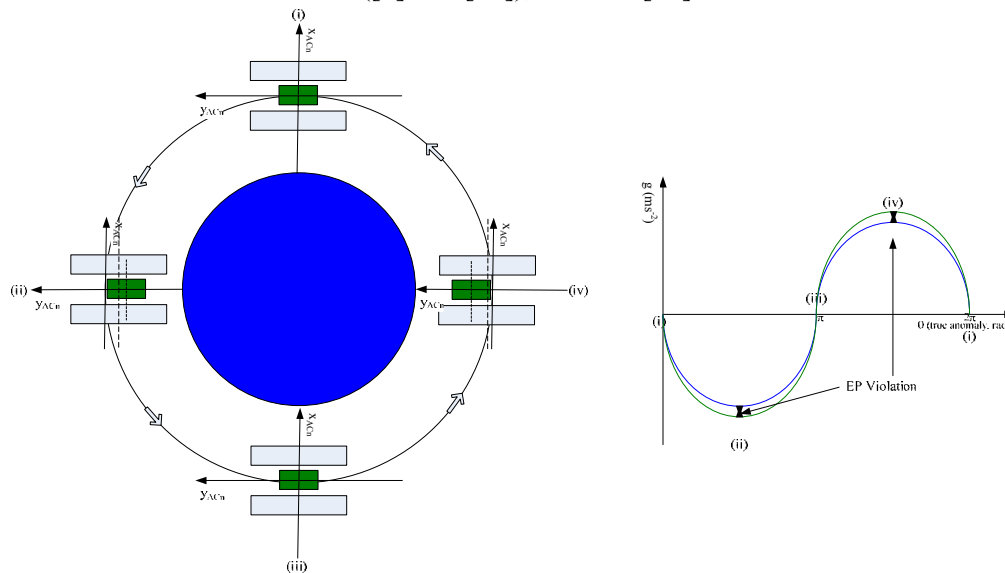
Figure 4.1- Test Mass Motion w.r.t. the Earth (FPE-B Mission Concept)
The three axis stabilised spacecraft orbits the Earth changing the orientation of the DAs sensitive axis w.r.t. the Earths gravitational field. The plot shows how the WEP violation will manifest over one orbit as a differential acceleration between each test mass.

The electrical signals of TM motion are detected and passed through the appropriate channel to the Front End Electronics (FEE) and then on to the Back End Electronics (BEE), which will convert the signals from the DAs into a digital format which is processed by the Data Processing Unit (DPU). The DPU shall also provide the appropriate signals to maintain the test masses at the 'null' position for calibration and DFACS. This nulling signal will be converted to an electrical signal by the set of electronics. The payload concept is shown in Figure 4.2.

The Accelerometer will provide the following signals:
- The **differential mode acceleration (DMA)** is the difference in acceleration due to gravity between the two test masses contained within a DA. If it exceeds known errors it will be a violation of the WEP.

- The ***common mode acceleration (CMA)*** is the acceleration measurement provided for the Drag Free Attitude Control System (DFACS). This is provided by the Electrostatic Positioning System (EPS) in all DoF with the exception of the sensitive SQUID axes (See Section (4.4.2)).

Figure 4.2 – FPE-B Instrument Function Block Diagram

4.4.2   Differential Accelerometer Design

There have been extensive studies conducted by NASA, ESA and Stanford University and others into a system for detecting the WEP from the relative motion of two Test Masses (TMs). This Section describes the design proposed in literature. The concept is shown in Figure 4.3.
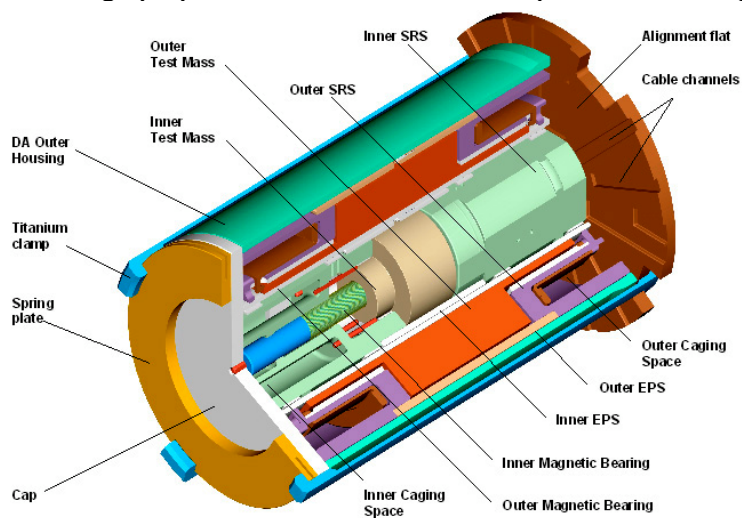
Figure 4.3 – A Possible Differential Accelerometer Implementation [37]

The accelerometer is composed of two cylindrical test masses one inside the other. They are hollow cylinders suspended by Quartz bearings providing magnetic levitation using a Super-Conducting Magnetic Bearing (SCMB). This bearing is complemented by a sub-system that will provide the means to position the TMs which is known as the Electrostatic Positioning System (EPS) (see Section (4.4.4)). It works on the same principle as the MICROSCOPE DA in that electrostatics are used to hold and measure the position of the TMs. The bearing for the inner tests mass surrounds it and the outer test mass has its bearing within. Each bearing is coated in thin film Niobium. Embedded in the thin film, are superconducting circuits generating levitation.

The persistent super-currents provide mechanical stiffness to hold the test mass in position. A higher level of stiffness (analogous to a mass-spring suspension) is maintained along all axes other than the sensitive axis, which is in the longitudinal direction of the test mass cylinder.

The differential mode is detected using the principle described in [30]. The coils to detect motion along the sensitive axis are in this case, of the pancake variety, positioned facing the 'belt'[*] of the outer TM. The inner TM has a set of pancake coils positioned at its ends. These two coils at either end are connected in parallel.

(a)

(b)
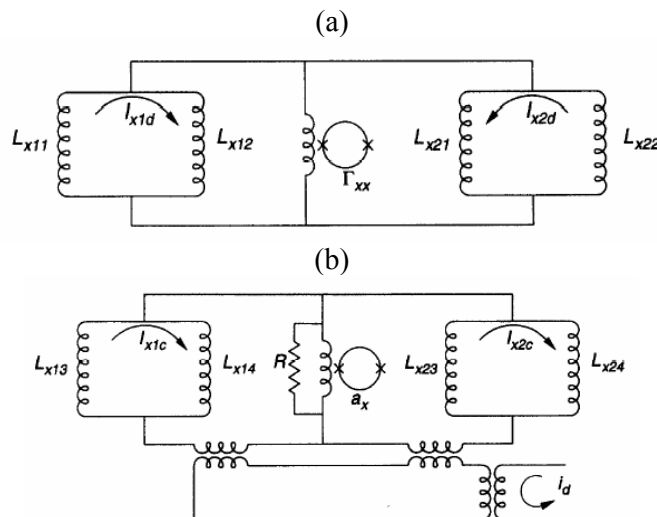
Figure 4.4 – Circuits for the detection of TM Motion along the Sensitive axis
a) The differential mode and b) the common mode acceleration signals [30]

The outer TM's belt motion towards or away from a coil changes the magnetic field in the coil and hence drives a change of current in the circuit. The same principle is true for the inner TM. However in this case the flow of the current of the coil-pair parallel circuit is designed to be in the opposite direction when induced. Both coil-pair circuits are connected in parallel to a SQUID. If there is a difference in currents between the outer and inner TM coil-pair parallel circuits a current will flow. The SQUID will detect this tiny current which is indicative of a *differential mode* acceleration signal. If there is no differential acceleration no current will flow to be detected by the SQUID, indicating equal and opposite currents in the pancakes coil-pairs relating to each test mass. The circuit is shown in Figure 4.4(a).

---

[*] The belt is a ring around the outer test mass, or the thicker area of the orange shape (test mass) in Figure 4.3.

The ***common mode*** acceleration signal is detected by a second set of outer pancake coils facing the outer TM belt and the end of the inner TM. However, this time the currents in them flow in the same direction. The combination of which is again detected in another parallel circuit by another SQUID. The circuit is shown in Figure 4.4(b). No cancellation will occur because the currents are in the same direction, only the increase proportional to an external force will be detected.

4.4.3   Sensitivity

The following equation describes the Power Spectral Density of a SQUID for the DA taken from [30].

$$S_a = \frac{8}{m_{TM}}\left[k_B T \frac{2\pi f_d}{Q_d} + \frac{(2\pi f_d)^2}{2\beta\eta} E_A(f) \right]$$

4.1

Where;

- $m_{TM} = 0.61$ kg (mass of the test mass, (taken as the smallest TM mass))
- $f_d = 0.001$ Hz (differential mode resonance frequency [30])
- $Q_d = 2$ x10^5 (quality factor[30])
- $T = 1.8$ K (temperature from STEP [5])
- $\beta = \eta = 0.5$ (transducer electromagnetic coupling coefficient and electrical coupling efficient of the SQUID respectively [30])
- $E_A(f) = 5\times10^{-31} F(f)$ input energy resolution of the SQUID [30]
- $F(f)$ = is a quantity dependant on the noise type (see Table 4.3)
- f = frequency

There are several sources of noise present and they are summarised in Table 4.3.

Source	Function, $F(f)$
White Phase Noise	$\left[1 + \frac{f^2}{(0.1mHz)^2} \right]$
Flicker Phase Noise	$\left[1 + \frac{f}{0.1mHz} \right]$
White Frequency Noise	1
Flicker Frequency Noise	$\left[1 + \frac{0.1mHz}{f} \right]$
Random Walk Frequency Noise	$\left[1 + \frac{(0.1mHz)^2}{f^2} \right]$

Table 4.3 – Sources of sensor noise and the frequency dependence
Adapted using p-73-75 of [16]

Each of the five sources of noise is plotted in Figure 4.5. In addition the quadratic RMS sum is plotted also, using the values of temperature and mass from this document.
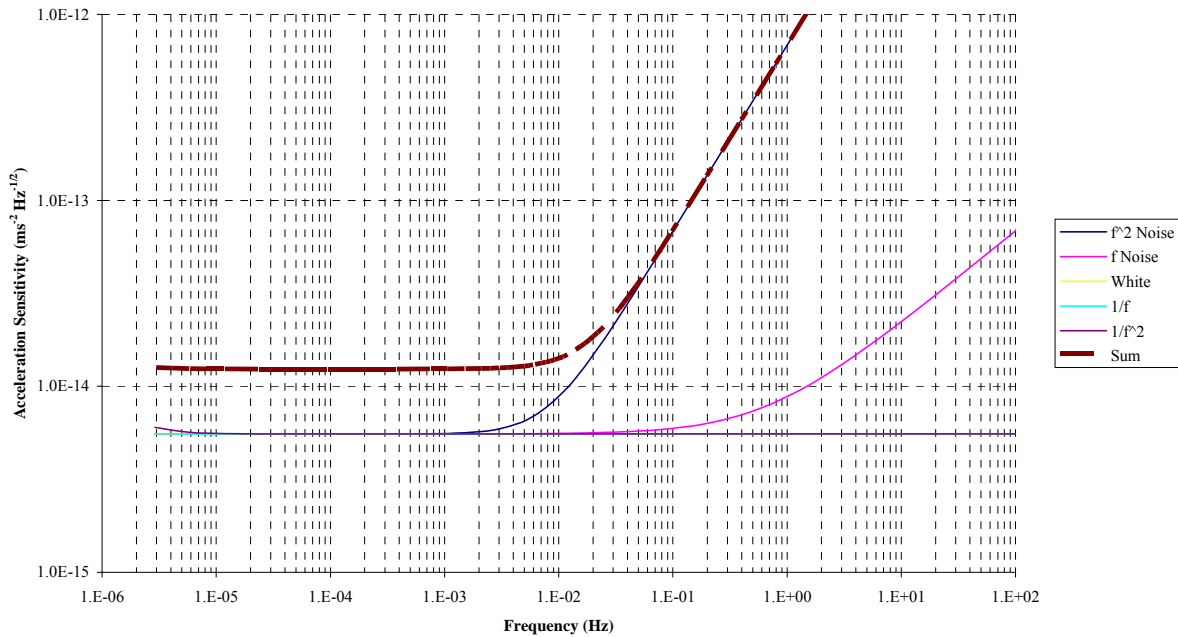
Figure 4.5 – Power Spectral Density of a DA SQUID
This plot uses Equation 4.1and Table 4.3

With a TM of 1 kg the sum of the noise is around 1 x 10^{-14} ms^{-2} Hz$^{-1/2}$. Increasing the size of test mass improves the performance of the SQUID. Thermal variations have a smaller effect on larger masses. Increasing the TM mass also has disadvantages. The most important is how the TM is caged for launch. Small stoppers are baselined in [30], but LPF with its larger TMs have a separate caging payload sub-system to release the TM without residual motion in a particular direction. With the values baselined for FPE-B smallest TM, the sensitivity is 1.24 x 10^{-14} Hz$^{-1/2}$ @ 0.5 mHz. To achieve the target of an WEP violation at 10^{-17} the measurement can be improved by integrating over a long period. The sensitivity which is quoted here is the one-shot noise. This integration time can be calculated using the formula $S_a(f) = \sigma^2(\tau)/2\tau$, where τ is the integration time (Table 2.2). For an WEP signal frequency of 0.33 mHz (two per 700 km orbit), the integration time required is 18 days for the sensitivity described in Figure 4.5.

A further option is to increase the quality factor, Q, of the SQUID sensor. An increase in a factor of 1.5 results in a sum sensitivity of 1 x 10^{14} ms^{-2} Hz$^{-1/2}$ for 0.33 mHz.

Increasing the sensitivity 1 x 10^{-14} ms^{-2} Hz$^{-1/2}$ at 0.33 mHz should be defined as a measurement goal, if not better, in an attempt to bring down the integration time. For this frequency it is 12 days. The heavier TMs may achieve this. However, the simple stopping devices may not be enough to protect the TM during launch.

4.4.4   Electrostatic Positioning System (EPS)

The accelerometer design includes also a dedicated sub-system to control the position of the TMs independently of the SCMB's as the purpose of these is to hold the TM for WEP measurements.

Comparisons can be drawn with electrostatic accelerometers to be used on the MICROSCOPE mission. Capacitive sensing is used to determine the position and rotation of the TMs. The functions of the EPS are as follows (this list also is found in [38]):

- Positional measurement of a TM so to release the caging mechanism (additional details are required) and initially position the TM in preparation for magnetic levitation. In addition, it holds the TM when not in drag free mode
- Implements the transition from 'standard' attitude control to drag free control
- Calibrates the SQUID sensors and sensitive axis (for clarity, it defines a sensitive axis)
- Relative alignment of test masses along the sensitive axis and radial direction
- Allows the dithering of the TMs for charge measurement
- Allows the dispersion of charged electrons once they have been liberated from the TM surface (see next section)

4.4.5   Charge Management System

A calculation is conducted in [30] and shows that the total charge on the TM should be no greater than **5×10^{-12} C** to ensure the coincident TM CoM is aligned to within a tolerance o**f 3×10^{-9} m.** An important value is that charging due to the South Atlantic Anomaly (SAA) is **2×10^{-14} C** per pass [30].

The EPS system is used to measure the charge on the test masses by applying a dither voltage to the electrodes. Oscillations between a positive and negative voltage will give rise to motion in the test masses either by attraction of repulsion. The frequency of which indicates the magnitude of the charge on the TM. The phase gives the sign. From this measurement a UV mercury lamp source is used to illuminate the TMs. This is done by using the cable channels in the housing to run an optical fibre to a point between the electrode and the test mass. The light then reflects backwards and forwards between the TM and electrode liberating electrons from the surface and discharging the mass. A bias is applied to the outer electrode to attract the free electrons. The whole discharge will take around 1000s [38].

4.4.6   Accommodation of the DAs

To assist in the stability of the DAs, they are encased in Quartz. They are positioned orthogonal to each other. Figure 4.6 shows a possible concept.
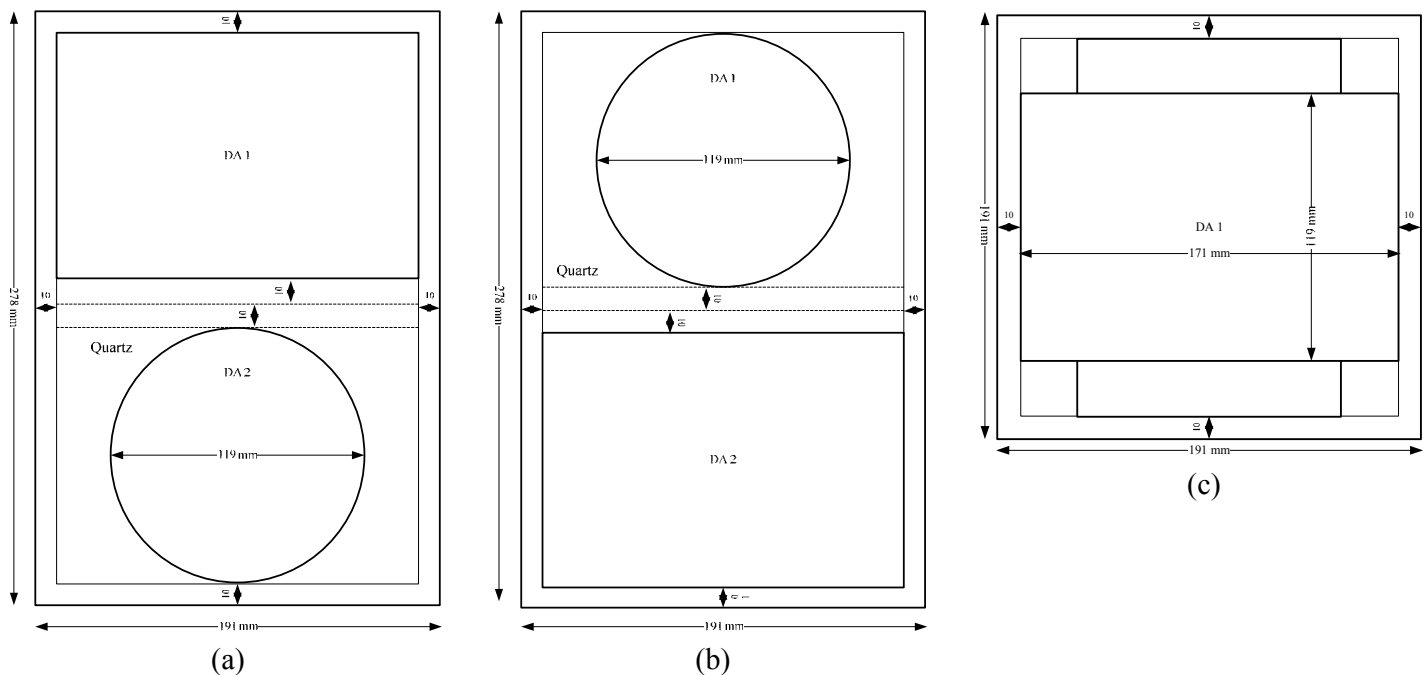
Figure 4.6 – Schematic showing the dimensions and possible layout of the EPI instrument.
(a)Lateral view, (b) second lateral view and (c) a planar view

4.5 Cryostat Definition

Superconducting DA's require the use of cryogenics. For FPE-B it has been decided that the Cryostat be part of the payload definition.

The cryostat is required to fit within LISA Pathfinder and provide an environment of around 1.8 K for the EPI. A single cryogen Helium cryostat was ruled out as a significant amount of Helium would be lost during launch preparation. Access to the payload after it has been integrated with the spacecraft is difficult. Therefore a dual cryogen concept was studied. A hydrogen tank would reduce the loads on the Helium during the Launch and Early Operations Phase (LEOP).

Venting is envisaged to be evenly space around the spacecraft to reduce the disturbance that it may produce.

Key issues that have been identified are:
- Development of small dual cryogen cryostat, completely new technology
- Restrictive lifetime, not realistic for a space mission
- Gas venting disturbances
- Motion of Helium within the tank creating variations in the local gravitational field

The parameters in Table 4.4 were determined using a thermal model based upon existing hardware. A margin on the radius is applied to allow for fixtures and fittings.

Mission and External Input			Mass Budget		
Pre-Launch	6	Days	**Helium**		
Operational	192	Days	**Helium Mass**	**8.2**	**kg**
Total Duration	198	Days	Margin	0	%
Abs.Av. Ther. Input ($\dot{Q}$)	214	mW	**Helium Mass (With Margin)**	**8.2**	**kg**
Margin	0	%			
Eff. Av. $\dot{Q}$	214	mW	**Hydrogen**		
Total Energy Input (Lifetime)	3657.8	kJ	**Hydrogen Mass**	**8.7**	**kg**
			Margin	0	%
Helium Lat. Heat of Vap.	23.93 x 10^3	J/kg K	**Hydrogen Mass (With Margin)**	**8.7**	**kg**
Helium Density	145.08	kg/m^3 @ 1.8K	**Tank and Other**		
Cryostat Geometry			Electronics/Sensors/Harness	9.00	kg
Helium Tank Volume	65.6	Litres	Cryostat Structure	92.3	kg
Hydrogen Tank Volume	99.5	Litres	**Cryostat Empty Mass**	**101.3**	**kg**
			Margin	20	%
			Cryostat Empty Mass (With Margin)	**121.5**	**kg**
Cryostat Dimensions (Cylinder)	846 x Ø740	Mm			
Cryostat Volume	0.36	m^3	**TOTAL Cryostat Subsystem**	**138.4**	**kg**

Table 4.4 – Cryostat Sub-System and Mass Budget for a Seven Month Lifetime

The EPI instruments fits into a rectangular space within the Helium tank with an interface at the top. Outside the Helium tank there is a shield consisting of empty space. Then the Hydrogen protective tank is surrounded by a shield vapour cooled, which is assumed in the model. The outer structure (known as the vacuum vessel) is also surrounded by Multi-Layer Insulation (MLI). A possible design is presented in Figure 4.7. The control wires for both the EPI and cryostat (sensor read-outs of temperature and pressure etc) control and processing electronics will interface with the spacecraft through the top. The electronics themselves controlling the payload and receiving the cryostat status will be accommodated on the SVM.

This design is very preliminary and it is the result of an initial sizing exercise. A larger cryostat may be required. More discussion on this can be found in Section (9.2.1).
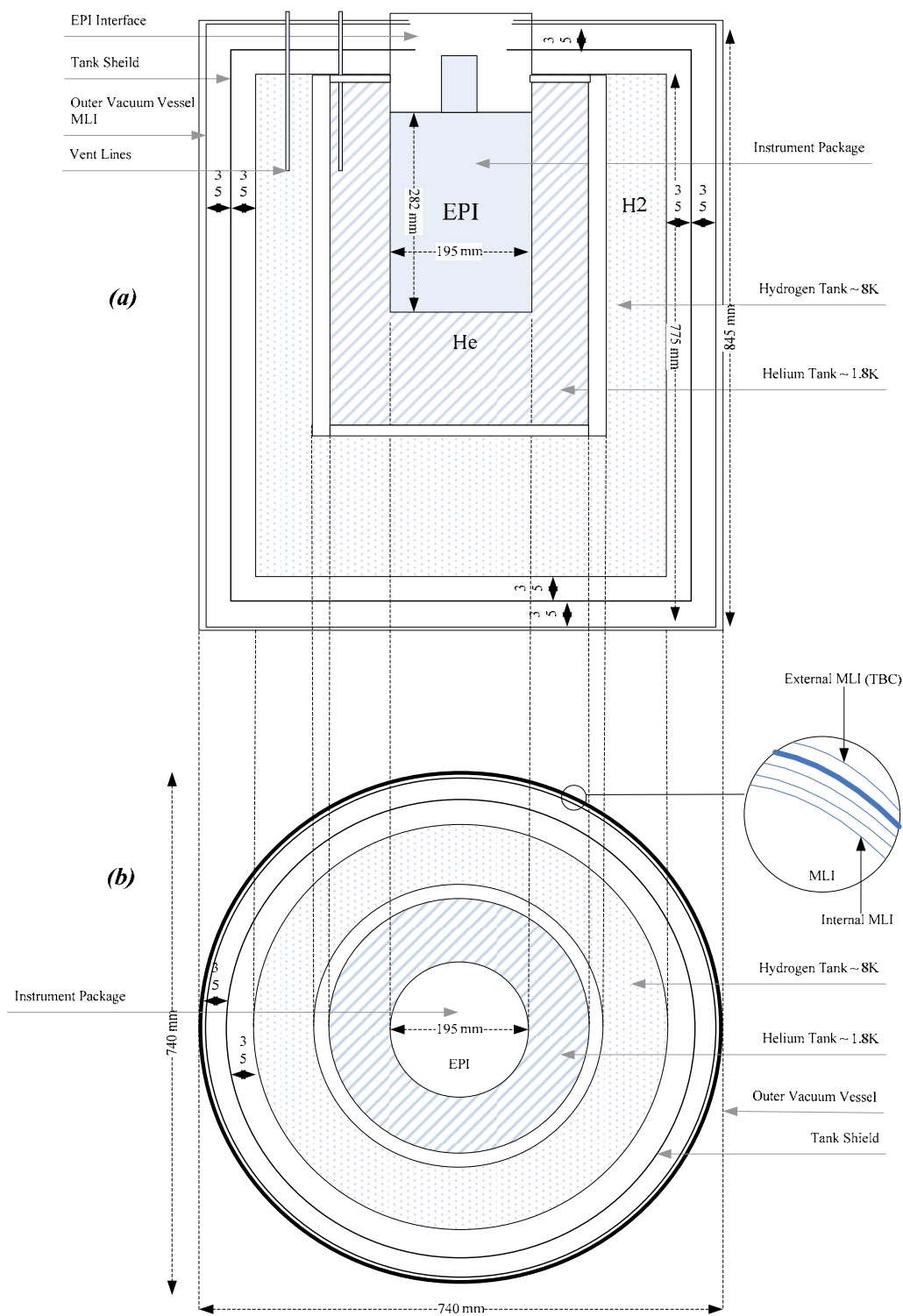
Figure 4.7 – A Possible Implementation of a Dual Cryogen Cryostat
(a) Shows a lateral view and (b) shows a polar cross section (dimensions) in mm

4.6   Payload System Requirements

This section summarises the resource budgets of the EPI and the cryostat which constitutes the payload of FPE-B. The estimates given are of a preliminary nature and not the result of a detailed design. However it does give an indication of the required allocations for future reference and is a starting point for further work.

4.6.1   Accommodation

Total payload volume (cryostat) is assumed to be **0.846 m x Ø 0.740 m** (length x diameter) cylinder. To increase lifetime a longer cryostat will be required as the radius is restricted by LISA Pathfinder's central cylinder.

4.6.2   Mass Budget

Item		Unit Mass (kg)	Margin (%)	Eff. Mass (kg)
DAS				
	Accelerometer 1	3.7	20	4.4
	Accelerometer 2	2.8	20	3.3
Mounting/Probe Assembly				
	DAS Casing	20.0	20	24.0
	Interface	20.0	20	24.0
	Harness	4.0	20	4.8
Electronics				
	Electronics	2.0	20	2.4
	DPU	4.0	20	4.8
	Power Converter Unit	1.0	20	1.2
Other				
	ESA Env. Monitor	1.0	20	1.2
	UV Charge Management	3.0	20	3.6
Cryostat				
	Structure and Electronics	101.3	20	121.5
	Helium	8.2	0	8.2
	Hydrogen	8.7	0	8.7
Total		**180.1**		**212.2**

Table 4.5 – Preliminary Mass Budget for the FPE-B Payload

A more detailed mass budget than Table 4.5 can be found in [TN3] derived from the design.

4.6.3   Power Budget

The power budget is shown in Table 4.6.

	Average (W)
EPI	
Positioning System	14.0
Front End Electronics	5.0
Back End Electronics	5.0
DPU	4.0
Power Converter Unit	3.0
UV Management	3.0
Abs EPI Total	**34.0**
Conversion Efficiency (0.7)	**48.6**
Support Instruments	
ESA Environment Monitor	2.0
Abs Support Total	**2.0**
Cryostat	**11.2**
Abs Payload Total	**61.8**
Margin (%)	30
Eff. Total	**80.3**

Table 4.6 – Preliminary Power Budget for the FPE-B Payload

4.6.4   Data Budget

The data budget is shown in Table 4.7.

Science Data	20	Hz
Dynamic Range	4	Orders
	14	Bits
DOF x 2 and DA x2	2240	Bps
Margin	20	%
	2688	**Bps**
EPS Positioning	20	Hz
Dynamic Range	3	Orders
	11	Bits
DOF x 5 and DA x2	4000	Bps
Margin	20	%
	4800	**Bps**
Cryostat and EPI Housekeeping	600	Bps (with Margin)
Margin	20	%
	720	**Bps**
Total Data Rate	**8208**	**Bps**

Table 4.7 – Preliminary Data Budget for the FPE-B Payload

The downloaded data is assumed to consist of the data signals of residual acceleration from the capacitive sensors of the EPS system, DMA and CMA from the SQUIDS on the sensitive axis and the cryostat status. The EPS data will give a measure of the external disturbances on the spacecraft and will bias towards an order of $10^{-7} – 10^{-11}$ ms^{-2}. The sensitive axis will be biased towards a dynamic range of 10^{-14}-10^{-18} ms^{-2}. Measurements are in the time domain (units of ms^{-2} rather than

$ms^{-2} Hz^{-1/2}$) and the PSD is computed later, hence the need for sample frequency of 20 Hz. This gives a large margin and many data points and is no problem as even the link at this data rate is not demanding.

4.6.5   Drag Free Control Requirements

The basic requirement of the DFACS is to compensate for the residual acceleration of the local environment to a level below the sensitivity of the Sensitive axis of the DA at the frequency of measurement.

The payload requirements of the AOCS sub-system are derived in the following way.

- **$1 \times 10^{-17} ms^{-2}$**. The goal of $10^{-17} ms^{-2}$ is the science requirement. The conversion from a time domain ($\sigma^2(\tau)$, the Allen Variance) to a PSD is $S_y(f) = \sigma_y^2(\tau)/2\tau$, where τ is the integration time (see Section (2.1.3) Table 2.2 White Noise is assumed here).
- **$1 \times 10^{-14} ms^{-2} Hz^{-1/2}$**. Given by an integration time of 12 days (10^6 secs) three orders of magnitude can be gained requiring a sensitivity of $1 \times 10^{-14} ms^{-2} Hz^{-1/2}$, which is nearly within the capabilities of the accelerometer. This denotes the sensitivity requirements of the SQUID sensor.
- **$1 \times 10^{-10} ms^{-2} Hz^{-1/2}$**. This is given based upon LISA Pathfinder's control loop gain a further four orders is achieved combined with the knowledge of how the TM is coupled to the spacecraft.
- **$0.75 \times 10^{-7} N Hz^{-1/2}$.** For an assumed spacecraft mass of approximately 750kg (as assumed by [TN4]) the thrusters must not exceed this noise level. (NB: For a 500 kg spacecraft the requirement is $0.5 \times 10^{-7} N Hz^{-1/2}$).

The frequency bandwidth these requirements demand is at a minimum twice per orbit if the spacecraft does not rotate. [TN4] selects a 700 km (see Section (6.6)), which results in a required band width of 0.3 mHz, as this is when the potential WEP is largest (see Section (4.4.1)).

5 FPE-C Bose Einstein Condensation

5.1 Science Requirements

The principle goals for FPE-C are listed in Table 5.1. The detailed requirements and further references can be found in the Sci-RD [TN1].

The advantage of space is that, unlike drop tower experiments, the time of free-fall is, in principle, perpetual, greatly improving the time of study. Moreover, the temperature of the BEC can be reduced to even lower levels (fK regime [TN1]) than on ground, and its size can be increased.

Code	Experiment	Requirements
C1	Ultra-Low Temperature Physics, Thermodynamics of degenerate quantum gases	• $10^5 - 10^6$ atoms cooled to hundreds of nK • Trap mechanism allowing adiabatic expansion (trap opening) • Tuneable trap frequencies (longer /shorter BEC lifetime experiments) • Temperature tuneable between hundreds of nK to fK • Long free evolution times • High resolution imaging system for sample detection ($10^2 - 10^3$ atoms etc). Baseline assumption of 2μm resolution is assumed.
C2	Coherence Properties	• $10^5 - 10^6$ atoms cooled to hundreds of nK • Trap mechanism allowing adiabatic expansion (trap opening) • Tuneable trap frequencies (longer /shorter BEC lifetime experiments) • Temperature tuneable between hundreds of nK to fK • Long free evolution times • High resolution imaging system for sample detection ($10^2 - 10^3$ atoms etc). Baseline assumption of 2μm resolution id assumed. • Coherent Matter Wave Splitting, support interferometric or Bragg Spectroscopy mechanisms
C3	Collective Excitation Modes in the Weak Trapping Regime	• $10^5 - 10^6$ atoms cooled to hundreds of nK • Trap mechanism allowing adiabatic expansion (trap opening) • Tuneable trap frequencies (longer /shorter BEC lifetime experiments) • Temperature tuneable between hundreds of nK to fK • Long free evolution times • High resolution imaging system for sample detection ($10^2 - 10^3$ atoms etc). Baseline assumption of 2μm resolution id assumed. • Excitation of the sample collective modes

C4	Degenerate Quantum Mixes	• Mixture of two species that co-exist as a BEC ($10^5 - 10^6$ atoms of each) • Long free evolution times • High resolution imaging system for sample detection ($10^2 - 10^3$ atoms etc). Baseline assumption of 2μm resolution is assumed. • Trap frequency and temperature variations could also be included
C5	Role of Dipolar Interactions	• $10^5 - 10^6$ atoms cooled to hundreds of nK • Trap mechanism allowing adiabatic expansion (trap opening) • Tuneable trap frequencies (longer /shorter BEC lifetime experiments) • Optical Dipole potential to confine the BEC • System to control the magnetic field for defining the quantisation axis and the orientation of the magnetic dipoles and scattering length • System to control the magnetic field for tuning the scattering length • Long free evolution times • High resolution imaging system for sample detection ($10^2 - 10^3$ atoms etc). Baseline assumption of 2μm resolution id assumed.
C6	Matter Wave Interferometry	• Tests of WEP with AIF

Table 5.1 – Science Requirements for FPE-C

In summary the goal is to study the BEC under differing conditions. The trap frequency is a switching of the magnetic field periodically to allow the most energetic atoms to escape, the process of evaporative cooling, usually in the RF-domain (see [51] for a description as to how). If the trap RF-frequency is varied, the process of evaporative cooling is changed (see [51] for a description as to how).

The formation is a one-shot process repeated several times. The trap produces the condensate, and then it is imaged, which results in its destruction. Therefore varying the time at which the BEC is released enables an analysis of the condensate after different periods of time. This could be from when a condensate has not formed to when it has.

The release temperature could also be varied, allowing the characteristics of the BEC to be studied still further (C1).

The BEC can also be excited by parametrically oscillating the system. This means that the magnetic field can be altered at a given frequency to observe the behaviour of the formation. The magnetic field can also be used to squeeze and shape the condensate to characterise it macroscopic properties.

Science goals C2 and C5 have not been studied at the present time and hence the required hardware has not been defined. They could be added at a later date. A means to detect Bragg scattering and interferometric patterns would be required. Mass penalties are not deemed to be too severe. Additional suggested science objectives of Matter Wave Interferometry have not been considered in this case and are left open to further study due to the required addition of Raman lasers (see [32] for

more details). Further this can be considered as a test of the WEP [TN1], which would be included in FPE-B. In addition to this a DFACS sensor at the level of FPE-B would be required.

As a first preliminary reference design, an instrument for creating and imaging a BEC has been defined in Sections (5.2) and (5.3).

5.2 *Payload Definition*

5.2.1 *Functional Architecture*

This section briefly outlines the payload concept. The initial design included a trap for containing and cooling the BEC, an imaging system, a control unit, ion pump, a UV source and a laser bench.
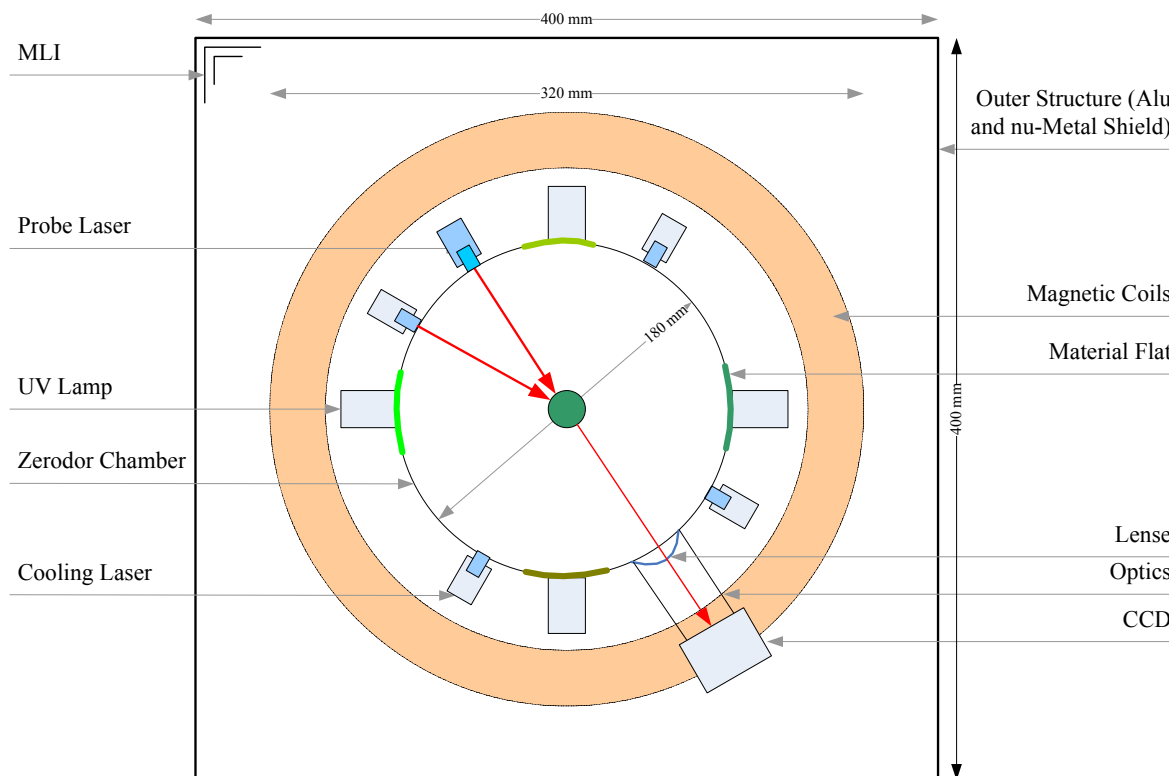
Figure 5.1 – FPE-C Payload Concept (Plan View)

BEC Trap Package (BTP)
The UHVIC or BEC Vessel is assumed to be Zerodur the same as the LPF optical bench. This allows easy access to the condensate for the cooling lasers, probe laser and CCD camera. It is assumed to be 2mm thick, although a detailed analysis would be required to determine the exact specifications to ensure testing and launch survival.

Embedded on the inner surfaces of the BEC Vessel are coatings of different atomic species to be tested. Fixed to the outside facing the material is a UV lamp, which when switched on, will dislodge

the atoms from the coating, releasing them into the chamber. The technique is described in [56]. The atomic species suggested by [TN1] are; Rb, Na, Li, K and Yb.

Fibre couplers bonded (in a similar way to how the mirrors on the LTP optical bench are mounted) provide access to the chamber for the cooling lasers. The laser is sourced from the Laser Bench (LB). This provides the optical molass (the mechanism which slows the atoms, see Section (3.2.3)).

Surrounding the chamber are two anti-Helmholtz coils (two coils with currents in opposition, only one is shown in Figure 5.1). This is an electromagnet which will provide the magnetic field to trap the atoms. The baseline is a set of copper coils. The radius of each is assumed to be 320 mm. For the Helmholtz condition the distance between the centres of each coil is required to be the same as the radius. This ensures the 'magnetic trap' is centred in the middle. Actuators will allow the adjustment of current and hence magnetic field. The adjustment should be varied in the RF domain. A schematic of a Magneto Optical Trap (MoT) as described is shown in Figure 5.2 and note that it differs from the single ion end-cap trap.
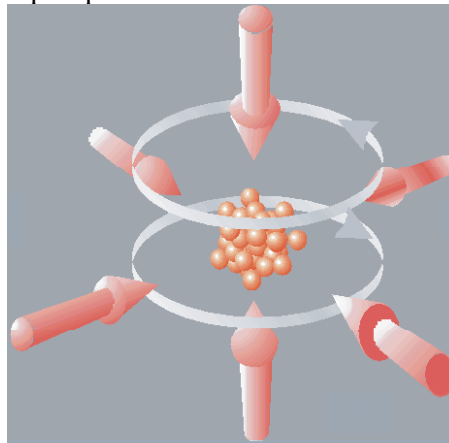
Figure 5.2 – MoT Trap Concept [53]

The BEC is observed in single shots by adsorption imaging. The probe laser is shone onto the BEC. Then CCD images the light after it has passed through the BEC (which casts a shadow).

The whole instrument is encased in a box providing support structures for the trap and coils and interfaces. The case consists of a is 1 mm thick aluminium primary structure augmented with a 0.5 mm mu-metal shield to attenuate external magnetic fields. MLI is included to assist in maintaining temperature stability.

Interfacing with the BTP, is the fibres containing the cooling laser (s) and probe laser. Also the output of the CCD is interfaced with Payload ECU, as are the environmental sensors. The actuation signal for the magnetic field, thermistors and control of the trap-formation-observation cycle are controlled by the Payload ECU.

External Units
The laser bench is similar to the PHARAO bench in that is provides several lasers of differencing frequencies. These should be switchable to allow the cooling of two species within the trap for experiments dedicated to mixtures (C4). This is required as each atomic species has a different

cooling transition. Other frequencies may be required as a degree of re-pumping or post-cooling could be necessary (see Section (3.2.3) Figure 3.7). The probe laser would also originate here.

A source for UV light is required for detaching the atoms from the patches on the sides of the chambers. It is assumed to be similar to the LTP Test Mass discharging unit.

5.2.2   Experiment Cycle

The creation and observation of a BEC is a one-shot event as the when the light is shone onto the condensate it is destroyed. The requirement of the cycle is to provide a BEC which has been parameterised differently in sequential fashion. Some parameters could be; BEC final temperature, trap depth, release time, magnetic field frequency variations, material type or free expansion before imaging time. A combination of these parameters while keeping others constant will provide a analysis of the behaviour. One important aspect is to fix all the parameters and image the BEC at different times after release into free expansion, viewing its development as a function of time.

The cycle could be defined as:
- The Ion Getter Pump clears the chamber of atoms, perhaps from a previous experiment.
- Pressure sensors verify the vacuum
- A picture is taken without any probe laser light.
- The probe laser is activated and another picture is taken.
- UV light is shined on one or more atomic patches releasing atoms into the chamber
- The cooling lasers switch on and provide the optical molass slowing the atoms' velocity.
- The cooling lasers are switched off and the magnetic field is applied to the cloud
- The RF frequency of the trap is varied to allow the most energetic atoms to escape, the evaporative cooling phase [51]
- After a pre-defined time the magnetic field is switched off and the atoms are released into free fall
- At this point the atoms may be manipulated to change the cloud shape or to apply an oscillating frequency
- The laser is then shone onto the cloud at a time appropriate for the stage of the experiment and the camera images the condensate (the third and final picture)

Recall that this cycle is varied so that the flight time or experiment parameters can be changed so the BEC can be observed at different stages of development.

Three pictures are taken to remove systematic errors and noise. An example is shown in Figure 5.3.
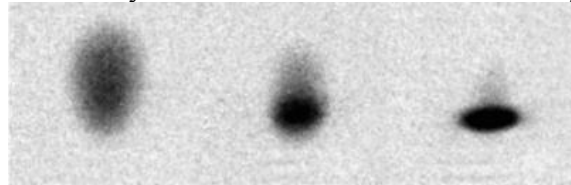
Figure 5.3 – Example Images of BEC [54]
Three separate images are shown, relating to three one-shot experiments using absorption imaging, for progressively lower temperatures (right to left). Image Size = 1.4 x 1.4 mm each.

5.3 Payload System Requirements

5.3.1 Accommodation

The trap is contained within a box. The laser bench, payload DPU and electronics are separate units. The ion pump is interfaced with the BTP. The preliminary estimates of envelopes are shown in Table 5.2.

Item	Envelope
	(Approx. Cuboid) mm
BTP	600 x 400 x 400
Laser Bench	529 x 330 x 178
DPU	245 x 240 x 120
UV Source	300 x 100 x 100
Environmental Sensors	200 x 100 x 50

Table 5.2 – FPE-C Payload subsystem Preliminary Envelope requirements

The key environmental requirements of the BTP are (which is the main driver):
- Vacuum shall be 10^{-12} mbar
- The trap shall be subjected to no external magnetic fields required if mu-metal shielding of the BTP.
- Temperature variations shall be minimised.

If AIF is implemented any effects leading to spurious accelerations need to compensated for below the level at which they generate a signal around the sensitivity of the accelerometer, at the frequency of interest.

5.3.2 Mass Budget

A summary is presented in Table 5.3.

Item	Mass (kg)	Margin (%)	Cont. Mass (kg)
Package Structure	13.3	20	16.0
BEC Vessel	8.9	20	10.7
Laser Bench	23.0	20	27.6
UV Source	6.3	20	7.5
Imaging System	0.6	20	0.7
Payload ECU	9.2	20	11.0
Environment Sensors	2.3	20	2.8
Total	**63.6**		**76.3**

Table 5.3 – Preliminary Mass Budget for the FPE-C Payload

5.3.3   Power Budget

A summary is presented in Table 5.4.

Item	Average (W)	Margin (%)	Average (W)
BEC Vessel	66.0	20	79.2
Laser Bench	33.0	20	39.6
CCD	2.0	20	2.4
Payload Control Electronics	32.5	20	39.0
Environment Sensors	6.0	20	7.2
Total			167.4

Table 5.4 – Preliminary Power Budget for the FPE-C Payload

5.3.4   Data Budget

A summary is presented in Table 5.4.

The picture assumptions made are; 16-bit pixel CCD, requiring 2µm resolution and size 1k x 1k pixels (image size shown in [54]). Monitoring of pressure is important as UHV is required.

Data Budget	Size	Units	Sample Rate (Hz)	Rate (bps)	Remarks
Measurement					
Picture	1.6E+07	3	1.000	4.8E+07	One set of three photographs per BEC cycle
Instrument Sensors (Mass/Power Allocation in Thermal Item)					
BEC Vessel Pressure	33.0	5	0.1	16.5	Monitoring, Continuous
BEC Vessel Temp	19.0	5	0.1	9.5	Monitoring, Continuous
Housekeeping Allocation					
20% of Total Data				9.60E+06	
Total w/o Margin				5.76E+07	
TOTAL with Margin	20	%		69.1	Mbps

Table 5.5 – Preliminary Data Budget for the FPE-C Payload

5.3.5   Drag Free Control Requirements

There are no specific DFACS requirements although disturbances should be reduced as much as possible removing any acceleration that could excite the condensate. Changes in the external disturbances over a few seconds to a few minutes are not severe. But the level of DFACS should be considered in greater detail to determine how the external disturbance couples to the BEC. Motion due to disturbances could increase the kinetic energies of the samples, thus impacting on the lowest BEC temperature.

It is assumed at this stage of the study that standard three axis-stabilisation is required. It should be noted that if an AIF is added then the DFACS requirements would become the same as FPE-B (Section (4.6.5)).

PART 3

MISSION ANALYSIS

6   Mission Analysis

Orbit selection is a compromise between science goals, the local environmental conditions, spacecraft technologies and available launchers. The chapter aims to select as an early baseline an orbit based upon these key areas. A small launcher is baselined (VEGA, with Rockot as an option).

6.1   Science Constraints and Requirements

6.1.1   FPE-A – Tests of Special and General Relativity

These tests aim to confirm the theoretical predictions of Special and General Relativity by determining the behaviour of light and Gravitational Red-Shift under differing laboratory frames. The spacecraft provides the laboratory platform.

An important quantity to consider is the relative change in the GRS as a function of altitude. Figure 6.1 shows the difference between GRS at perigee and apogee for a given eccentricity. The perigee is fixed. It can be seen that eccentricity improves the shift whereas altitude is less important. This is because if altitude is increased rather than eccentricity the gravitational potential reduces (*1/r*, (Equation (2.7)), thus the effect decreases. The restriction imposed on the eccentricity is by the desire for the orbit to be SSO.
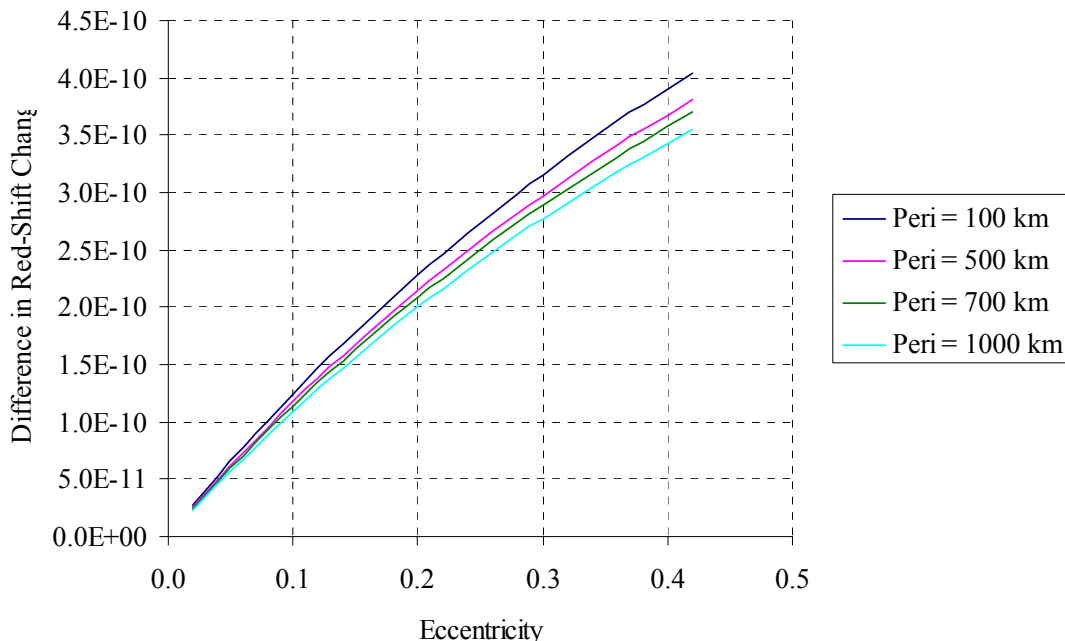
Figure 6.1 – The difference between the red-shift at perigee and apogee for a given eccentricity.

The main drivers for orbit selection imposed by the science requirements are;

- Eccentricity. A height differential allows a variation in the red-shift between space and ground and the comparison of the OR and OAC for the universality of GRS (see Section (2.2.2)).
- High level of thermal stability to maximise the performance of the reference cavities (both for the ORB and the OAC (see Section (3.6.1)))

In summary the selected orbit should be elliptical with a large as possible altitude differential, whilst remaining within the limits of the DFACS system. The orbit should aim to be thermally stable to minimise thermal expansion of the spacecraft and instruments improving accuracy (further detail can be found in the Sci-RD [TN1] or Payload Definition Document [TN2]). Eclipse free periods should be maximised. This all implies a Sun-Synchronous Orbit (SSO). The lowest perigee altitude should be compatible with drag free thruster performance.

6.1.2   *FPE-B – Tests of the Weak Equivalence Principle*

The requirement is to provide the strongest acceleration possible to maximise the magnitude of the differential.

However, the altitude should allow for a drag force no larger than that the DFACS thrusters can compensate for. SSO is chosen to allow for thermal stability. Power can be maintained throughout the orbit with a constant Sun vector, which will remove the need to adjust attitude or cant the solar array. Motion of the spacecraft will affect the spacecraft changing the radial gravitational vector w.r.t. the payload, which is unacceptable. This approach also removes the need to cant the solar arrays so they track the sun. Moving the solar array would be incompatible with using LISA Pathfinder as a platform and also introduce mechanical noise into the spacecraft affecting the experiment.

6.1.3   *FPE-C – Tests of Bose Einstein Condensates*

The requirements of this are similar in terms of FPE-A and B. SSO is desired to maintain temperature stability. An altitude high enough to allow the FEEPs system to compensate for external disturbances is also desired (although the DFACS requirements are yet to be determined).

There are no constraints relating to gravity, GRS or pointing for the BEC. Therefore only undisturbed microgravity conditions are required.

In summary the requirements of the FPE-C orbit shall be an SSO circular orbit. The altitude should allow for a drag force that the FEEP thrusters can compensate for. SSO is chosen to allow for thermal stability. A Dawn-Dusk SSO is desirable remove the requirement of cantable solar arrays (see Section (6.1.2)).

6.2   *Orbital Environmental Constraints*

- **Environmental Stability** – The orbit is desired be as benign as possible. Thermal variations will cause the expansion and contraction of the experimental payload. An SSO will provide

long eclipse free sessions and also maintains the spacecraft thermal gradient as constant. These factors are important for the Differential Accelerometers [TN3], the cavities that the lasers are locked to [TN2] and the kinetic energy of the BEC condensate [†]. Therefore the goal would be to select an orbit that assists the spacecraft in providing ideal conditions for the payload.

- **Altitude** – This is a common driver for the choice of orbit. It affects the launch vehicle performance, the length of eclipses, the degree of the external residual forces and the inclination required for an SSO. Clearly the altitude is coupled to the above environmental discussion. Residual forces will affect the performance the payload and the degree of these forces (with the exception of solar and earth radiation pressure and earth albedo) are driven by altitude. Also at certain altitudes the radiation environments are much more severe, which will impact on test mass charging. Magnetic gradients could affect atomic trap performances.

- **Inclination** – As the inclination increases the radiation environment is changed, as is the magnetic field. One specific implication of changing inclination is the altitude at which the orbit is sun-synchronous (which is ideal for FPE-B).

- **Launch Date** – Eclipse durations and seasons over the entire mission will be affected by the position of the sun at time of launch. A launch just after an eclipse season would maximise the time of thermal stability. Also the solar cycle affects the atmosphere which at its height increases the environmental disturbances.

- **Location of Centre of Gravity** – If the CoM is offset from the centre of pressure a torque will be created. The longer this lever arm is the higher larger the torque. So it may be desirable to design the spacecraft symmetrically and as a single body (e.g., no protruding solar panels)

Rather than environmental stability being a driver, it is driven by the choice of altitude, inclination and launch date of the orbit and mission.

As a summary the major affects on the payload due to various orbital influences are summarised in Table 6.1.

More specifically for FPE-A is the fact that an elliptical orbit is required, thus eclipses are affected by the position of the argument of perigee (AoP) and Right Ascension of the Ascending Node (RAAN). Also the orbital environment is further complicated by the changing environment over an orbit depending on eccentricity (which drives both velocity and altitude over the whole orbit).

Parameters 4-8 in Table 6.1 are important for sizing the drag-free control system. Figure 6.2 shows the magnitude the linear acceleration illustrating that all are important in terms of the WEP test accuracy desired. Figure 6.4 shows the Torque the spacecraft is likely to encounter of each of these as a function of altitude.

[†] FPE-C Tests of Quantum Gases is yet to be assessed in great detail but the disturbances on the spacecraft are expected to influence orbit choice in a similar way to FPE-B. The payload is also expected to be similar.

	Parameter	FPE-A Affects	FPE-B Affects	FPE-C Affects	Driven By
1	Radiation	Damage to electronic and optical components	Charging of TMs. Damage to electronic components	Momentum and energy transfer to the BEC	Altitude, Inclination
2	Gravity Gradient	n/a (there are spacecraft torque effects)	WEP signal mimicking due misalignment of the TMs CoMs Strength of gravity	n/a (there are spacecraft torque effects)	Altitude, *(Inclination to some degree as the magnitude of J2 depends on it also)*
3	Eclipses (when and duration)	Cavity stability due to thermal gradients	TM Thermal Gradients	BEC Thermal Gradients	Launch date, Arg. of Perigee, RAAN, Altitude, Eccentricity
4	Solar Radiation Pressure	Cavity stability by residual forces	Disturbance of test masses due to residual forces	Disturbances increasing BEC kinetic energy (temp)	Solar season (hence launch date)
5	Magnetic Field	Magnetic effects on the trap. Residual forces on cavity.	Disturbance of test masses due to residual forces	Performance of MOT trap from stray fields	Altitude, inclination, solar season (hence launch date)
6	Aerodynamic Drag	Cavity stability by residual forces	Disturbance of test masses due to residual forces	Disturbances increasing BEC kinetic energy (temp)	Altitude, solar season (hence launch date)
7	Earth Radiation Pressure	Cavity stability by residual forces	Disturbance of test masses due to residual forces	Disturbances increasing BEC kinetic energy (temp)	Altitude, solar season (hence launch date)
8	Earth Albedo	Cavity stability by residual forces	Disturbance of test masses due to residual forces	Disturbances increasing BEC kinetic energy (temp)	Altitude, solar season (hence launch date), inclination
9	Moons Gravity	n/a (there are spacecraft torque effects)	WEP signal mimicking due misalignment of the TMs CoMs	n/a (there are spacecraft torque effects)	Altitude
10	Suns Gravity	n/a (there are spacecraft torque effects)	WEP signal mimicking due misalignment of the TMs CoMs	n/a (there are spacecraft torque effects)	Altitude

Table 6.1 – Influences on the selection of an FPE orbit

There are other factors which determine the orbital environment, most notably radiation, which is important in terms of Test Mass (TM) charging. Figure 6.3 shows the radiation environment in the vicinity of the Earth. The key aspects to note are the polar horns, as an SSO is recommended and the South Atlantic Anomaly may be encountered, therefore flight through these areas is unavoidable. However the effect can be minimised by having a low altitude below the majority of the Van Allen belts. This will not be possible for elliptical orbits of the order shown in Figure 6.1 as they will encounter radiation. But the radiation environment is more important mainly for TM charging.

Eclipses are another factor which can be dependant on altitude, even in SSO. There will be times during the year when the Sun has a declination high (or low enough depending on the season) such that even in an Dawn-Dusk SSO the spacecraft may eclipse at high latitudes.

If the Test Masses are slightly misaligned such that one is closer to the Earth than the other a differential acceleration will be detected between them. This would mimic a WEP signal violation. The TMs could be aligned to within 3×10^{-9}m. This will create the differential acceleration of greater magnitude than the WEP violation.

The detailed calculations and background is provided in [TN5]. The calculations assume a reference spacecraft and other assumptions as described in Table 6.2.

Mass (kg)	750
x-length (m)	1.9
y-Length (m)	1.9
z-Length (m)	0.9
Ix (kg m^2)	276.3
Iy (kg m^2)	276.3
Iz (kg m^2)	451.3
A of x-y (m^2)	3.6
A of x-z and y-z (m^2)	1.7
Coefficient of Drag	2.2
CoP – CoM offset (m)	0.95
Reflectivity	0.6
Residual Magnetic Moment (A m^{-2})	5.0
Test Mass CoM Misalignment (m)	1.0×10^{-8}
Off Axis Pointing (deg)	1.0

Table 6.2 – Spacecraft data assumed for disturbance sizing
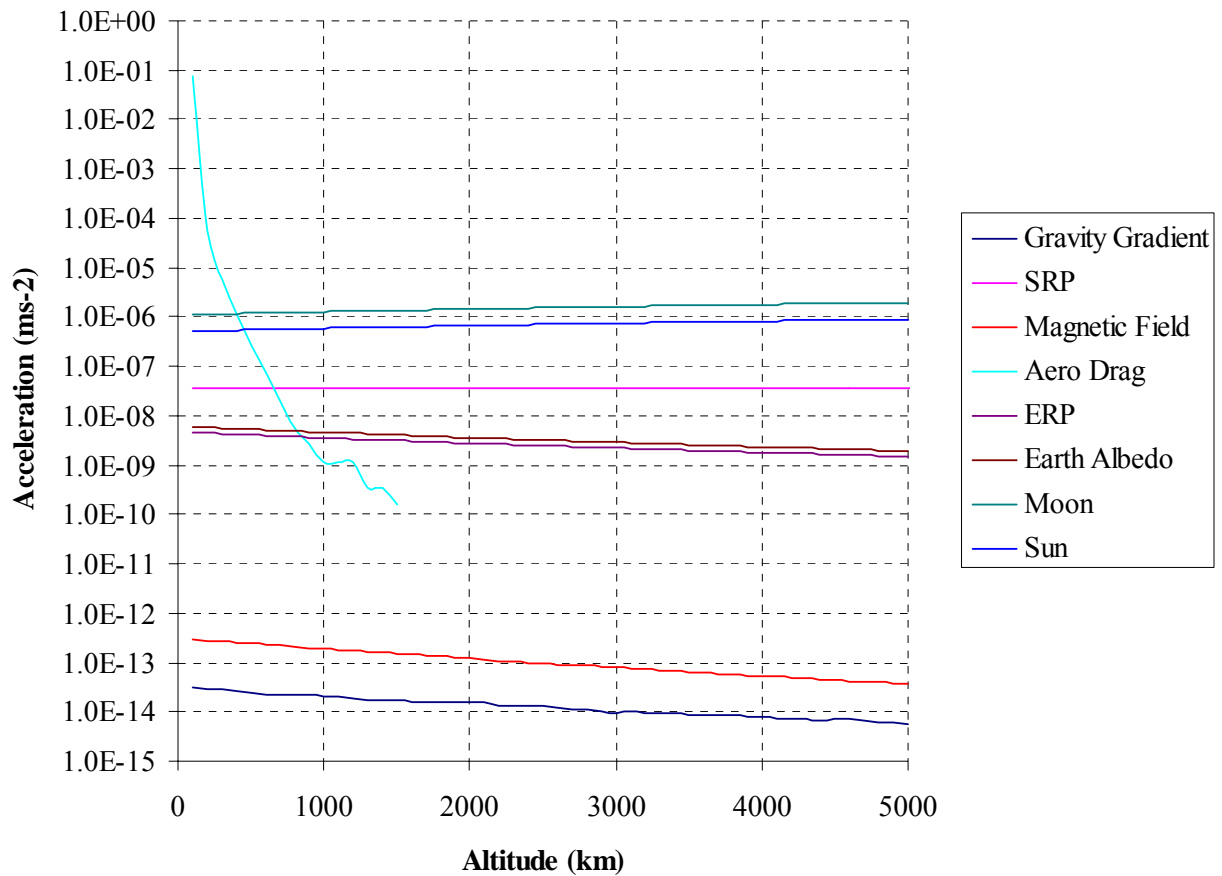
Figure 6.2 – Orbital Linear Acceleration Disturbance Sizing as a Function of Altitude
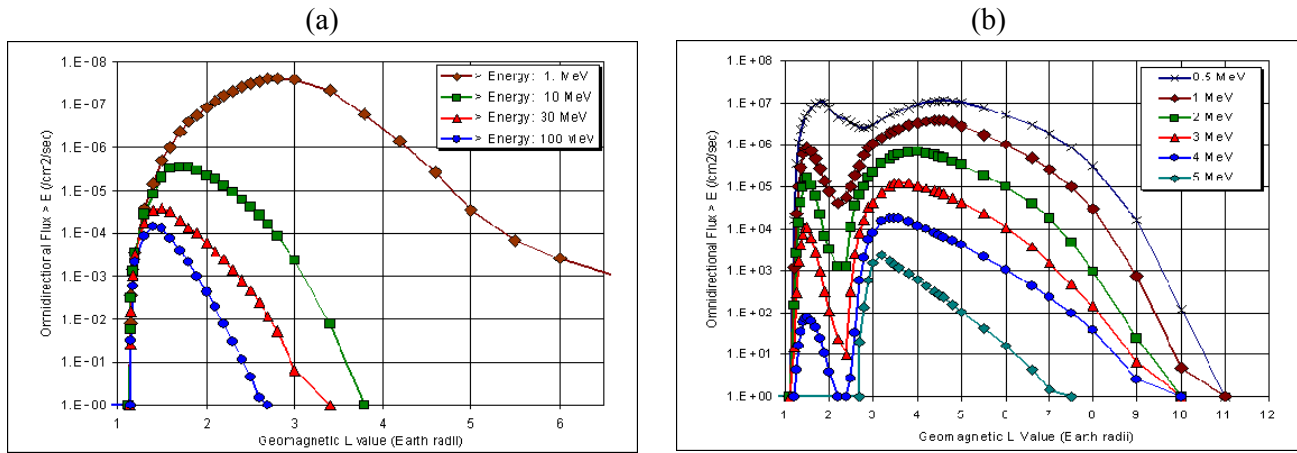
Figure 6.3 – Flux Density of the Radiation Belts as a function of Altitude.
(a) The Proton radiation belts and (b) the Electron radiation belts taken from [40].
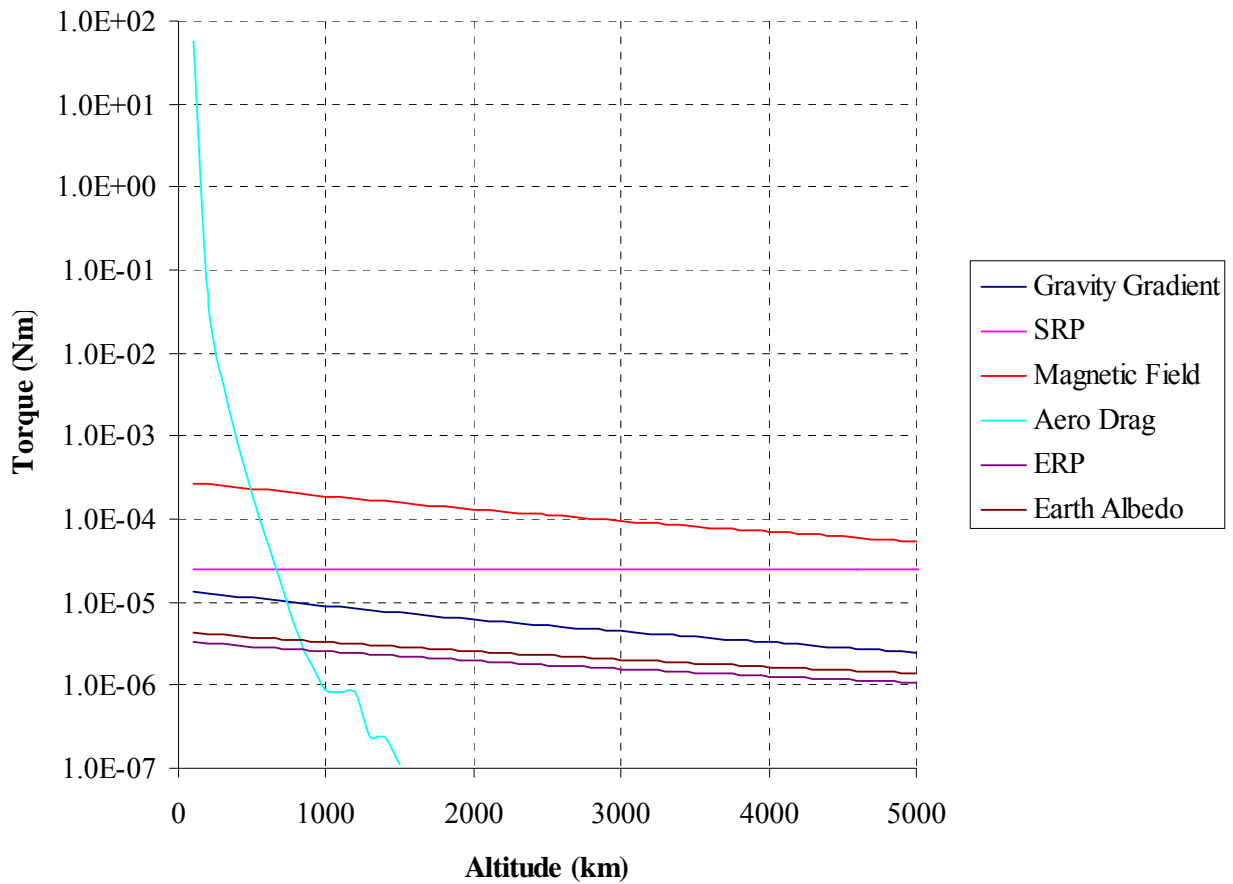
Figure 6.4 – Orbital Disturbance Torque Sizing as a Function of Altitude

6.3   Sun-Synchronous Orbit Constraints
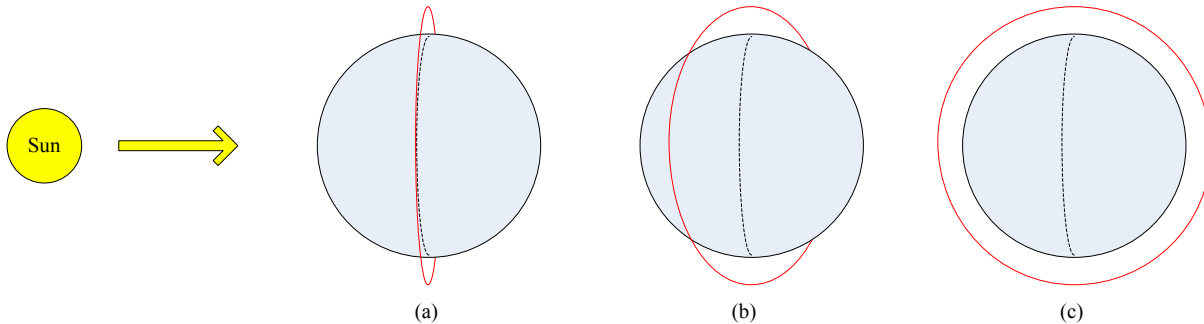
Figure 6.5 – Examples of possible SSO
(a)Dawn/Dusk, (b) Mid-Afternoon/Mid-Night and (c) Noon-Midnight (The dotted line shows the terminator).

A Sun-Synchronous orbit (SSO) is an orbit which the regression of the Right Ascension of the Ascending Node (RAAN), due the Earth oblateness J2 effect is equivalent, to 2π in one year.

The following equation expresses inclination as function of semi-major axis and eccentricity bounded by a fixed rate of regression (2π, Sun Synchronous),

$$\cos i = -\frac{4\pi a^{7/2}(1-e^2)^2}{3J_2 R_E^2 \sqrt{\mu}\tau_{YR}}$$

6.1

Where J_2 = zonal coefficient relating to the equatorial bulge, R_E = the Earths radius (m), a = semi-major axis (m), e = the eccentricity, and i = the inclination (rad), τ_{yr} = time in seconds for one year and τ is the orbital period.

A Dawn-Dusk is selected as this will minimise eclipses to seasonal periods around the solstices. The length of the season and longest eclipse duration is dependant on the inclination and altitude. A spacecraft with a low inclination has longer eclipses and more frequent seasons, whereas a near 90^0 is shorter and less respectively. The types of SSO are shown in Figure 6.5 including the Dawn-Dusk.

Figure 6.6 shows inclination as a function of altitude. It is clear there is a limit on the altitude. The calculation is repeated in Figure 6.7 for some elliptical cases. There are more constraints on altitude for an elliptical orbit. If we assume a maximum realistic inclination of 110^0, a range of acceptable orbits can be seen in Figure 6.8. When compared with Figure 6.1 there is a limit to magnitude of relative GRS.

Changing the rate of regression results in fewer restrictions on the inclination and altitude, however there is no direct benefit to the FPE-A science, as these orbits will have regular eclipses. Analysis is performed in [TN4].
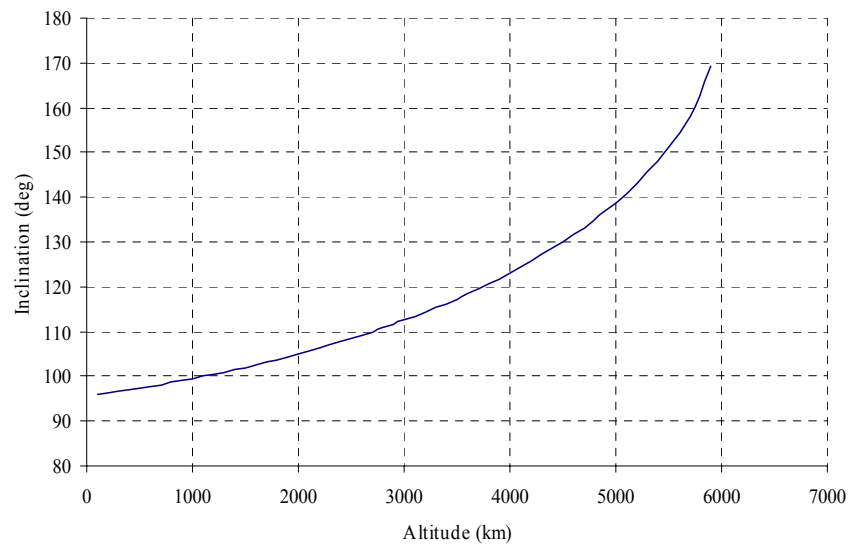
Figure 6.6 – Circular SSO Inclination for a given Altitude
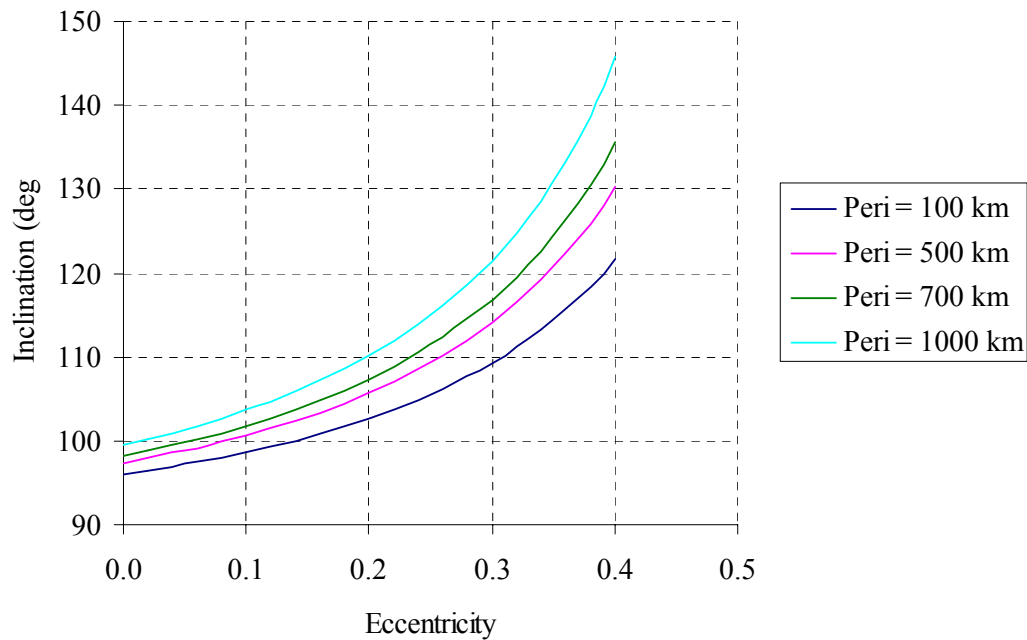
Figure 6.7 – Inclination as a function of Eccentricity for a SSO
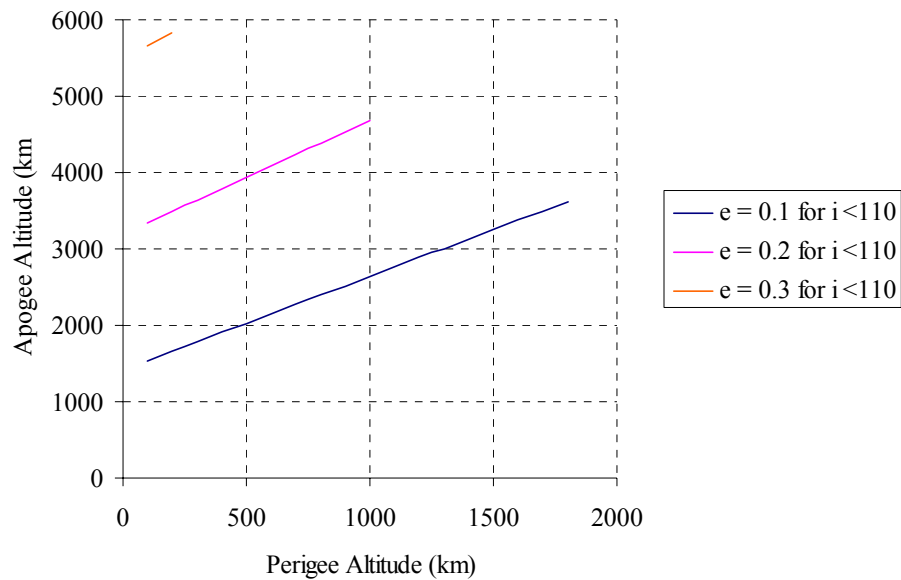
Figure 6.8 – Perigee against Apogee for Practical SSOs for a Given Eccentricity

6.4   Launcher and DFACS Constraints

6.4.1   Launchers

The launcher should be in keeping with the goal of implementing a low cost mission and ESA policy. For this reason the launcher option considered is VEGA [41] and Rockot [42] as reserve. They are both small low-cost European launchers. The performance specification for VEGA is shown in Figure 6.9
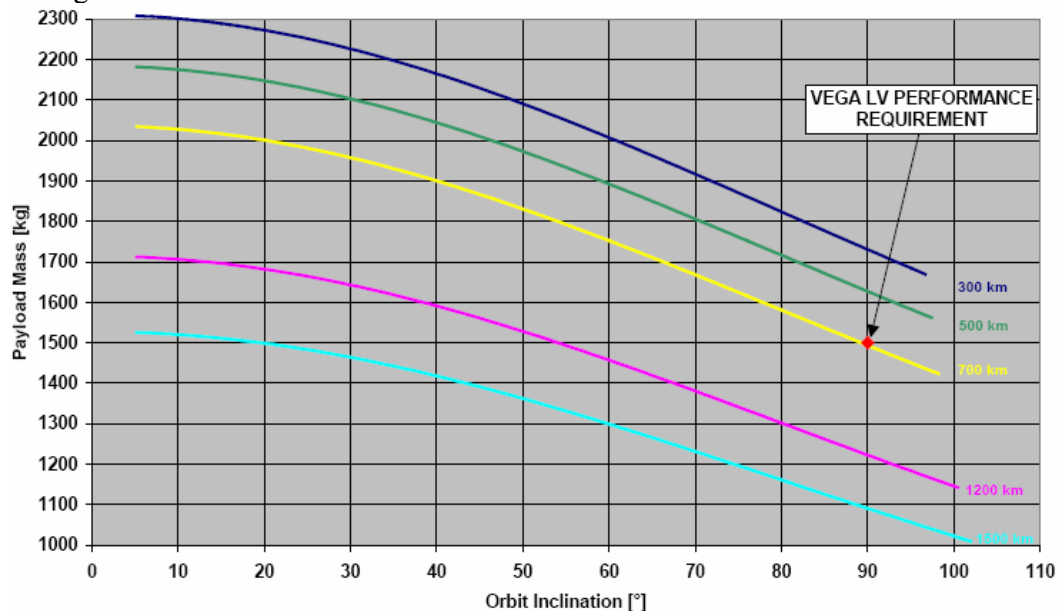
Figure 6.9 – VEGA Launch Payload Performances into Circular orbit [41]

The computation of the performance of an elliptical orbit is much more complex than the circular case and has to be defined specifically. Two cases were considered and computed. They were chosen to gain a feel of the boundaries of performance. A perigee of 500 km was chosen to be a compromise between an orbit too low incurring drag penalties at 1000 km being too high for incurring radiation penalties. Two inclinations for this perigee were chosen, 45^0 and 90^0, with a required payload of 750 kg. The objective was to determine the maximum apogee. The results are presented in Table 6.3.

	Case A	Case B	Case C	Case D	Case E (500 kg Payload)
Inclination	45 deg	90 deg	105 deg	105 deg	105
Perigee Altitude	500 km	500 km	700 km	500 km	700 km
Apogee Altitude	7103 km	4489 km	2860 km	3190 km	4750 km

Table 6.3 – VEGA Performance for Elliptical Orbits
Assuming $M_{S/C}$ = 750 kg, 90 kg fuel reserve and two burns by the AVUM (fourth stage)
(Credit: ESA)

6.4.2   FEEP Performance

The constraint on orbit selection is driven by the maximum thrust of the DFACS actuator or thruster. As we are considering LISA Pathfinder's potential for re-use, so FEEPs are used as a reference.

The thrust of a DFACS thruster is assumed to be 75-150 µN from ARC Seibersdorf Indium [43] or the ALTA Cs FEEP. A choice is yet to be made. For a 750 kg spacecraft this amounts to an acceleration of $1 \times 10^{-7} – 2 \times 10^{-7}$ ms^{-2}. The torque that can be created assuming a lever arm of 0.95 is 1.43×10^{-4} Nm.

6.5   FPE-A Orbit Trade Study

The starting point is to take advantage of the SSO for power and thermal stability reasons. Eclipses are minimised as is attitude adjustments to maintain sun pointing for a fixed solar panel. As considered in the early parts of Section (6.2) altitude and inclination are the key parameters. The choices of which are limited by the SSO constraint. One must be chosen to be fixed, which is used to base the trade upon. The choice is inclination. The value is chosen to be 105^0 as the maximum allowable SSO inclination keeping in mind Vega performances. It is believed that an inclination higher would be un-realistic.

The aim is to choose an orbit which, when perigee altitude is traded, satisfies:
- Minimise thermal instability, for cavity stability and hence clock accuracies [TN2]
- SSO (see Section (6.3))
- Acceptable for the Vega launch vehicle (see Section (6.4.1))
- Largest possible eccentricity (see Section (6.3))
- Lowest possible external disturbances, so not to exceed the FEEP capabilities (see Section (6.2) and (6.4.2))
- Minimises the eclipse duration and season

- Maximise the relative red-shift (see Section (6.1.1))
- Maximise measurement accuracy for Red Shift (see Section (6.1.1))

The results are shown in Table 6.4. A summary of the trends are shown in Table 6.5. As the perigee increases the apogee decrease so to compensate and so the orbit remains an SSO. However this reduces the eccentricity which we desire to maximise. An increase in perigee reduces the magnitude of the non-gravitational forces. A reduction in the time spent in eclipse is seen due to the reduced time in behind the Earth at the Solstices. The relative G-RS reduces as the eccentricity reduces.

Table 6.3 shows the performance of the Vega launcher. At 105^0 and higher perigees result in payload mass penalties. LISA Pathfinder is around 500 kg so orbits up to a perigee of 700 km will be acceptable.

If SSO is deemed to be too expensive in terms of launch vehicle, a move away from SSO would be possible allowing larger eccentricities. The penalty is the reduction in eclipse free periods of the orbit and the loss of constant sun pointing. To optimise the eclipse free periods it is suggested that the position of the argument of perigee should be considered in detail such that it is near the south pole for the winter solstice and at the north for the summer solstice (for the northern hemisphere). An analysis of the precession of the line of apsides is required for this.

High apogees are more susceptible to being perturbed by the Sun and Moon [TN4]. The important quantities to assess are the non-gravitational linear accelerations and all potential torques. The Sun and Moon are more important with regards to orbit maintenance rather than for disturbance force compensation.

The thermal stability requirements are very stringent as can be seen in [TN2]. If, at any time the spacecraft enters eclipse, science measurements are no longer possible.

The perigee is not desired to be lower than 700 km as a 150 µN thruster (Section (6.4.2)) can only provide 1×10^{-7} ms^{-2} in total acceleration compared with the total perturbation. The total torque available (1.43×10^{-4} Nm) is lower than the max torque disturbance (from 2.7×10^{-4} Nm). This assumed a large lever arm and CoM to CoP offset of 0.95 m so in principle could be lower. However the FEEPs could be assisted by a magnetic torquer. Reaction wheels are noisier and undesirable. Another option is to minimise the residual magnetic moment of the spacecraft. This is considered because the magnetic field is the dominant torque in these altitude ranges generally. A reduction of the residual magnetic moment to 1 A m^2 at 700 km reduces the torque to 4.3×10^{-5} Nm, which is more within FEEP capabilities.

If the spacecraft mass is 500 kg, the total acceleration that can be generated is 3×10^{-7} ms^{-2}, allowing a little more margin when compared to the local residual acceleration. A 600 km may be possible but allowing for a margin makes 700 km more sensible, and reduces the magnitude of the torques. However, if in the program the mass of the spacecraft increases dramatically, the implications on orbit selection would be severe, possibly resulting in delay due to orbit re-design. Also launcher performance would be affected (see Table 6.3).

Perigee (km)	Max Ecc.	Apogee (km)	Linear (@ perigee)		Angular (@ perigee)		VEGA Performance (Yes/No)	Eclipse (Longest mins, Season days)	Relative Red-Shift $((\Delta v/v)_{apo} - (\Delta v/v)_{per})$
			Dominant/Max Perturbation (ms-2)	Total Perturbation (ms-2)	Dominant/Max Perturbation (Nm)	Total Perturbation (Nm)			
100	0.24	4191	9.4×10^{-2} (drag)	9.4E-02	7.0E+01 (drag)	7.0E+01	Yes	TBD	2.65E-10
300	0.22	4067	7.2E-06 (drag)	7.3E-06	5.2E-03 (drag)	5.4E-03	Yes	TBD	2.39E-10
500	0.20	3939	3.1E-07 (drag)	3.6E-07	2.3E-04 (Mag Field)	5.0E-04	Limit	TBD	2.15E-10
600	0.18	3664	8.3E-08 (drag)	1.3E-07	2.2E-04 (Mag Field)	3.2E-04	Payload < 750kg	TBD	1.94E-10
700	0.17	3599	3.5E-08 (SRP)	6.9E-08	2.1E-04 (Mag Field)	2.7E-04	Payload < 600 kg	TBD	1.82E-10
1000	0.14	3402	3.5E-08 (SRP)	4.5E-08	1.9E-04 (Mag Field)	2.3E-04	Payload < 500 kg	TBD	1.47E-10

Table 6.4 – Elliptical Orbit Trade Study for FPE-A

Perigee is the trade parameter and the resulting eccentricity is constrained by an inclination of no more than 105^0. The eccentricity shown results in an SSO with this inclination. The moon and sun gravitational perturbations are not included in the trade as they are assumed affect both payload and spacecraft at a common CoM. Relative forces between payload and spacecraft due to the sun and moon are assumed to be negligible. Other forces change at a much higher frequencies. Radiation is not included in trade as there is not a practical way of avoiding the belts due to the requirement of an elliptical orbit. The effect is more important in terms of Test Mass charging (FPE-B). The perturbation calculations are based upon the incident forces at perigee.
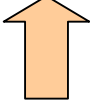
Perigee	Ecc	Apogee	Perturbations (@Perigee)	Launcher Performance	Eclipses Longest (Season)	Relative Red-Shift	Relative RS Accuracy
Up	Down	Down	Down	Down	Down (down)	Down	Down

Table 6.5 – Trend Summary for FPE-A Orbital Trade
Cream = trade parameter, Red = Disadvantage, Green = Advantageous.

The final consideration is the reduction of the perigee altitude to increase the eccentricity of the orbit. This is only possible if the choice of thrusters is changed from FEEP's to a thruster capable of more. The result may be an increase in thruster noise and lower specific impulse (e.g. cold gas) increasing propellant requirements. A reduction in scientific performance may result, due to affects on cavity stability. A further constraint is the objective of reusing LPF, which provides FEEP's anyway. Requiring a different thruster would require changes to LPF, if it was to be re-used.

The orbit selected is highlighted in Table 6.4 and is described in more detail in Table 6.6.

Type	Dawn-Dusk SSO	Thermally stable, seasonal eclipse periods
Inclination	105.4^0	At the limit of the launch vehicle. Reductions in eccentricity may have to be made to compensate to lower inclination
Perigee	700 km	Total disturbances compatible with FEEP's
Apogee	3599 km	
Eccentricity	0.17	
Launcher	VEGA	Could be a difficult orbit to reach, imposing more mass restrictions. Spacecraft could be limited to < 600 kg
RAAN	90^0 on 21st March	Position at the vernal equinox so to provide Dawn-Dusk
Relative Red-Shift	1.82E-10	

Table 6.6 – Summary of selected orbit for FPE-A

It provides the following:
- Perigee altitude within the domain of the LPF FEEP thrusters.
- An eccentricity providing a relative red-shift better than that described in the Sci-RD [TN1 p-12]
- Marginally within the launch vehicle requirements
- Sun-synchronous Dawn-Dusk (Type (a)) and hence thermally stable for long periods
- Eclipses minimised due to Dawn-Dusk SSO

An orbit of higher altitude does not provide much more gain in terms of red-shift magnitude as the effect of G-RS reduces as altitude increases. As an example the differential red-shift between perigee/apogee for 10000/36000 km is 1.65 x 10^{-10}. The orbit has an eccentricity of 0.44.

6.6   FPE-B Orbit Trade Study

As for FPE-A a SSO is desirable for power and thermal stability reasons. Eclipses are minimised as are attitude adjustments that would be required to maintain sun pointing for a fixed solar panel. As considered in the early parts of Section (6.2) altitude is the key parameter.

The aim is to choose an orbit which, when altitude is traded, satisfies:
- Minimise thermal instability
- Minimise charging effects on the Test Masses
- SSO (see Section (6.3))
- Acceptable for the Vega launch vehicle (see Section (6.4.1))
- Maximise the magnitude of the WEP signal, i.e., the strongest possible gravitational field.
- Lowest possible external disturbances, so not to exceed the FEEP capabilities (see Section (6.2) and (6.4.2))
- Minimises the eclipse duration and season

The results of the trade study are shown in Table 6.7 and a trend summary is shown in Table 6.8.

The important quantities to assess are the non-gravitational linear accelerations and all potential torques. The Sun and Moon are more important with regards to orbit maintenance rather than the attenuation of forces for measurement purposes.

As the altitude is increased the total perturbations (not including Sun and Moon) lower until at around 700 km the FEEPs are able to compensate for the linear accelerations. In terms of torque at all the altitudes shown the FEEPs will require assistance from magnetic torquers for the same reason as FPE-A (Section (6.5)). An increase in altitude to around 1000 km will result in a more severe radiation environment rather than just the SAA (which affect orbits above 350 km).

This would require more discharging sessions of the Test Masses which would impinge on a limited measurement time (cryogen lifetime). VEGA performance is acceptable for SSO inclinations to just above 2000 km. But the altitude limit is mainly imposed by the radiation belts.

The eclipse season durations are lowered as around the solstices, the spacecraft is further from the Earth reducing the time spent behind.

Unlike FPE-A, FEEPs are the required thrusters for drag compensation. Other thrusters are too noisy, so therefore replacing them with a more powerful alternative will be undesirable. The minimum altitude is therefore difficult to redefine.

| Range (km) | Linear (non-gravitational) | | Angular | | TM CoM Misalignment Grav Grad (ms^{-2}) | Radiation Flux P>10Mev, E>1MeV $(cm^{-2} s^{-1})$ | VEGA Performance (kg) | Eclipse (Longest mins, Season days) | SSO Requirements (inclination) |
	Dominant/Max Perturbation $(ms-2)$	Total Perturbation $(ms-2)$	Dominant/Max Perturbation (Nm)	Total Perturbation (Nm)					
100-500	7.9E-02 (aero drag) – 2.6E-07 (aero drag)	7.9E-02 – 3.1E-07	5.6E+01 (Drag) – 2.3E-04 (Mag Field)	5.6E+01 – 4.6E-04	3.0E-14 – 2.5E-14	Small. Highest avg flux is at poles order 10 for protons and $1x10^4$ for electrons	1550 – 2300	TBD	$96.0^0 – 97.4^0$
500-1000	2.6E-07 (aero drag) – 3.5E-08 (SRP)	3.1E-07 – 4.5E-08	2.3E-04 (Mag Field) – 1.9E-04 (Mag Field)	4.6E-04 – 2.3E-04	2.5E-14 – 2.0E-14	Beginnings of the Van Allen belts at 1000 km. Highest flux constant over whole orbit >1000 for protons and $1x10^5$ at the poles for electrons	1250 – 2190	TBD	97.4 – 99.5
1000-2000	3.5E-08 (SRP) – 3.5E-08 (SRP)	4.5E-08 – 4.2E-08	1.9E-04 (Mag Field) – 1.3E-04 (Mag Field)	2.3E-04 – 1.7E-04	2.0E-14 – 1.5E-14	Most of orbit in P+E radiation belts. Protons $5x10^4$ max and electrons $1x10^5$ for nearly ¼ orbit.	650-1850	TBD	99.5 – 104.9
2000-5000	3.5E-08 (SRP) – 3.5E-08 (SRP)	4.2E-08 – 3.9E-08	1.3E-04 (Mag Field) – 5.4E-05 (Mag Field)	1.7E-04 – 8.4E-05	1.5E-14 – 5.8E-15	At 5000km avg. is $5x10^4$ for protons when crossing the equator. For electrons flux is $5x10^5$ towards $1x10^6$.	1100 – n/a	TBD	104.9 – 138.6

Table 6.7 – Circular Orbit Trade Study for FPE-B

The launcher performances are between best cases near launch latitude for the lowest altitude to worst case SSO inclination for the largest altitude. The Sun and Moon gravitational effects are not included as the spacecraft is required to naturally follow the local geodesic. If the Sun or Moon were to pull on the TMs differently that in itself is a violation of the equivalence principle. The effect needs to be monitored as the orbit may require correction. The linear gravity gradient is not included as the effect could also be a WEP violation (see [TN4] Section (2.3.1)).
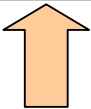
Altitude	Perturbations (@Perigee)	TM Misalignment Gravity Gradient	Radiation	Launcher Performance	Eclipses Longest (Season)	SSO Inclination	Gravity
Up	Down	Down	Up	Down	Down (down)	Up	Down

Table 6.8 – Trend Summary for FPE-B Orbital Trade
Cream = trade parameter, Red = Disadvantage, Green = Advantageous

The orbit selected is highlighted in Table 6.7 and is described in more detail in Table 6.9.

Type	Dawn-Dusk SSO	Thermally stable, seasonal eclipse periods
Inclination	98.19^0	
Altitude	700 km	Total disturbances compatible with FEEPs. Torquers to provide assistance
Eccentricity	0	
Launcher	VEGA	Maximum mass of spacecraft 1400 kg
RAAN	90^0 on 21st March	Position at the vernal equinox so to provide Dawn-Dusk
Test Mass Misalignment Gravity Gradient (3×10^{-8} m)	2.31×10^{-14} ms^{-2}	Adjustment required to measurements in post processing.

Table 6.9 – Summary of selected orbit for FPE-B

It provides the following:
- Perigee altitude within the domain of the LPF FEEP thrusters.
- Within the launch vehicle requirements up to 1400 kg.
- Sun-synchronous Dawn-Dusk (Type (a)) and hence thermally stable for long periods
- Eclipses minimised due to Dawn-Dusk SSO
- Minimises radiation by staying below the Van Allen belts. However it should be noted that passes through the SAA may occur. Detailed orbit design may provide a profile to avoid it.

Knowledge of the TM CoM alignment is required as accelerations due to this could be higher than the WEP signal.

6.7   FPE-C Orbit Trade Study

The orbit is baselined to be similar to FPE-B in that the altitude is the main driver. The BEC itself does not have any pointing or orbital requirements. An environmentally quiet environment would be desirable. Thus the comfort zone identified for FPE-B would be adequate for FPE-C. However, a particular area that would need more consideration is the magnetic effects on the trap reducing its performance.

The aim is to choose an orbit which, when altitude is traded, satisfies:
- Minimise thermal instability
- Minimise magnetic effects
- SSO (see Section (6.3))
- Acceptable for the Vega launch vehicle (see Section (6.4.1))

- Lowest possible external disturbances, so not to exceed the FEEP capabilities (see Section (6.2) and (6.4.2))
- Minimises the eclipse duration and season

Unfortunately the desire to have a thermally stable orbit and low magnetic fields are contradicting factors. An SSO will be thermally stable, but passing through the magnetic horns at higher latitudes. In complete opposition at the equator the thermal stability will be harder to control. Since FPE-C experiment has no specific altitude, eccentricity, pointing and gravitational requirements (just microgravity), the FPE-B solution seems ideal. The mission analysis for both missions will be similar reducing the need for detailed trades and analysis, building on the FPE-B orbital heritage.

The FPE-B orbit is selected for FPE-C and can be seen in Table 6.9.

PART 4

ADAPTABILITY OF LISA

PATHFINDER

7   Introduction

LISA Pathfinder (LPF) is a precursor to the LISA mission aiming to study gravitational waves from distant parts of the galaxy. This technique will allow the direct detection of black holes, which is not possible currently without inferring their existence from local phenomena such as accreting binary systems and high energy x-ray sources. LPF will demonstrate drag-free control and test the interferometric technology needed to detect the gravitational waves. The science part of the spacecraft will be delivered to L1 by a dedicated propulsion module, using a manoeuvre consisting of a number of burns designed to increase altitude incrementally. The measurement of gravitational waves will lead to some testing of fundamental physics.

To these ends it is being considered that LPF may be an option as a spacecraft platform for FPE. This section aims to compare LPF with the constraints imposed by the FPE payloads, to determine its suitability. This will include analysis of the available resources and how LPF may need to be adapted.

LISA Pathfinder is presently in phase C/D and the detailed design is being finalised. On this basis, the summary of the spacecraft presented here is subject to further evolution.

8   LPF Description

8.1.1   Orbit

A maximum 1910 kg launch mass is injected into a Lissajous orbit at L1, at distance varying during the mission between 1.1 and 1.7 Million km. A 400 N main engine contained within a dedicated propulsion module using incremental burns to raise the apogee and then transfer to L1 with a ΔV totalling 3100 ms^{-1} [48]. The launcher is baselined to be Rockot. It should be noted that studies are on going to determine the compatibility of LPF with the new Vega launcher.
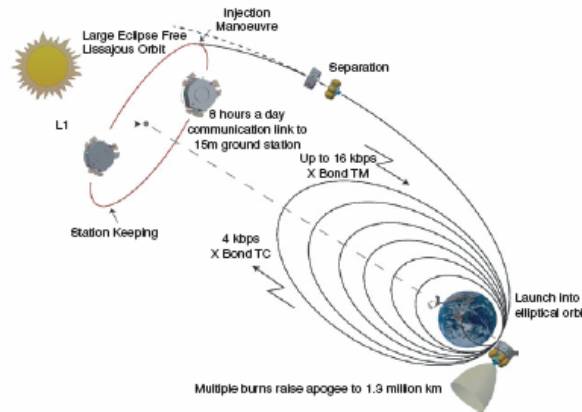
Figure 8.1 – The Mission Scenario of LISA Pathfinder (LPF)

Clearly this defines a set of intermediate orbits to allow for two tracking passages and 8 hrs for orbit manoeuvre preparation. Allowed for in this time is the design and uploading of commands for the upcoming manoeuvre with enough ground station contingency. Enough contact time between the spacecraft and ground has to be allowed, for the spacecraft to be properly prepared. The sequence of orbits must be designed to minimise the radiation dosage and minimise fuel consumption throughout the transfer to L1.

The amount of propellant takes into account deviations from the ideal case due to the use of finite duration burns. Missed burns incur penalties due to extra time spent in particular orbits thus needing increased propellant for attitude control due to perturbations such as J2 and aerodynamic drag dependant on altitude.

The apogee raising manoeuvres (15 burns) takes approximately 15 days. This does not include the LEOP spacecraft commissioning, contingency or the transfer to L1 from the last burn. The timeline proposed for mission operations is 90 days from launch to the start of science operations in the Lissajous orbit.

8.1.2   Science Objectives

LISA Pathfinder is to study the model of geodesic motion in space of a free test mass. This includes the study and characterisation of all possible effects on such an instrument from itself, the spacecraft and the external environment.

The determination of these factors involved will allow the physical models to be confirmed and allow the gravitational motion of a Test Mass to be determined.

Some of the contributors to the motion are (more detail in [44]):

- Patch Fields – Spatial variations of the work function change the magnitude of the electrical potential or patches, which influence the motion of the TM in its cage.
- Brownian Motion – Damping from this is a random force and is expected to be due to residual particles in the vacuum chamber hitting the TM (the Brownian motion if the particles surrounding the TM). Also there can be non-contact forces inducing a small damping effect. They are known as surface dielectric losses.
- Radiometer effects and Thermal Gradients – Particles with higher momentum striking the surface of the test mass due to higher temperature than compared with a lower temperature on the other, create a residual force. The same is true if one electrode is hotter than the others.
- Cosmic Rays – Charged particles striking the TMs will change the electric potential across it. Clearly this will change how the TM responds to the electrostatic field surrounding it.
- Characterisation of Magnetic Effects – Magnetometers will create magnetic fields around each TM to characterise their response and thus attaining a good knowledge of the effect of stray magnetic fields.

Flying one TM drag free and monitoring its behaviour by controlling the other can only be performed on a drag free spacecraft.

The results of these experiments would be advantageous to FPE, as it would provide experience of the characterisation of Inertial Sensors (IS) and DFACS.

8.1.3   The LISA Technology Package (LTP) (Payload)

The LTP itself consists of an Inertial Sensor Sub-system, and Optical Metrology Sub-system, which are distributed in an opto-mechanical assembly (LCA) and the related electronics. In addition there is a Data and Diagnostics Sub-system containing a computer and a set of diagnostic instruments.

The inertial sensors are free floating Test Mass (TM) based. Within their housing is a set of electrodes providing capacitance sensing of the position of the TM. The motion of the TM will cause a differential capacitance across one pair of electrodes. One set of electronics per TM provides a read of the capacitance detecting the motion and rate of the test mass. Each TM is contained within a vacuum chamber to reduce disturbances. Charging due to cosmic rays is discharged by applying ultraviolet light periodically to the TM surface. There is a caging mechanism built in to lock the TMs firmly during launch and more softly in safe mode. In addition it is used as a mechanism to position the test masses at the centre of the electrode housing.

The area between the green test mass chambers is the optical bench which provides the means to measure the differential displacement between the two TMs by means of interferometry. A delay in the laser between the two masses will cause an interference pattern corresponding to a change in the relative distance between the TMs. In the LISA baseline the TMs are located 5×10^9 m and the change in this distance is caused by many effects, including the passage of a gravitational wave. The LTP is designed to test the principle of a gravitational wave and characterise the disturbances and its performance. It cannot detect due to the distance, any gravitational waves.
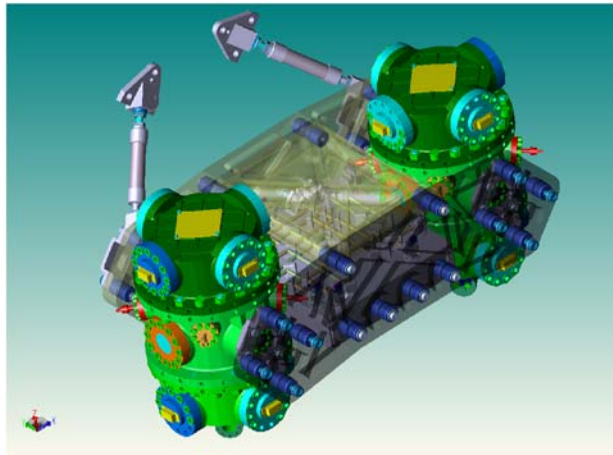
Figure 8.2 – A 3D Model of the LISA Technology Package

We now turn our focus to the inertial sensors themselves, a description of the components can be described. One single inertial sensor weighs 20 kg. Essentially the test mass is contained within a vacuum enclosure at 10^{-5} Pa, an extremely high vacuum. There is 38 cm between test masses and each is a cube of width 46 mm. Material wise, they are 73/27 Gold/Platinum alloys and weigh 1.96 kg. A dedicated getter pump is used to maintain the vacuum system. Space itself is deemed to be too dirty to be used as the method of evacuation. Quantitative are data taken from [TN7].

Larger TMs unlike those employed on MICROSCOPE require a locking mechanism. Forces experienced during launch will cause impact damage if TM is left free. One example was in the testing of the DRS locking mechanism. Rather than clamping the TM, the design opted for small rods for the TM to knock against. During vibration tests the rods drilled precise small holes into the TM causing significant damage. The importance of a method of locking the TM cannot be overstated. The LTP TM's are held by rods at each of its four corners. Fifth and sixths rods are present and their purpose is to position the test mass. An actuation mechanism releases the rods pushing away from the TM. This must be done to make sure the TM is released evenly across all the rods. Any force differential will cause a torque, which may make the TM tumble (Figure 8.3).
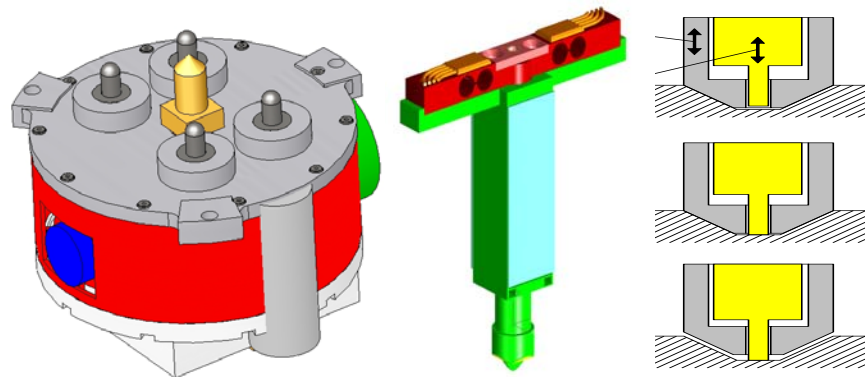
Figure 8.3 – Caging Mechanism for the TM during launch [TN7]

A set of UV lamps are used to discharge the TMs. In space the TMs will be subject to charging from cosmic rays. There are two options with which to discharge a TM. The first is by using a contact wire, which is the case in the MICROSCOPE accelerometer. The second is by shining UV light on the surface (mercury lamp). The photo electric effect causes the discharge. The method can be continuous or over discrete intervals. The electrode housing can also be discharged.

The Inertial Sensors provide the reference masses (also drag free attitude information). An optical bench is placed between each test mass. A laser is incident on the TM surface via a window in the can. The laser beams are then recombined by a set of mirrors on the bench to form an interference pattern, which is compared to a reference to provide a measure of a gravitational wave. The bench base is composes of Zerodur. Each mirror is bonded to the base plate using a silicate. It is not desirable for the mirror to shift from its designed nominal position.

The LTP has the following demands of the spacecraft.

	'w' Margin
Power	165 W
Mass	150 kg
Telemetry	1900 bps

Table 8.1 – LTP Mass, Power and Telemetry requirements
Power is the most demanding LTP mode

Ideally we would want the FPE payload to stay within these bounds otherwise the required LPF sub-systems would have to be adapted. Although, higher data rates could be accommodated as LPF flies at L1 and the FPE is envisaged to be placed into LEO. It should be noted that the inertial sensors would be included in the mass budget above as the package is integrated.

The LTP is designed to perform with the following noise spectrum. This goal comes from the LISA requirements, but at one order of magnitude lower. Figure 8.4 shows the Power Spectral Density (PSD) of the performance.
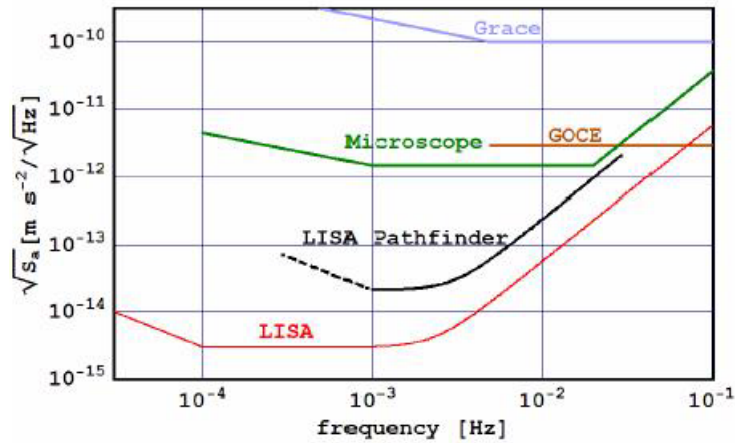
Figure 8.4 – Comparison of science requirements expressed as a PSD, showing the LPF goals [44]

In principle the thrusters must be provide a noise performance that allows an unhindered operations of the LTP sensors.

The requirements of the LPF system differential acceleration noise is,

$$S_a^{1/2} = 3x10^{-14}\left[1+\left(\frac{f}{3mHz}\right)^2\right]ms^{-2}Hz^{-1/2}$$

8.1

For 1mHz<f<30mHz [44].

8.1.4   Structures and Configuration

The entire spacecraft including the propulsion module has a height of 2.7 m and a maximum outer diameter of 2.1 m.

The area of particular interest is the science spacecraft where the FPE payload would be placed. This is hexagonal in shape with the payload situated in a central cylinder. See Figure 8.5.
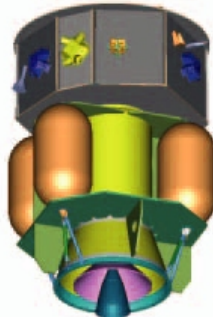
Figure 8.5 – LISA PF in its launch configuration.
Note the larger lower propulsion module and the upper (grey) science spacecraft.

The internal configuration is designed to accommodate the spacecraft equipment in a gravitationally symmetric fashion, to prevent any bias on the LTP, an aspect very important for FPE-B. A central cylinder is surrounded by 8 compartments. The height of which is 478 mm and a diameter of 788 mm.

(a)   (b)
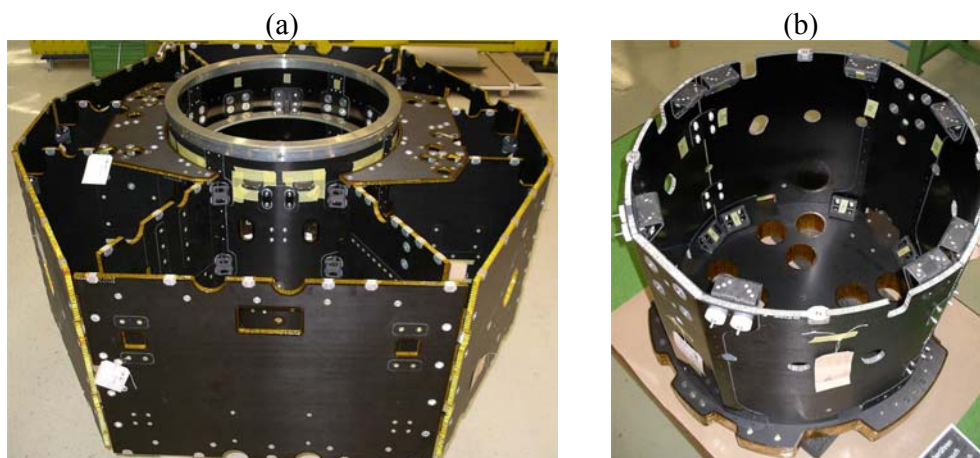
Table 8.2 – Structural Design of LPF
(a) Complete science spacecraft structure and (b) the Central Cylinder for the LTP (Credit: ESA)
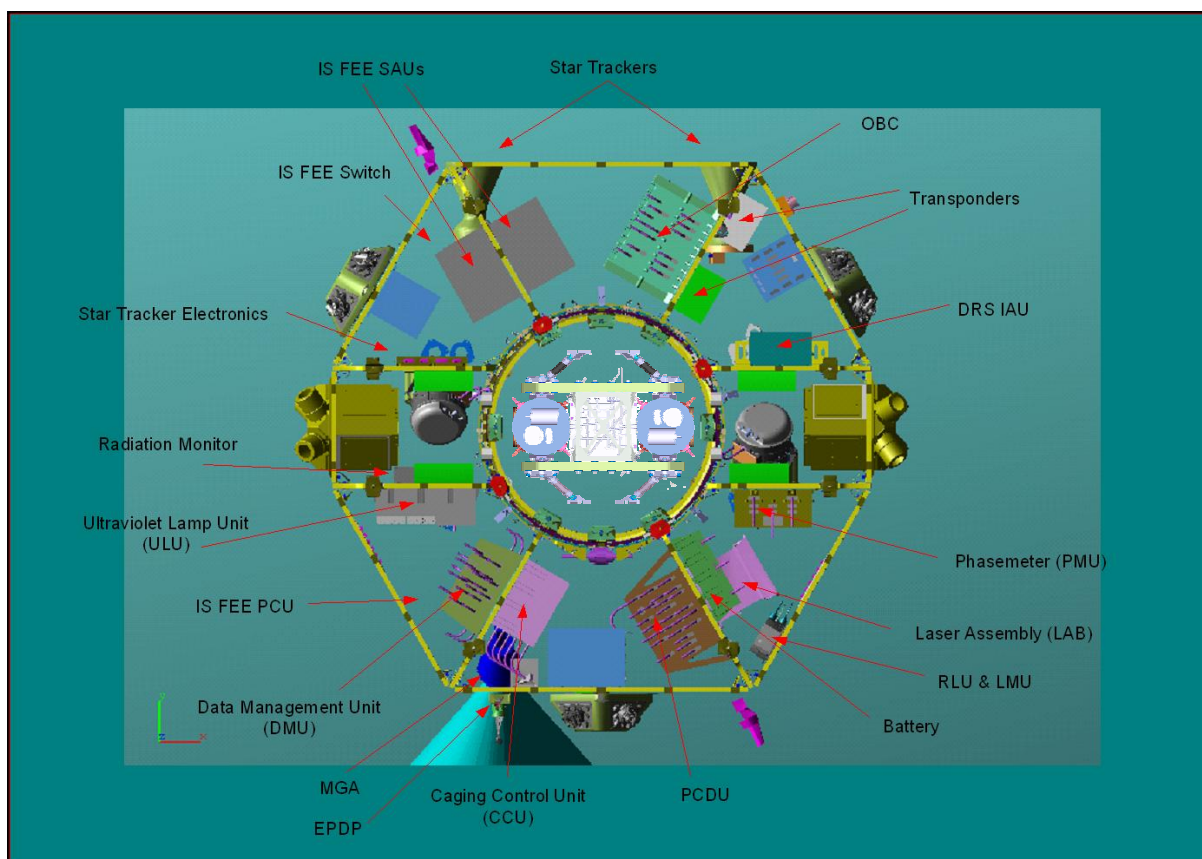
Figure 8.6 – Configuration of Spacecraft Hardware [TN7]

8.1.5   Thermal Control System

The main features of the thermal control system are as follows:
* Sun-shield between the solar array and the main body of the spacecraft
* The central cylinder is made from Carbon Fibre Reinforced Plastic (CFRP)
* The DRS radiator is conductively attached to the central cylinder as is the mounting panel.
* The DRS electronics are mounted directly on the shear panel for a conductive path. Local compartment is made from CFRP.
* The LTP mounts are coated in Vacuum Deposited Aluminium (VDA) MLI.
* As with the other electronic equipment, the mounting to the shear walls allows heat dissipation to the external radiator panels.
* Heater circuits for the laser assembly for operating temperature control
* A network of thermistors and a total of 66 heater circuits. They are considered in two groups, 1) temperature monitoring and 2) monitoring of key areas in each heater circuit.
* There is external MLI covering 65% of the spacecraft
* 35 % of radiator coverage on the spacecrafts external surfaces.

8.1.6   AOCS

For the implementation of the very demanding science goals, this sub-system is critical for success. It consists of three distinct control systems, distinguished by purpose.

* **CACS** – Composite Attitude Control System is for control during LEOP and the transfer to L1.
* **MPACS** – Micro Propulsion Attitude Control System is for non-science mode operations on station.
* **DFACS** –Drag Free Attitude Control System. This control system is used during science operations to provide drag-free control to a specific degree of freedom as required by the experiments. The DFACS modes can be considered to consist of:
   o **Accelerometer Mode** – A very stiff suspension of the TM's with the main objective of bringing the TMs to their initial reference position and attitude following their release from the hold mechanism (caging).
   o **Science Mode** – Designed to provide drag-free control to the axis passing through both TMs, using nominally, one TM as reference. It also provides drag-free control to an additional 5 DoF of the TMSs. The remaining DoF of the TMs are controlled to maintain them in the required range. Within this mode different usage of capacitive sensing and laser metrology create other sub-modes.
   o **DRS Mode** – In this mode the spacecraft provides measurements of the TM position and attitude to the DRS computer, which runs a dedicated drag-free control algorithm. The DRS then requests the spacecraft to apply forces and torques to the TMs and to the spacecraft, therefore actuating its own drag-free control.

Now we must consider the actuators. Currently there are two competing thrusters, which are awaiting selection, the Arc Indium Needle FEEP (see [46]) and the ALTA Caesium Slit FEEP (see [47]). Examples of the emitters are shown in Figure 8.7.

The emitter containing the propellant is fed along a tube to the tip of a needle/slit without active pumping due to capillary action. The electric field generated by the voltage difference between emitter and accelerator (the ring) creates local instability in the liquid metal after a certain amount of time. Gradually a cone forms at the end of the emitter slit/needle due to the electric field (known as a Taylor Cone). When the ionising voltage is released the atoms at the tip of the cone ionise and accelerate through the potential difference established by the voltages applied by the emitter and accelerator. This creates the thrust. A neutraliser is present to maintain the jets neutrality and prevent spacecraft charging. The disadvantage of such a system is that currently the needles are difficult to manufacture.

The noise specifications of the Alta Cs FEEP are as follows [TN8]:

- $\log[PSD] = 0.01 \left(\dfrac{0.1}{f} \right) \mu N^2 \, Hz^{-1}$ for $0.1mHz – 0.1Hz$

- $\log[PSD] = 0.01 \ \mu N^2 \, Hz^{-1}$ for $0.1Hz – 1Hz$

(a)   (b)
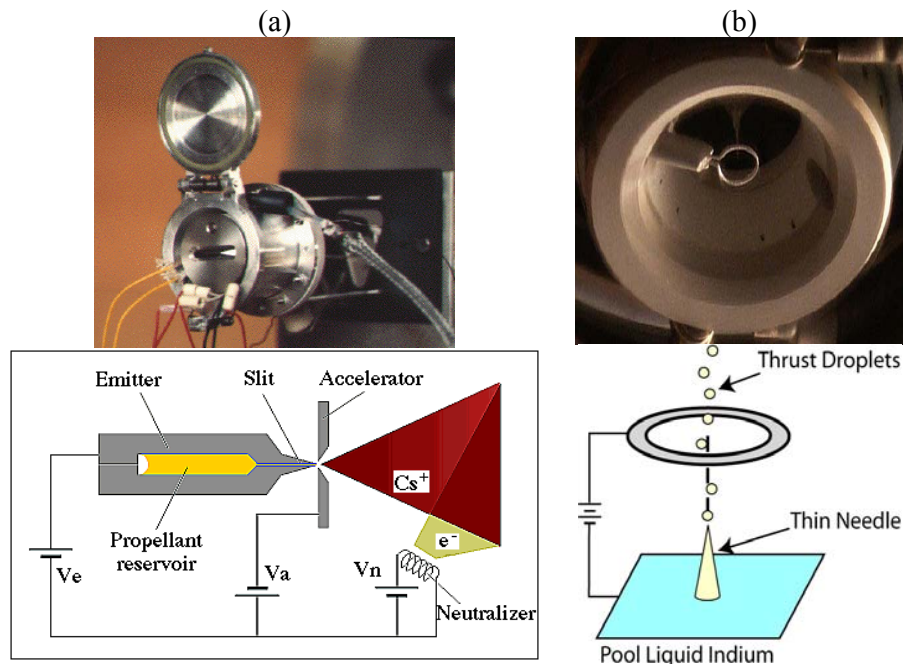
Figure 8.7 – ALTA Slit (a) and Arc Needle (b) types of FEEP Emitter [18]

The performance of an Indium FEEP manufactured by ARC is shown in Figure 8.8.
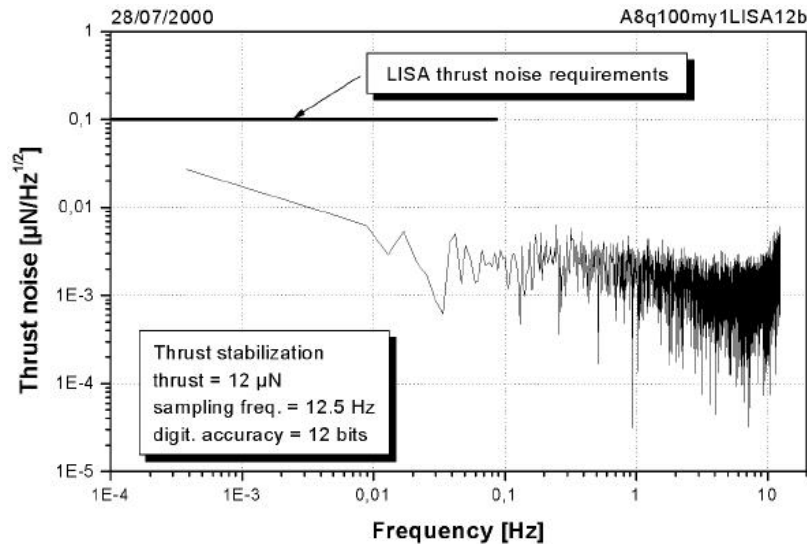
Figure 8.8 – Arc Indium Needle FEEP Measured PSD Results [43]

The performance of each type of FEEP is very similar and the decision will be made based upon technical and programmatic maturity.

The software used to control the AOCS sub-system including the MPACS and DFACS is run in the main On-Board Computer (OBC).

8.1.7   Electrical Power

This sub-system includes a solar array, Power Control and Distribution Unit (PCDU) and a battery. The solar array is composed of triple junction GaAs cells with a specified EOL power of 650 W. The battery is chosen to be re-chargeable Lithium Ion. The PCDU regulates the power in sunlight, while the battery is directly connected to the power bus to provide energy during eclipses. The batteries are directly connected to the bus. The bus itself is regulated 29.4 V during LEOP and transfer phases. Nominal operations are conducted at 28 V.

8.1.8   Data Handling Sub-System

The Data Handling Sub-System (DHS) is composed by a single computer connected via a MIL-1553 with the rest of the system. Both the spacecraft management and AOCS applications are running on the same computer. The AOCS application is replaced by the DFACS during the science operations.

8.1.9   Tracking, Telemetry and Control (TTC) (X-Band Comms)

The LPF TTC subsystem is designed to provide modulation and demodulation for the X-Band. The Cebreros (35 m, 66.0 dB gain up and 68.2 gain down) ESA station is to be used during nominal operations for ground receipt and transmission of telecommands and telemetry [28].

On the spacecraft, two hemispheric antennas provide near-omni-directional coverage. They are accommodated on the outside of the science module. Both are X-Band Helix antennas and of low gain. A third antenna, the Medium Gain Antenna (MGA) is a horn. The position of the MGA is shown in Figure 8.6. A dual redundant transponder is baselined.

The communications window is around 8 hours per day.

The data rate is supported by three modes (based on the latest information from the LPF project);
- High: **60.0 kbps** in LEOP
- Medium: **30.0 kbps** in on station nominal
- Low: **512 bps** emergency link through the LGA's only

Due to the frequency of interest for the scientific objectives, both instruments (LTP and DRS) generate a low amount of scientific data per second.

8.1.10   Resource Budget Summary

This section will present a summary of the mass, power and link budget for LISA PF. It should be noted as FPE mission will not require the propulsion module (as the launch vehicle is assumed to do all the orbit insertion) it is not included in the budget below. The detailed sub-system breakdowns are shown in the previous sections. The values presented in Table 8.3 are not fixed and are subject to change.

Sub-System	Mass (kg)	Power# (W)
Service Module		
Data Handling	16.5	41.7
Power	69.1	10.5
X-Band Comms	9.7	54.0
AOCS	18.4	19.6
Structure	80.8	0.0
Thermal	7.4	11.6
FEEP μProp	44.9	167.9
Total	**246.8**	**305.3**
Payload Module		
LTP*	150.0	152.3
DRS*	50.5	78.0
Balance Mass	10.0	0.0
Total	**210.5**	**230.3**
Science Spacecraft Total		
TOTAL	**457.4**	**535.6**

Table 8.3 – LISA Pathfinder Science Spacecraft Mass and Power Budget as of Early 2007
*The data is taken from the latest available LPF information provided by the project and included margins.
#Joint mode operations is assumed in the example.

9 Resource Comparison and Required Adaptability

The goal of this section is to compare what is required of LPF by the FPE mission profile and payload. The comparison between what *is* required what is *available* can be made. Specifically it is useful to define and determine the *changes* that are needed. As starting point it is assumed that the LTP will be removed in its entirety, hence removing the support hardware outside of the central cylinder (electronics, phase meter etc(see Figure 8.6)). No further changes to the platform are envisaged.

The first comparison to make is between the LTP itself and the FPE payload requirements. This is shown in Table 9.1. The assumption made is that the US-DRS is present. This consideration is applied as it is assumed that the LPF is sized for *both* the DRS and LTP (see section (8.1.3)). Later however the power and TLM demands will be assessed more formally once the additions to LPF have been identified.

Resource Demand	LTP+DRS	FPE-A Payload	FPE-B Payload	FPE-C Payload[#]
Mass (kg)	210.5	127.8	212.2	<80
Power (W)	230.5	195.9	80.3	<170
TLM (kbps)	3.8	0.25	8.2	<70 000

Table 9.1 – Comparison of LPF and FPE payloads.
Note that quantities are including margins to reflect an upper safety limit.
*Joint mode operations
#Initial Allocation

The FPE payloads appear to be within the scope of the LISA Pathfinder platform in terms of mass and power although there may be issues with accommodation which are addressed later.

The following is a schematic (Figure 9.1) showing the configuration of LPF. The red boxes are pieces of equipment relating to the LTP which in principal, when the LTP is removed, are redundant as they support it. Note that the implications of removing of the Inertial sensor, which is part of the LTP (see Section (8.1.3)), is considered in Section (9.1.2).

It also should be noted that the configuration is subject to change during the design process and some units could be omitted due to the perspective of Figure 9.1. The schematic is split into segments each with a letter assigned. Segment B also contains elements of the DRS.

Key
1. LTP
2. IS (LTP) Sensing and Actuation Unit
3. IS (LTP) Sensing and Actuation Unit
4. Radiation Monitor/Magnetometer
5. UV Lamp Unit
6. LTP DMU
6a.IS (LTP) PCU
7. Caging Control Unit
8. Ref. Laser Unit & Laser Metrology Unit
9. Laser Assembly
10. Phasemeter
11. DRS IAU (Other equipment located here)
12. FEEP Assembly 3
13. FEEP Assembly 1
14. FEEP Assembly 2
15. Electric Propulsion Diagnostic Package
16. AOCS Gyro 1
17. AOCS Gyro 2
18. Colloid Assembly 2
19. Colloid Assembly 1
20. MGA
21. LGA 2
22. LGA 1
23. TTC Transponder
24. TTC Transponder
25. OBC
26. Star Tracker
27. Star Tracker
28. Battery
29. PCDU
30. Star Tracker Electronics

Figure 9.1 – Configuration of the LISA Pathfinder, adapted from Figure 8.6
The equipment highlighted in RED is related to the LTP, spacecraft hardware is in GREEN and the DRS is in PURPLE.

9.1   FPE-A – Optical Atomic Clocks and Cavity Resonators

9.1.1   Accommodation of Payload

An analysis of the relevant/non-relevant/adaptable pieces of equipment is shown in Table 9.2 for the LTP and Table 9.3 for the DRS.

The most significant consequence of removing the LTP on the AOCS sub-system is the loss of the inertial sensor. This requires a replacement. One solution is to adapt a MICROSCOPE like differential accelerometer [31] to provide inertial measurements in the absence of the LTP (more detail in Section (9.1.2)).

The advantages of these removals are the availability of space in segments A, C, D and E. Some space becomes available in segment H where it is assumed a new laser package will be installed more suited to FPE-A needs.

The Optical Atomic Clock (OAC), Optical Resonator Bench (ORB), Probe Laser Stabilisation Cavity (PLSC) and Frequency Comb (FC) are located in the central cylinder, Segment I. Also located here is the ONERA-like Electrostatic Inertial Sensor (IS) to replace the lost LTP IS.

Item (Figure 9.1 ref.)	Retained	Remarks
LTP (1)	No	Payload not adaptable to FPE-A science requirements
Inertial Sensor (IS) FEE (2 and 3)	No	Required by the LTP and likely to be specifically designed for it
Radiation Monitor and Magnetometer (4)	Yes	Would be useful to monitor the magnetic and the radiation environment to monitor clock health
UV Lamp Unit (5)	Adapted	Required to discharge test masses, not applicable to FPE-A payload, but will be necessary for replacement inertial sensor.
LTP DPU (6)	Adapted	Replaced with payload computer as discussed in [TN2]. But similar unit envisaged.
IS (LTP) PCU (6a)	Adapted	A PCU is required but changes maybe necessary to make it compatible with FPE-A architecture
Caging Control Unit (7)	No	Relates to test mass release, not applicable to FPE-A payload, but will be necessary for replacement inertial sensor.
Ref Laser & Laser Metrology Unit (8)	No	Laser reference in this form is not necessary as a laser bench will be needed for the cavities and clocks, likely requiring different wavelengths and powers.
Laser Assembly (9)	Adapted/No	Changes required as more than one laser wavelength is needed. A new system could be the better option, tailored for the Optical Clock, cavities and comb
Phasemeter (10)	No	Some measure of phase and wavelength maybe useful to FPE-A as back-up to the primary frequency measurements. However assumed not to be required.

Table 9.2 – Retained and removed LTP elements with reference to FPE-A payload definition

Item (Figure 9.1 ref.)	Retained	Remarks
Colloid Thruster Assemblies (18 and 19)	No	Not required as there is cold gas and FEEPS available. They also directly relate to the DRS sensors.
DRS DPU (11)	No	Payload designed as a technology demonstrator not required for FPE associated with the colloid thrusters

Table 9.3 – Retained and removed DRS elements with reference to FPE-A payload definition
Note that there are other elements to the DRS contained in the vicinity of item (11) or the DRS IAU and also below the LTP.

The goal was minimise the movement of equipment that is to be retained. In some cases elements relating to payload were moved so to be in a more convenient place. A description of the accommodation process relating to Figure 9.2 can be found below.

- The colloid thrusters and DRS have been removed in addition to the LTP and the LTP FEE electronics.
- The radiation monitor was moved to create space for the OAC laser bench to the space vacated by the removed DRS electronics.
- Replacing the colloid thrusters in Segment E is the laser bench for the OAC. The lasers could be placed as close to the OAC UHV to minimise fibre lengths preventing attenuation of high frequencies, but they are mounted on external walls so the heat dissipated can be radiated to space.
- Immediately next to the OAC laser bench (2) is the electronics both digital and analogue (ECU and feedback electronics). The output of the photo detectors required for the stabilisation loop is directed here.
- The same system is in place for the ORB laser sources (9) stabilised by PDH stabilisation placed in Segment A along with the electronics (8).

- The frequency comparison hardware is placed near to the central cylinder in Segment F reducing fibre harness length.
- The UV unit is moved to Segment D to make room for the positioning of the frequency comparison and counter electronics.

Key
1. OAC, Cavities, and Frequency Comb
2. OAC Laser Sources
3. OAC Feedback FEE, ECU and PCU
4. Radiation Monitor/Magnetometer
5. UV Lamp Unit
6. P/L Control DPU
6a. P/L PCDU
7. Caging Control Unit
8. ORB Feedback FEE, ECU and PCU
9. ORB Laser Sources
10. MWL Link Transponder
11. Frequency Comparison Electronics
12. FEEP Assembly 3
13. FEEP Assembly 1
14. FEEP Assembly 2
15. Electric Propulsion Diagnostic Package
16. AOCS Gyro 1
17. AOCS Gyro 2
18. Inertial Sensor (IS) 1
19. Inertial Sensor (IS) 2
20. MGA
21. LGA 2
22. LGA 1
23. TTC Transponder
24. TTC Transponder
25. OBC
26. Star Tracker
27. Star Tracker
28. Battery
29. PCDU
30. Star Tracker Electronics
31. IS1 Analogue and Digital Electronics
32. IS2 Analogue and Digital Electronics
*Changes are in in red

Figure 9.2 – Adaptation of LPF due to accommodation of FPE-A payload
The equipment highlighted in RED may require moving, possible adaptation or are new.

- The P/L control DPU and PCU retain their positions as they could be adapted from the LPF versions.
- ONERA microStar-like accelerometers are placed in the central cylinder as close to the CoM as possible. The associated electronics make use of the space available in Segment C due to one of the removed LTP FEE units.
- The Phasemeter is removed as it a component for interferometry measurements from the LTP optical bench.
- The new inertial sensors are assumed to have an integrated launch cage mechanism. Implying that they will still require the control unit.
- The caging control unit is moved to where the phasemeter was, allowing the MWL link transponder to be placed there. This ensures proximity to the both LGA 2 and the MGA. The MGA could be used for this taking advantage of the higher gain for the required high stability of the link.

NOTE: This description is preliminary and mass distribution issues may drive the position of units if a more detailed design is pursued.

9.1.2   Payload Change Implications on AOCS

The AOCS sub-system requires adaptation to account for the loss of the LTP.

There are two options. The first retains the inertial sensors of the LTP. This requires significant adaptation as the optical bench has been removed. There is also the optical window for the laser incident on the test mass which is no longer required. The second option is to use electrostatic accelerometers similar to MICROSCOPE, possibly from ONERA, as the inertial sensor. The level of drag free provided enables a test of the equivalence principle, although at a lower accuracy than FPE-B, but will be adequate for FPE-A. Clearly this requires modifications of charge management and caging hardware and possibly some re-design of the accelerometer. In both cases new software would be required for the DFACS. In summary modification to each option would be required tailored for the mission needs. So the choice therefore depends on the resource demands.

	Mass (kg)	Envelope (mm)
LTP IS	18.0	Ø246 x 440
Electronics	15.0	278 x 185 x 185
ONERA [12]	8.0	Ø100 x 250
Electronics [12]	5.5	240 x 180 x 180

Table 9.4 – Comparison of accelerometer hardware

Note that the resources are based upon one unit and is an estimate for rough comparison. In the ONERA case the digital electronics are omitted.

The LTP IS is more demanding in terms of size so the ONERA providing good performance would be the chosen baseline in terms of the adaptation.

The absolute requirement to have a DFACS system needs further study. The applicability of using the gyros and star trackers to provide the necessary attitude information for AOCS needs to be assessed. This may lead to the option of de-scoping AOCS saving on cost and complexity.

9.1.3   AOCS Performance Requirements Comparison

This section considers the requirements of the FPE-A payload on the AOCS system to determine if the LPF hardware can provide the performance required to measure the violations in special and general relativity. The same platform is to be used for FPE-B as A. B has more stringent requirements so if these are met, by default FPE-A's will also be met. They are stated here for completion. A further system consideration is that the local environment is much less benign than for L1. The thrusters must be able to perform in a more noisy and strenuous environment.

In LEO the use of FEEPs is deemed to be possible as they are an on-going development for not only LPF but also Microscope and GAIA. From this one can assume that FEEPs are possible in LEO and this is one of the reasons for the high thrust specification.

The FPE-A requirements are stated in Section (3.6.5) and can be compared to the performance specifications stated in Section (8.1.6) for the FEEPs. As can be seen the Indium FEEPs are

compatible with the system requirements. Table 9.5 shows the comparison as a summary for reference.

	LPF (ALTA Cs FEEP)	LTP Req.	FPE-A Req.
Max Thrust (μN)	150-250	150	74.0*
Min Thrust (μN)	0.1	0.1	0.6
Resolution (μN)	0.1 for <100 0.3 for > 100	0.1	0.6

Table 9.5 – AOCS (DFACS mode) performance comparison
The ALTA FEEP is assumed for comparison purposes. 500 kg is assumed for LPF mass

The comparison shows that for attitude control at least LPF is compatible with the needs of the FPE-A payload. The maximum thrust is comparable with the local disturbances.

Noise performance appears to be acceptable considering the minimum thrust requirements are quite high. If the noise requirement flicker floor is assumed to be 0.6 μN the ALTA FEEP and also the Indium FEEP (Figure 8.8) could meet the requirements. A PSD of the cavities in question (this drives the performance requirements [TN1]) compared with FEEP noise would be a more rigorous test.

9.1.4   Mission Profile Changes

The orbit selected in is;
*   700/3599 km elliptical orbit with an eccentricity of 0.17 and an inclination of 105^0. This orbit is sun-synchronous.

An elliptical orbit implies the following differences with LPFs current profile:
*   Larger disturbances with atmospheric drag much more dominant. Although at 700 km SRP is the largest. Possibility of larger propellant mass.
*   Varying thermal conditions over the orbit from the Earth.
*   Infrequent ground contacts of the order 10 mins every hour if one assumes a single ground station, although an analysis shows this not to be a problem (see Section (9.1.5)).
*   Launch vehicle ascent profile and possible mass penalties due to a highly energetic orbit.
*   The Radiation environment may be more severe due to passages through the Van Allen belts [TN4].

For an analysis of the required propellant the following three stages are considered:
*   Sun acquisition/ operational attitude slew manoeuvre
*   Linear acceleration compensation due to eternal disturbances
*   Torque compensation due to eternal disturbances

The ΔV and torque budget for the FEEPs are given by Table 9.6. The calculations of the magnitudes of the perturbations are found in [TN4], where the spacecraft assumptions are also stated as well as Table 6.2. It should be noted that the torque is the upper limit and most likely will be reduced bringing it into line with the FEEP capabilities (1.4×10^{-4} Nm). The Sun and Moon are included as corrections may be required to maintain the chosen orbit.

Perturbation	Torque	Residual Acceleration	ΔV	Linear Thrust
	Nm	ms^{-2}	ms^{-1}	μN
Gravity Gradient	1.03E-05	2.31E-14	0.00	0.00
SRP	2.52E-05	3.54E-08	1.12	26.57
Magnetic Gradient	2.14E-04	2.19E-13	0.00	0.00
Aero Drag	1.73E-05	2.43E-08	0.77	18.22
ERP	2.74E-06	3.85E-09	0.12	2.89
Earth Albedo	3.56E-06	5.00E-09	0.16	3.75
Moons Gravity	0.00E+00	1.22E-06	38.54	916.49
Suns Gravity	0.00E+00	5.61E-07	17.70	420.91
Total	**2.73E-04**	**1.85E-06**	**58.40**	**1388.83**

Table 9.6 – ΔV and Torque estimate for FPE-A
Assuming: S/C Mass = 750 kg, Thruster lever arm 0.95 m, 1-year lifetime [TN4]

As a continuous drag-free environment is required, the propellant is sized to allow thruster firings for the entire mission lifetime. This is assumed to be one year for these calculations. The orbital correction manoeuvres could be implemented during eclipse periods so valuable science measurement time is not used.

The sun acquisition time may cause a problem as FEEPs are used. If the maximum thrust is restricted to 150 μN then the total time to slew from a worst case anti-sun direction (slew angle of 180^0) to a sun-pointing direction could be 76 minutes assuming a lever arm of 0.95 m (see Table 6.2). This could require the extra addition of new thrusters to cope with these demands, although the timescale is within the battery initial lifetime of around 2 hrs. The slew time however is significantly longer than the specified 15 minutes for LPF. However the thrusters used will be the noisier propulsion module allowing larger thrusts on shorter timescales. A further option to consider is the actual need for FEEPs. The science requirements, with further analysis, could allow more thruster noise. This would make it possible for a higher thrust system. The problem would still remain for FPE-B however.

The propellant budget is shown in Table 9.7.

	Propellant (per FEEP kg)	Propellant (kg)	Remarks
Sun Acquisition Slew	Negligible	Negligible (1.74 x 10^{-5} kg)	Assumed 180^0 slew and includes acceleration and deceleration over 76 minutes
Linear Accelerations	0.37	1.12	Includes sun moon
Torques	0.07	0.22	Includes Sun Moon
Total	**0.45**	**1.34**	
With Margin (20%)		**1.6**	

Table 9.7 – Estimated required propellant for FPE-A Orbit Maintenance

Typically from [TN8] each FEEP cluster has 14 g of propellant. From Table 9.7 this will need to increase and the changes in design assessed.

9.1.5   TT&C Requirements and Ground Segment

Link budget should not pose a problem to LPF as the data rate is comparably low and FPE-A will be at a lower altitude. However the configuration of the antennas must be considered as the spacecraft is assumed to be three-axis stabilised. LPF at L1 maintains pointing in the antenna Earth direction. The spacecraft does not vary its attitude w.r.t. the Earth greatly. In LEO 360^0 coverage is required as the spacecraft antenna will not necessarily be pointing at the ground station in view. It is not possible to re-point as this would affect science measurement, as the cavities would move relative to the cosmic microwave background. Therefore an additional MGA may need to be added to complement the current set (two LGA and one MGA).

The data requirements of FPE-A assume an orbital period of 7837 s (see Section (6.5)). If a 2kbps spacecraft and 8.2 kbps payload is assumed, a downlink once per orbit with a 10 minute communication window requires a data rate of 29.4 kbps.

The requirements of the adapted TTC sub-system are:
- Receive telecommands (TLC)
- Transmit spacecraft operation TLM
- Transmit science data

In addition to the current LPF configuration:
- Provide K-Band for the high frequency clock comparisons.
- Provide S-Band for use in determining ionospheric corrections when compared with the K-Band

The following presents two options for the communications architecture. It is assumed for this exercise that a clock will be present at the ground station.

The first is to provide a system in all three bands, allowing the clock comparisons (MWL package in S-Band and K-Band) and transmission of TC/TLM (X-Band). This would be the modular system. The implication of this is the need for extra antennas to ensure that clocks can be compared while the spacecraft is being commanded and monitored. The same antenna could not be used for TLC and TLM (X-Band) and for clock comparisons (S-and K-Band) at the same time. There would be two new antennas in addition. This has the advantage of allowing the MWL package to function as a separate entity.

The alternative is to dispense with the X-Band system present on LPF and use the S-Band link (ionospheric corrections) for spacecraft housekeeping and data retrieval (from other experiments). The antennas would remain part of the spacecraft TTC system rather than, as described above, within the payload. An additional MGA would be required on the opposite side of the spacecraft to ensure full coverage of the high stability link. If the spacecraft were to tumble, there would still be available antennas on both sides of the spacecraft.

K-Band requires passage regularly over ground receivers that are capable of receiving such signals. Within Europe K-Band facilities are only present at Cebreros and Redu-2.

Dispensing with the X-Band system is recommended as this would not be required in LEO in any case. The spacecraft housekeeping would be carried by the S-Band, i.e. routed from the spacecraft

transponder. In some cases spacecraft commanding and telemetry receipt would not be done at the same time as a clock comparison (this of course depends on where the ground clocks are situated). Doing so makes the X-Band redundant. This is advantageous as almost all ground stations will be able to receive the S-Band and stations without clocks could be used for reception of data, increasing the number of available ground stations.

The approach taken is to define a reference link budget based upon the LPF link budget, hardware and mission profile and compare this to a hypothetical S-Band FPE Budget for sizing purposes [TN5]. This is done rather than reproducing an accurate representation, which would be time consuming. The K-Band is not envisioned to have major problems other than the significantly reduced number of K-Band ground stations.

Reference Link Budget (X-Band - 8.5 GHz with a slant range of 1 785 259 km)
This is the nominal on-station scenario for LPF in science mode. The data rate in this case is assumed to be **30.0 kbps** with a required **E_b/N_o** (Energy per bit to noise ratio) of **2.8 dB**. The E_b/N_0 is Binary Phase Shift Keying (BPSK) with Viterbi and Reed-Solomon coding. The RF power output is assumed to be 7 W (TBC).

The ground station and spacecraft antennae data are shown in Table 9.8. The link budget is shown in Table 9.9. The ground station data can also be found in [28]. LPF presently assumes Cebreros as the prime ground station. **All other values (blue) are calculated independently.** The data rate is assumed to include the LTP requirements.

The reference budget is calculated for the purpose of this exercise and may not reflect the true LPF link budget as some input values are to be confirmed.

Transmitting Antenna (LPF)			Receiving Antenna (Cebreros)		
Type	Horn		Type	Parabolic	
Diameter	0.097	m	Diameter	35	m
Physical Area	0.007	m2	Physical Area	962.113	m2
Efficiency	0.520		Efficiency	0.550	
Effective Area	0.004	m2	Effective Area	529.162	m2
Gain	15.924	dB	Gain	67.274	dB
Half-Power Beam width	26.059	deg	Figure of Merit	50.800	dB/K
Pointing Error	13.030	deg	Half-Power Beamwidth	0.071	deg
			Pointing Error	0.006	deg

Table 9.8 – Reference Transmitting (Tx) and Receiving Rx Antennas for link comparison (X-Band)

	Scenario				
	Slant Range	1785259000	m	185.0	dBm
	Frequency	8.50E+09	Hz	198.6	dBHz
	Wavelength	3.53E-02	m	-29.0	dBm
A	**Spacecraft**				
	Transmitter Power	7*	W	8.5	dBW
	Transmitter Line Loss			-3.5	dBW
	Tx Antenna Gain			15.9	dB
	Tx EIRP			**20.9**	**dB**
B	**Propagation**				
	Free Space Loss	2.475E-24	W/m2	-236.1	dB
	Antenna Pointing Loss			-3.0	dB
	Antenna Noise Temp	53.5	K	17.3	dBK
C	**Ground Station/Internal**				
	Rx Antenna Pointing Loss			-0.1	dB
	Rx Antenna Gain			67.3	dBW
	Rx Noise Temp	44.4	K	16.5	dBK
	Boltzmann			**-228.6**	**dB**
	Output of Receiver				
D	**System Noise Temperature**	97.9	K	19.9	dB
	Noise			-208.7	dB
	Received Carrier Power			-151.0	dB
	Received Carrier to Noise			57.7	dB
	Data Rate	3.00E+04	bps	44.8	dB
	Link Effective Eb/No			12.9	dB
E	**Link Margin**			**10.1**	**dB**

Table 9.9 – Reference LPF DownLink Budget for On-Station Science Mode (X-Band)
Possible trade parameters are shown are shaded
*Assumed value (TBC)

FPE-A LGA Link Budget (S-Band - 2.5 GHz with a slant range of 3 599 km)
The LGA Helical antenna is assumed. There are two positioned on opposite sides of the spacecraft. Other than the situation twice per orbit when both antennas point tangentially w.r.t. the orbit plane or in other words perpendicular to the nadir direction a good link will be maintained.

For FPE assuming the S-Band the following assumptions for the link budget are required:
- S-Band Frequency assumed to be **2.5GHz.**
- The downlink required is to be **29.4kbps** over an assumed 10 minute window.
- Primary antenna is a **Helix** due to the low frequencies. The gain is assumed to be **1 dB ±90^0**. This is because we have moved to lower frequencies. Earth coverage is required so the

spacecraft does not have to be moved to point at the ground station with this omni-directional antenna.
- Slant range is assumed to be the orbit apogee at worst case **3599 km**.
- The atmospheric noise temperature is increased to **290 K** to account for the greater proximity to Earth of the spacecraft.
- The primary ground station is changed to Svalbard (13 m [28]) to account for the SSO orbit. This will impact on the figure of merit (G/T) of the receiver, which is now **23 dB/K** [28].

The link margin is 32.6 dB, which should cause no problems.

LEOP Telecommands (TC) and TLM could be done over the S-Band also. LPF assumes 60 kbps for this phase and when this is inserted into the budget above the link margin becomes 29.5 dB. In principle the S-Band can be used for all communications not involving the microwave K-Band clock comparison. Hence the X-Band transponder can be replaced/modified.

FPE-A MGA Link Budget (Ku-Band – 14.7 GHz with a slant range of 3 599 km)
The band is assumed to be the same as the ACES link.

The required E_b/N_o SNR ratio is dependant on the bit error probability, P_b. If BPSK is assumed then the following error function is valid,

$$P_b = \frac{1}{2} erfc\left(\sqrt{\frac{E_b}{N_0}}\right)$$

9.1

The assumption chosen is based on the instability of the clock, as errors of a greater probability would prevent the transmission of the clock performance. The clock instability is required to be 10^{-17}, so 10^{-18} is assumed to account for a margin. E_b/N_0 is required to be 38.34 or **15.84 dB.** The data rate is assumed to be **88 bps**, which is two 12 digit numbers of 44 bits (the time interval data and the clock frequency) of a GHz frequency measurement transmitted from the spacecraft once per second. The spacecraft is not included as this a link between institutional users and it.

The ground station assumed needs to be capable of receiving Ku-Band and be at high latitude as the spacecraft is in SSO. The chosen baseline is based upon REDU-2 Ka-Band receiver. This is not of particularly high latitude and windows of opportunity could be limited. Also the specified frequencies of the station are 18 – 20 GHz. The mission may depend on smaller ground user receivers.

The following changes to the reference link budget are required:
- Frequency will now be 14.7 GHz
- The data rate is changed to 88.1 bps so to take into account only interval data and the clock frequency. The purpose of this link is solely for clock comparisons. Housekeeping and further data retrieval are transmitted on the S-Band.
- The ground station is REDU-2 (13.5 m) which is near to the range of the ACES link. Further study in this area may be required. This affects the antenna size (13.5) and figure of merit (42.5 dB/K).

- The required SNR (E_b/N_0) is changed to 15.84 dB to reflect the higher demands on bit accuracy.

The link margin is calculated to be 66.6 dB.

The link has a large margin. However the ground segment may also consist of smaller portable receivers stationed near the ground clock. It is assumed that a primary ground clock would be used for red-shift measurements, but for all other measurements (and red-shift too) would be done by institutions with a *smaller* receiver. If an average diameter of 30 cm and a figure of merit of 15 dB/K is assumed the link margin reduces to 34.7 dB. If the data rate for such a system were to increase to 2 kbps for the same small receiver, then the margin is 21.1 dB. Care has to be taken in this area. The driver is mainly due to instability rather than signal strength.

Conclusions

Budget	Band (GHz)	Data Rate (kbps)	Figure of Merit (dB/K)	Receiver Gain (dB)	Transmitter Power (W)	Effective E_b/N_o (dB)	Required E_b/N_o (dB)	Margin (dB)
Reference*	8.5	30.0	50.8	67.3	7	12.9	2.8	10.1
FPE-A LGA	2.5	29.4	23.0	48.1	7	35.4	2.8	32.6
FPE-A LGA	2.5	29.4	23.0	48.1	1	27.0	2.8	24.2
FPE-A MGA	14.7	0.088	42.5	63.8	7	82.5	15.8	66.6
FPE-A MGA	14.7	2.0	15.0	30.7	7	37.0	15.8	21.1

Table 9.10 – Comparison of Reference LPF Link Budget with Various Hypothetical FPE-A Link Budgets
*The reference budget is calculated for the purpose of this exercise and may not reflect the true LPF link budget.

Table 9.10 shows the LPF reference budget compared with the calculated budgets using the input parameters described above (example FPE input parameters).

The issues that should be highlighted are:
- Confirmation of required bit error probability for clock comparison Ku-Band link
- The quality of the receivers and transmitters is a critical area that could contribute to the degradation of the clock signal from space. This requires further study. Also to be considered is the infrastructure for receiving the ACES-based Ku-Band signal from the space-clocks.
- Small intuitional receiver gain and link margin.
- Data to be carried on Ku-Band link (PN-Code etc)
- Number of ground stations able to receive the K-Band with regular access to the satellite from an SSO, emphasising the need for local receivers (possibly intuitional)
- Replacement of X-Band transponder with an S-Band system the payload will use.
- An additional antenna may be required

The link margins themselves do not appear to pose a problem, but care needs to be taken in designing the institutional ground receiver. In general the critical issue for the TTC sub-system is the ground architecture and the availability of ground clocks and ground stations with K-band receivers and the proximity of the clocks to these.

9.1.6   FPE-A Mass and Power Budget

Shown in this section is a hypothetical mass budget for the adapted LPF. The new units are included and the adapted units are highlighted. This exercise aims to confirm that launcher margins on Vega are not exceeded. The mass budget assumed to be the latest from the LPF project. The changes to equipment are shown by sub-system.

Sub-System	LPF w/margin(kg)	FPE-Assumption w/margin (kg)	Relative change (kg)
Service Module			
Data Handling	**16.5**	**16.5**	**0.0**
Power	**69.1**	**69.1**	**0.0**
S-Band Comms	**9.7**	**11.6**	**+1.9**
Additional MGA Antenna	1.9	3.8	+1.9
AOCS	**18.4**	**34.4**	**0.0**
ONERA IS x 2	0.0	16.0	+16.0
Structure	**80.80**	**80.8**	**0.0**
Thermal	**7.40**	**7.4**	**0.0**
FEEP µProp	**44.90**	**46.5**	**+1.6**
Propellant	0.04	1.6	+1.6
Total	**246.8**	**266.25**	**+19.5**
Payload Module			
LTP	**150.00**	**0.0**	**-150.0**
FPA-A Payload	**0.00**	**130.6**	**130.6**
DRS	**50.50**	**0.0**	**-50.5**
Balance Mass	**10.00**	**0.0**	**-10.0**
Total	**210.50**	**130.6**	**-79.9**
Consumables			
Consumables	**0.0**	**0.0**	**0.0**
Total	**0.0**	**0.0**	**0.0**
Science Spacecraft Total			
TOTAL DRY	**457.30**	**396.9**	**-60.5**
TOTAL WET	**0.00**	**0.0**	**0.0**
TOTAL	**457.30**	**396.9**	**-60.5**

Table 9.11 – Mass Budget for FPE-A Using LPF

In summary the major changes occur from a payload perspective. The only major spacecraft changes foreseen could be the addition of a higher thrust propulsion system at the expense of mass (lower I_{sp}, hence more propellant) and the addition of an extra MGA. FPE-A could have a mass of around 400 kg. This will reduce demands on the required thrust (drag compensation), potentially allowing a lower perigee.

The K-band transponder is included in the payload (MLW link). The power budget is within the EOL capabilities of the 650 W solar panel.

Sub-System	LPF w/margin (W)	FPE-Assumption w/margin (W)	Relative change (W)
Service Module			
Data Handling	**41.7**	**41.7**	**0.0**
Power	**10.5**	**10.5**	**0.0**
S-Band Comms	**54**	**29**	**-25.0**
SSPA	30.0	5.0	-65.0
AOCS	**19.6**	**30.6**	**11.0**
ONERA IS x2	0.0	11.0	+11.0
Structure	**0**	**0**	**0.0**
Thermal	**11.6**	**11.6**	**0.0**
FEEP µProp	**167.9**	**167.9**	**0.0**
Total	**305.3**	**291.3**	**-14.0**
Payload Module			
LTP	**152.3**	**0**	**-152.3**
FPE-A Payload	**0**	**195.9**	**195.9**
DRS	**78**	**0**	**-78.0**
Total	**230.3**	**195.9**	**-34.4**
Science Spacecraft Total			
Sub-Total	**535.6**	**487.2**	**-48.4**
Final Joint Ops	**535.6**	**487.2**	**-48.4**

Table 9.12 – Power Budget for FPE-A Using the LPF Platform

9.2 FPE- B – Cryostat Supported Differential Accelerometers

9.2.1 Accommodation of Payload

This section refers to the configuration of LPF shown in Figure 9.1. The same procedure is to be followed assessing each aspect of LPF to determine re-use. Table 9.13 and Table 9.14 show the retained and removed units. The key aspect is there are no optical elements aside from the UV discharging unit (5) which is more of an operational element rather than part of the science payload.

Item (Figure 9.1 ref.)	Retained	Remarks
LTP (1)	No	Payload not adaptable to FPE-A science requirements
Inertial Sensor (IS) FEE (2 and 3)	No	Required by the LTP and likely to be specifically designed for it
Radiation Monitor and Magnetometer (4)	Yes	Would be useful to monitor the magnetic and the radiation environment to monitor local environment for Test Mass charging estimates
UV Lamp Unit (5)	Yes	Required to discharge test masses. Definitely required for the FPE-B Differential Accelerometers (DA).
LTP DPU (6)	Adapted	Replaced with payload computer. But similar unit envisaged. Could even be the same unit with different software.
IS (LTP) PCU (6a)	Adapted	A PCU is required but changes maybe necessary to make it compatible with FPE-B architecture.
Caging Control Unit (7)	No	Relates to test mass release, not applicable to FPE-A payload as mechanical stoppers are included in the DA design.
Ref Laser & Laser Metrology Unit (8)	No	Laser systems are not required for FPE-B in any capacity.
Laser Assembly (9)	No	Laser systems are not required for FPE-B in any capacity.
Phasemeter (10)	No	There is no measurement of the frequency of a laser.

Table 9.13 – Retained and removed LTP elements with reference to FPE-B payload definition

The key aspect to the adaptation of FPE-B to LPF is the accommodation of the cryostat. The sizing was designed from a starting point of placing the cryostat inside LPF therefore the radius was fixed to allow a fitting within the central cylinder.

Item (Figure 9.1 ref.)	Retained	Remarks
Colloid Thruster Assemblies (18 and 19)	No	Not required as there is cold gas and FEEPS available. They also directly relate to the DRS sensors.
DRS DPU (11)	No	Payload designed as a technology demonstrator not required for FPE associated with the colloid thrusters

Table 9.14 – Retained and removed DRS elements with reference to FPE-B payload definition

A possible configuration is shown in Figure 9.3. One of the most striking aspects of the configuration is the reduction of units. The spaces are left emphasise this. A description of the accommodation process relating to Figure 9.3 can be found below:

- The colloid thrusters and DRS have been removed in addition to the LTP and the LTP FEE electronics.
- The LTP IS FEE electronics are no longer required and are replaced by the electronics necessary for operation of the DA. These packages (2 and 3 in Figure 9.3) include both the analogue and digital electronics.
- The cryostat is accommodated in the central cylinder replacing the LTP.
- The UV unit (5) is retained in its original position.
- The laser assembly and phasemeter is removed leaving space in Segment H.

Key
1. Cryostat (DA Suite and assembly)
2. DA1 FEE
3. DA2 FEE
4. Radiation Monitor/Magnetometer
5. UV Lamp Unit
6. EPI DPU
6a.EPI PCU
7. Cryostat Electronics
8.
9.
10.
11.
12. FEEP Assembly 3
13. FEEP Assembly 1
14. FEEP Assembly 2
15. Electric Propulsion Diagnostic Package
16. AOCS Gyro 1
17. AOCS Gyro 2
18.
19.
20. MGA
21. LGA 2
22. LGA 1
23. TTC Transponder
24. TTC Transponder
25. OBC
26. Star Tracker
27. Star Tracker
28. Battery
29. PCDU
30. Star Tracker Electronics
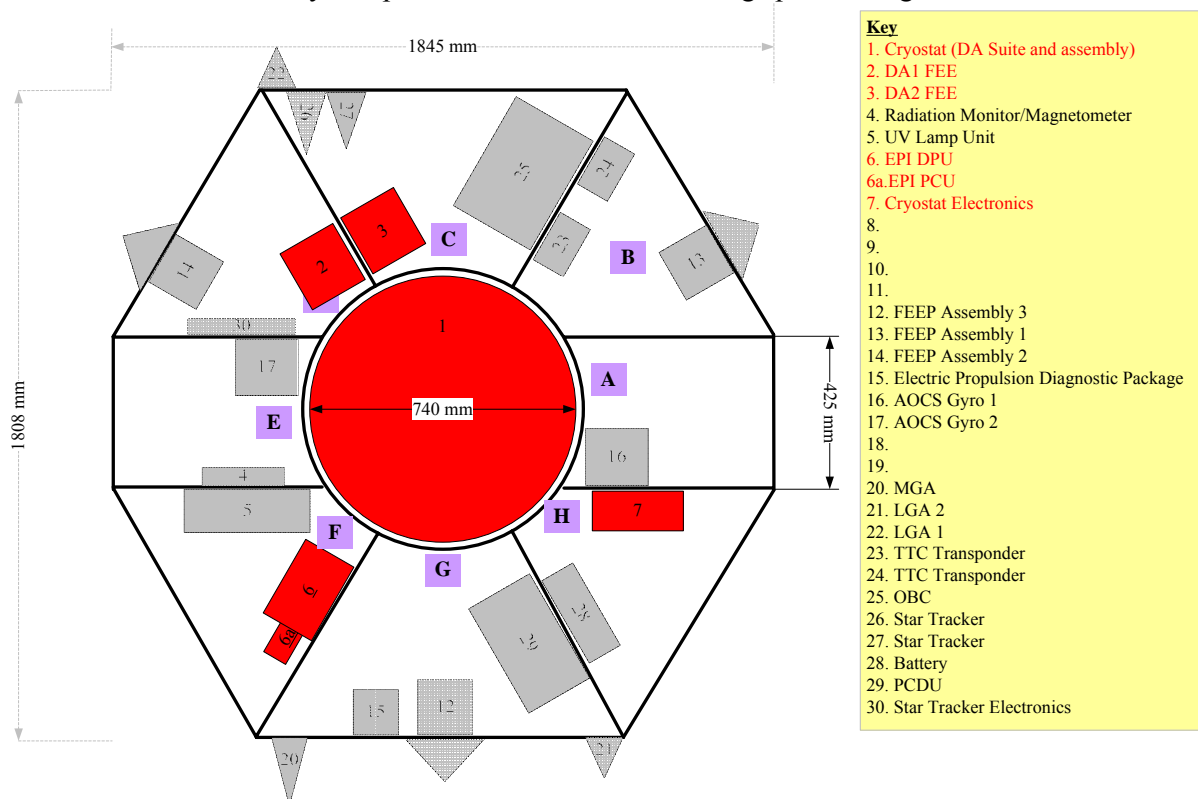
Figure 9.3 – Adaptation of LPF due to accommodation of the FPE-B Payload

From the above analysis it can be stated that it is no trivial matter including the cryostat within the LTP. To gain a 198 day lifetime, while fixing the cryostat radius at 740mm, the height required is 846 mm. As the more detailed design progresses the margins allowed on the radius of 7 cm (all sides) could be found to be inadequate. As it appears to be squeezed in, this area (the central cylinder) of LPF may need to be expanded as the cryostat is developed.

It is useful to return to the cryostat model used for the initial payload sizing to emphasise the effects of changes in size (for lifetime extensions) to assess any added complexity in adapting LPF. The first trade is a fixed radius which implies a lengthening of the cryostat. The second consideration is a fixed height, which would have implications on the structural design of the central cylinder and main spacecraft structure. The data is presented in Table 9.15. The sizing is done using a model deriving from previous cryostats, deriving tank volume and mass. GP-B data is included for comparison. [Note that the GP-B cryostat Dewar also includes a guard tank containing He I for launch-integration-test phases [3]. This maintains the main Helium II preventing losses for up to 3 months. The guard tank can be re-filled much easier. This is the general idea behind the Hydrogen cryogen so to extend the Helium lifetime for FPE-B.]

Lifetime (Month (Yr))	Radius (m)	Height (m)	Tank Mass (kg)	Hydrogen		Helium	
				Mass (kg)	Volume (m^3)	Mass (kg)	Volume (m^3)
8 (0.67)	0.370	1.171	126.1	13.9	0.291	12.3	0.099
8 (0.67)	0.428	0.846	120.3	13.4	0.284	12.1	0.097
9 (0.75)	0.370	1.479	158.1	18.8	0.378	16.1	0.129
9 (0.75)	0.470	0.846	142.6	17.2	0.354	15.3	0.122
10 (0.83)	0.370	1.938	205.9	26.3	0.509	21.6	0.173
10 (0.83)	0.518	0.846	194.9	22.2	0.445	19.44	0.156
GP-B[3], 16.5	1.100	3.000	810.0	12.4*	0.990*	338.0	2.328

Table 9.15 – Lifetime Extension Implications on cryostat design
*Guard tank of He I at 4.2 K

It can be clearly seen that the increase in lifetime increases the radius/height of the cryostat such that it exceeds the dimensions of the LPF central cylinder.

Any changes in the central cylinder will have many repercussions throughout the spacecraft. Due to the noticeable reduction in equipment units a widening of the central payload cylinder may be possible but impacting on the placement of these units. A possible reason for widening the central cylinder is to shorten the height of the cryostat to prevent protrusions below the spacecraft, anti-sun side. This could cause issues relating to the placing of the spacecraft in the launch fairing. A structural element would have to be included to prevent the cryostat being a load bearing structure.

Another option is to place the cryostat entirely outside the LPF platform suspended below it with a set of umbilical connections for power and data transfer. This has the obvious advantage of only requiring small modifications to the science spacecraft, notably an adapter to attach the service module (LPF science spacecraft without the LTP). However launch vehicle integration becomes an issue as the cryostat becomes the load bearing structure at launch. This then would require a new structural element. The complexity and most importantly mass and size increases.

Favouring placing the cryostat within LPF implies modifying the structure of LPF such that it compensates for the increase in cryostat height, widening the central cylinder or adding cryostat module beneath. An entirely new structural design would have to be assessed and studied in all cases. All the loads across the spacecraft would be become different. Hence we can assume that to increase lifetime beyond six months, LPF requires significant structural changes.

The venting of hydrogen and helium requires accurate control to minimise the effects on the orbit of the spacecraft and hence the performance of the payload as a residual acceleration would be created. A design incorporating a significant degree of symmetry would be required assisting the drag free control system providing the disturbance free environment. This is necessary as unlike GP-B the drag-free control system on LPF does not have cold gas thrusters as a baseline using the cryogen vapour as propellant.

9.2.2   Payload Change Implications on AOCS

As with FPE-A removing the LTP removes the Inertial Sensors (IS) for drag-free control. But, unlike FPE-A, B compensates for this using the Differential Accelerometers as the drag-free sensors also. The sensitive axis of the sensor, not only provides an opportunity to detect the EP signal, but also common mode acceleration. In addition the TM is free to move along this axis. The other degrees of freedom operate to hold the test mass by electrostatic suspension. The forces that are applied by the capacitors to 'hold' the TM are used to drive the actuation of the thrusters.

These changes would have to be reflected in the control law of the DFACS system as a new sensor is being used. Changes of the same kind as with FPE-A in terms of adapting DFACS to account for a new sensor. In this case the IS is part of the payload itself so this development will coupled to the development of the differential accelerometer. More detail on the accelerometer which is based upon the STEP instrument can be found in [30].

9.2.3   AOCS Performance Requirements Comparison

The drag-free modes are considered.

	LPF (ALTA Cs FEEP)	LTP Req.	FPE-B Req.
Max Thrust (μN)	150-250	150	74.0
Min Thrust (μN)	0.1	0.1	0.075
Resolution (μN)	0.1 for <100 0.3 for > 100	0.1	0.075

Table 9.16 – AOCS (DFACS mode) performance comparison
The ALTA FEEP is assumed for comparison purposes.

The LTP sensitivity requirements are shown in Equation 8.1. Assuming a sensitivity of 3.3×10^{-14} ms^{-2} Hz$^{-1/2}$ @ 1mHz. Through the gain of the feedback loop (assumed to be 10^4 orders), for a 500 kg spacecraft the thrust noise is $0.17\mu N$ Hz$^{-1/2}$ @ 1mHz. The requirement is then set at $0.1~\mu N$ Hz$^{-1/2}$ @ 1 mHz to allow some margin (Section (8.1.6)).

THE FUNDAMENTAL PHYSICS EXPLORER
TECHNOLOGY REFERENCE STUDY
issue 1 revision 0 – 12/12/2007

SCI-PA/2007.025/FPE/DB

page 143 of 166

The Indium FEEP noise spectrum is shown in Figure 8.8. If it is compared with the SQUID sensor requirements of the FEEPs (Section (4.6.5)), it is very much border line around 0.075 µN, especially around the WEP signal band which is nominally 0.33 mHz currently. The thrust noise value at this frequency on this PSD is not shown. Extrapolation of this curve would indicate that work is required to improve thrust noise at lower frequencies.

Potential solutions are:
- The production of a FEEP that is more within the requirements, say to 0.05 µN $Hz^{-1/2}$ @ 0.33 mHz.
- Increase the integration time requiring a lower sensitivity measurement. Reducing the sensitivity requirements to 3.3×10^{-14} ms^{-2} $Hz^{-1/2}$ @ 0.33mHz requires an integration time of 129 days. But the thruster noise requirement is 0.25 µN $Hz^{-1/2}$ @ 0.33mHz. The sensitivity limit of the sensor may be reached much earlier also as measuring indefinitely will not always produce better results.
- Increase the frequency of the WEP signal, more rotations of the spacecraft per orbit. Three rotations per orbit allow a shift of the equivalence principle signal to 1 mHz. The signal of the WEP signal achievable at a frequency of 1 mHz is (over the same integration time 12 days) is still 10^{-17} as the sensitivity of the SQUID is $\sim10^{-14}$ at this frequency (Figure 4.5). But the thrusters perform better at these frequencies (1 mHz).

Shifting the frequency of the signal is the favoured solution as FEEP's are still under development and the performance goals may not be reached. At 1 mHz Figure 8.8 shows a noise of 0.02 µN $Hz^{-1/2}$. An increase in integration time is not practical as this would reduce the number of measurement sessions, which is already restricted by cryostat lifetime. Improvements to the accelerometer could reduce to integration time requirements, lowering the curve (Figure 4.5) similar the discussion in Section (4.4.3).

Maximum thrust requirements are slightly lower than FPE-A as the velocities are lower due to the circular orbit and hence the drag is lower as compared with a higher perigee velocity.

9.2.4   Mission Profile Changes
The orbit selected for FPE-B is a 700 km circular orbit. This is a compromise between the severity of the Van Allen radiation belts and the magnitude of the external disturbances.

- Larger disturbances with atmospheric drag much more dominant. Although at 700 km SRP is the largest. Possibility of larger propellant mass.
- Varying thermal conditions over the orbit from the Earth.
- Infrequent ground contacts of the order 10 min every hour if one assumes a single ground station, although an analysis shows this not to be a problem (see Section (9.2.5)).

The only consideration w.r.t. LPF is the charging of TM's, which is likely to be more severe in LEO than at L1.

The mission lifetime is 6 months if no changes are made to LPF's structure. The longer duration missions would have a larger ΔV for corrections. The ΔV budget and propellant budget is shown in Table 9.17 and Table 9.18.

Perturbations	Torque	a	ΔV	Thrust
	Nm	ms-2	ms-1	μN
Gravity Grad	1.03E-05	2.31E-14	0.00	0.00
SRP	2.52E-05	3.54E-08	0.56	26.57
Magnetic Gra	2.14E-04	2.19E-13	0.00	0.00
Aero Drag	1.48E-05	2.08E-08	0.33	15.57
ERP	2.74E-06	3.85E-09	0.06	2.89
Earth Albedo	3.56E-06	5.00E-09	0.08	3.75
Moons Gravity	0.00E+00	1.22E-06	19.27	916.49
Suns Gravity	0.00E+00	5.61E-07	8.85	420.91
Total	**2.70E-04**	**1.85E-06**	**29.14**	**1386.18**

Table 9.17 – FPE-B ΔV Budget based for a 6 Month lifetime
Based upon 750 kg S/C, over 6 months and data from [TN4]

The key concern is that FEEPs are certainly required for FPE-B. If FEEPs are the only form of propulsion the slew time for sun acquisition as discussed for FPE-A is a concern. The addition of an orbital manoeuvring system in addition may be required.

	Propellant (per FEEP kg)	Propellant (kg)	Remarks
Sun Acquisition Slew	Negligible	Negligible (1.74×10^{-5} kg)	Assumed 180^0 slew and includes acceleration and deceleration over 76 minutes
Linear Accelerations	0.19	0.56	Includes sun moon
Torques	0.04	0.11	Includes Sun Moon
Total	**0.23**	**0.67**	
With Margin (20%)		**0.80**	

Table 9.18 – Estimated Propellant budget for FPE-B
Based upon 750 kg S/C, FEEP Isp of 4000s, over 6 months and data from [TN4]

9.2.5   TT&C Telemetry Requirements and Ground Segment

Link budget should be no problem. Changes from FPE-A are a higher data rate (but not higher than LPF) and a 700 km max altitude. S-Band could be used to make equipment procurement similar to FPE-A. But there would be no need for a change to the LPF X-band. If the X-Band were retained the link margin would only increase. The antenna architecture remains the same as for the LPF baseline. The data rate is low enough and the frequency of the S-Band allows the use of the LGA Helix.

If a 2 kbps spacecraft and 8.8 kbps payload is assumed, a downlink once per orbit with a 10 minute communication window requires a data rate of 0.1 Mbps.

FPE-B LGA Link Budget (S-Band - 2.5 GHz with a slant range of 700 km)
A required E_b/N_o (Energy per bit to noise ratio) of **2.8 dB** was assumed from Binary Phase Shift Keying (BPSK) with Viterbi and Reed-Solomon coding.

Receiving Antenna (Svalbard)		
Type	Parabolic	
Diameter	13	m
Physical Area	132.732	m2
Efficiency	0.550	
Effective Area	73.003	m2
Gain	48.042	dB
Figure of Merit	23.000	dB/K
Half-Power Beam width	0.646	deg
Pointing Error	0.059	deg

Table 9.19 - Svalbard Receiving Rx Antenna for link comparison (S-Band)
Frequency is assumed to be 2.5 GHz, which the gain is also dependant on.

	Scenario				
	Slant Range	700000	m	116.9	dBm
	Frequency	2.50E+09	Hz	188.0	dBHz
	Wavelength	1.20E-01	m	-18.4	dBm
A	**Spacecraft**				
	Transmitter Power	1	W	0.0	dBW
	Transmitter Line Loss			-3.5	dBW
	Tx Antenna Gain			1.0	dB
	Tx EIRP			**-2.5**	**dB**
B	**Propagation**				
	Free Space Loss	1.861E-16	W/m2	-157.3	dB
	Antenna Pointing Loss			-3.0	dB
	Antenna Noise Temp	290	K	24.6	dBK
C	**Ground Station/Internal**				
	Rx Antenna Pointing Loss			-0.1	dB
	Rx Antenna Gain			48.0	dBW
	Rx Noise Temp	319.3	K	25.0	dBK
	Boltzmann			**-228.6**	**dB**
D	**Output of Receiver**				
	System Noise Temperature	609.3	K	27.8	dB
	Noise			-200.8	dB
	Received Carrier Power			-114.9	dB
	Received Carrier to Noise			85.9	dB
	Data Rate	1.00E+05	bps	50.0	dB
	Link Effective Eb/No			35.9	dB
E	**Link Margin**			**33.1**	**dB**

Table 9.20 – FPE-B DownLink Budget for a Science Mode (S-Band) at Apogee
Red and blue numbers are changes from the reference budget and calculated values respectively

The changes required from the LPF reference link budget for FPE-B are:
- The S-Band is used rather than X-Band.
- The required data rate is 0.1 Mbps
- Slant range is assumed to be 700 km.
- Ground station assumed to be Svalbard (13 m) (S-Band receiver) with a figure of merit of 23.0 dB/K.
- Antenna is assumed to be a **Helix with 1 dB** of gain
- Atmospheric noise temperature adjusted to 290K to reflect the Earth in closer proximity.
- Transmitter power 1W.

The receive antenna data is shown in Table 9.19 and the link budget is shown in Table 9.20 with the changes to the reference budget (Table 9.9) shown in red.

The transmitter power could be reduced to below 1 W and still retain a good link margin. Also if the X-Band is used, there would be still margins for further improvements.

9.2.6   FPE-B Mass and Power Budget

Shown in this section is a hypothetical mass budget for the adapted LPF. The new units are included and the adapted units are highlighted. The mass budget assumed to be the latest from the LPF project. The changes to equipment are shown by sub-system.

Sub-System	LPF w/margin(kg)	FPE-Assumption w/margin (kg)	Relative change
Service Module			
Data Handling	16.5	16.5	**0.0**
Power	69.1	69.1	**0.0**
S-Band Comms	9.7	9.7	**0.0**
AOCS	18.4	18.4	**0.0**
Structure	80.8	80.8	**0.0**
Thermal	7.4	7.4	**0.0**
FEEP µProp	44.9	45.7	**+0.8**
Propellant	0.04	0.8	+0.8
Total	246.8	247.6	**+0.8**
Payload Module			
LTP	150	0.0	**-150.0**
FPA-B Payload	0	212.2	**212.2**
DRS	50.5	0.0	**-50.5**
Balance Mass	10	0.0	**-10.0**
Total	210.5	212.2	**1.7**
Consumables			
Consumables	0.0	0.0	**0.0**
Total	0.0	0.0	**0.0**
Science Spacecraft Total			
TOTAL DRY	457.3	459.8	**2.5**
TOTAL WET	0.0	0.0	**0.0**
TOTAL	457.3	459.8	**2.5**

Table 9.21 – Mass Budget for FPE-B Using LPF

In summary the major changes occur from a payload perspective. The only major spacecraft changes would be the structural changes required to accommodate the cryostat. FPE-B would have an estimated mass of 460 kg. This will reduce demands required for drag compensation, potentially allowing a lower perigee. The table shows that the only major hardware changes are payload related.

The power budget is within the EOL capabilities of the 650 W solar panel (reduced when compared to FPE-B). FPE-B power requirements are deemed to be compatible with LPF.

Sub-System	LPF	FPE-Assumption	Relative change
	w/margin(kg)	w/margin (kg)	(W)
Service			
Data Handling	**41.7**	**41.7**	**0.0**
Power	**10.5**	**10.5**	**0.0**
S-Band Comms	**54.0**	**29.0**	**-25.0**
SSPA	30	5	-25.0
AOCS	**19.6**	**19.6**	**0.0**
Structure	**0.0**	**0.0**	**0.0**
Thermal	**11.6**	**11.6**	**0.0**
FEEP mProp	**167.9**	**167.9**	**0.0**
Total	**305.3**	**280.3**	**-25.0**
Payload			
LTP	**152.3**	**0.0**	**-152.3**
FPE-B Payload	**0.0**	**80.3**	**80.3**
DRS	**78.0**	**0.0**	**-78.0**
Total	**230.3**	**80.3**	**-150.0**
Science Spacecraft Total			
Sub-Total	**535.6**	**360.6**	**-175.0**
Final Joint Ops	**535.6**	**360.6**	**-175.0**

Table 9.22 – Power Budget for FPE-B Using the LPF Platform

9.3   FPE- C – BEC

9.3.1   Accommodation of Payload

This section refers to the configuration of LPF shown in Figure 9.1. The same study procedure has been followed, assessing each aspect of LPF to determine re-use. Table 9.23 and Table 9.24 show the retained and removed units.

There is a reduction of units. The following changes are made to the accommodation (see Figure 9.4):
- The colloid thrusters and DRS have been removed in addition to the LTP and the LTP FEE electronics.
- The LTP IS FEE electronics are no longer required as the LTP is removed
- The BTP is accommodated in the central cylinder

- The UV unit (5) is retained in its original position.
- The laser assembly and phasemeter is removed leaving space in Segment H.
- A new laser bench is placed in Segment A and mounted on the outer wall to allow heat to radiate into space.

Item (Figure 9.1 ref.)	Retained	Remarks
LTP (1)	No	Payload not adaptable to FPE-C science requirements
Inertial Sensor (IS) FEE (2 and 3)	No	Required by the LTP and likely to be specifically designed for it
Radiation Monitor and Magnetometer (4)	Yes	Would be useful to monitor the magnetic and the radiation environment
UV Lamp Unit (5)	Adapted	Required for dislodging atomic species from the BEC Vessel. The exact needs of the unit may not be identical.
LTP DPU (6)	Adapted	Replaced with payload computer. But similar unit envisaged.
IS (LTP) PCU (6a)	Adapted	A PCU is required but changes maybe necessary to make it compatible with FPE-C architecture
Caging Control Unit (7)	No	Not required its LPF form. Although if a drag free sensor is required it would be adapted for the new IS. Only required if DFACS is required.
Ref Laser & Laser Metrology Unit (8)	No	Laser reference in this form is not necessary as a separate laser bench is baselined, likely requiring different wavelengths and powers.
Laser Assembly (9)	Adapted/No	Changes required as more than one laser wavelength is needed. A new system could be the better option, tailored for the cooling of different BECs
Phasemeter (10)	No	Assumed not to be required.

Table 9.23 – Retained and removed LTP elements with reference to FPE-C payload definition

The assumption made is that the AOCS inertial sensors will be based upon the Sun and Earth sensors and the star tracker. Further attitude and orbit maintenance information can be provided by the ground.

| Item (Figure 9.1 ref.)	Retained	Remarks
Colloid Thruster Assemblies (18 and 19)	No	Not required as there is cold gas and FEEPS available. They also directly relate to the DRS sensors.
DRS DPU (11)	No	Payload designed as a technology demonstrator not required for FPE associated with the colloid thrusters

Table 9.24 – Retained and removed DRS elements with reference to FPE-C payload definition
Note that there are other elements to the DRS contained in the vicinity of item (11) or the DRS IAU and also below the LTP.
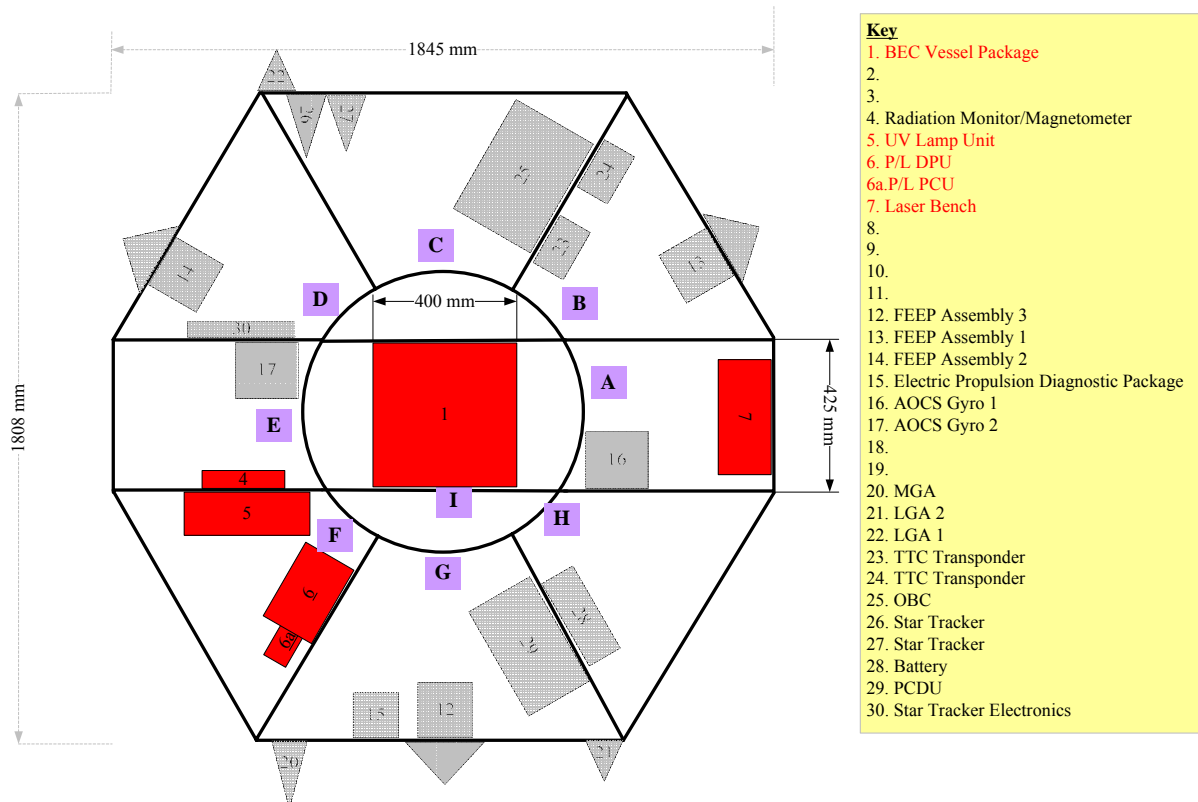
Figure 9.4 – Adaptation of LPF due to accommodation of the FPE-C Payload

9.3.2 Payload Change Implications on AOCS

Removing the LTP and not replacing the drag-free inertial sensor requires the adaptation of the AOCS and GNC sub-systems to account for changes in the control law. Attitude and determination would be dependant on measurements from the Sun sensor, star tracker and ground providing an orbit prediction. These tools would be used to determine if and/or when orbital corrections will be required. These manoeuvres may be lengthy due to the presence of FEEPs which have lower thrust performance than cold gas for example.

It must be noted that the addition of DFACS in a similar mould to FPE-A would require accelerometers capable of higher accuracy measurements. This would not have great mass and power penalties as FPE-C's payload is lower than B and A.

9.3.3 Mission Profile Changes and AOCS Performance Requirements

The orbit has been defined as the same as FPE-B, a 700 km circular SSO, on the same premise of a trade between magnitude of disturbances and the intensity of radiation. For completion the ΔV and propellant budgets are presented in Table 9.25 and Table 9.26 respectively. A 12 month lifetime is assumed. This could also be used as a comparison with FPE-A and B to show the difference between an elliptical 12-month mission and a 6-month circular case.

Perturbations	Torque	a	ΔV	Thrust
	Nm	ms-2	ms-1	μN
Gravity Grad	1.03E-05	2.31E-14	0.00	0.00
SRP	2.52E-05	3.54E-08	1.12	26.57
Magnetic Grad	2.14E-04	2.19E-13	0.00	0.00
Aero Drag	1.48E-05	2.08E-08	0.65	15.57
ERP	2.74E-06	3.85E-09	0.12	2.89
Earth Albedo	3.56E-06	5.00E-09	0.16	3.75
Moons Gravity	0.00E+00	1.22E-06	38.54	916.49
Suns Gravity	0.00E+00	5.61E-07	17.70	420.91
Total	**2.70E-04**	**1.85E-06**	**58.29**	**1386.18**

Table 9.25 – FPE-C ΔV Budget based for a 12 Month lifetime
Based upon 750 kg S/C, over 12 months, at 700 km and data from [TN4]

	Propellant (per FEEP kg)	Propellant (kg)	Remarks
Sun Acquisition Slew	Negligible	Negligible (1.74 x 10^{-5} kg)	Assumed 180^0 slew and includes acceleration and deceleration over 76 minutes
Linear Accelerations	0.37	1.12	Includes sun moon
Torques	0.07	0.22	Includes Sun Moon
Total	**0.44**	**1.34**	
With Margin (20%)		**1.60**	

Table 9.26 – Estimated Propellant budget for FPE-C
Based upon 750 kg S/C, FEEP Isp of 4000s, over 12 months and data from [TN4]

The amount of propellant is estimated to be comparable to FPE-A.

9.3.4   TT&C Telemetry Requirements and Ground Segment

Referring to Table 9.1 it can be seen that the data rate is much higher. Therefore it is important to assess whether or not LPF can support such a link. The approach is the same as before comparing the reference link budget (Table 9.9). The changes to the budget are outlined and then the budget is presented in the same format.

FPE-C MGA Link Budget (X-Band – 8.5 GHz with a slant range of 700 km)
The MGA is chosen as the data download would likely be done with this antenna due to the high data rate. The assumed link margin is 2.8 dB.

The changes are as follows:
- The S-Band is used rather than X-Band.
- Payload data rate is **683 Mbps** rather than the LTPs **30.0 kbps** (Table 9.1).
- Slant range is assumed to be 700 km.
- Ground station assumed to be Svalbard (13 m) (X-Band receiver) with a figure of merit of **32.0 dB/K**. To account for high latitudes.
- Antenna is assumed to be a **Horn with 15.9 dB** of gain (Table 9.8)
- Atmospheric noise temperature adjusted to 290K to reflect the Earth in closer proximity.

The receive antenna data is shown in Table 9.27 and the link budget is shown in Table 9.28 with the changes to the reference budget (Table 9.9) shown in red.

Receiving Antenna (Svalbard)		
Type	Parabolic	
Diameter	13	m
Physical Area	132.732	m2
Efficiency	0.550	
Effective Area	73.003	m2
Gain	58.671	dB
Figure of Merit	32.000	dB/K
Half-Power Beamwidth	0.190	deg
Pointing Error	0.017	deg

Table 9.27 - Svalbard Receiving Rx Antenna for link comparison (X-Band)
Frequency is assumed to be 8.5 GHz, which the gain is also dependant on.

	Scenario				
	Slant Range	700000	m	116.9	dBm
	Frequency	8.50E+09	Hz	198.6	dBHz
	Wavelength	3.53E-02	m	-29.0	dBm
A	**Spacecraft**				
	Transmitter Power	7*	W	8.5	dBW
	Transmitter Line Loss			-3.5	dBW
	Tx Antenna Gain			15.9	dB
	Tx EIRP			**20.9**	**dB**
B	**Propagation**				
	Free Space Loss	1.610E-17	W/m2	-167.9	dB
	Antenna Pointing Loss			-3.0	dB
	Antenna Noise Temp	290	K	24.6	dBK
C	**Ground Station/Internal**				
	Rx Antenna Pointing Loss			-0.1	dB
	Rx Antenna Gain			58.7	dBW
	Rx Noise Temp	464.7	K	26.7	dBK
	Boltzmann			**-228.6**	**dB**
D	**Output of Receiver**				
	System Noise Temperature	754.7	K	28.8	dB
	Noise			-199.8	dB
	Received Carrier Power			-91.5	dB
	Received Carrier to Noise			108.3	dB
	Data Rate	6.83E+08	bps	88.3	dB
	Link Effective Eb/No			20.0	dB
E	**Link Margin**			**17.2**	**dB**

Table 9.28 – FPE-C DownLink Budget for a Science Mode (X-Band)
The gain of the Horn is from the LPF project of 15.9 dB. Red number and blue numbers are changes to the reference
budget and calculated values respectively
*Assumed value

It can be seen that the data rate is not critical. Data compression would allow further reductions. A reduction in RF power is not recommended as the link margin is within 7.1 dB of the LPF reference of 10.1 dB.

9.3.5 FPE-C Mass and Power Budget

The only change to the spacecraft is the payload and related units as described in Section (9.3.1). The science spacecraft mass is reduced from 457.3 kg to 325 kg as the LTP and DRS are removed and replaced with a lighter payload. Power is reduced to 447.7 W.

In terms of mass, power and data rate FPE-C appear compatible with the VEGA launcher and LPF.

10   Conclusions

The main goal of the analysis described in this chapter was to determine whether or not the reference FPE payloads defined in Part 2, could be accommodated into the LPF platform with relatively modest design changes.

The design drivers for FPE-A are:
- High level of thermal stability
- Elliptical orbit with a minimum number of eclipses
- SSO for thermal stability
- Accommodation of optical elements of a high stability requirement (FPE-A)
- Thermal control relating to the lasers
- Changes in the TTC sub-system to accommodate both an S-Band and K-Band link. X-Band system removed.
- Ground visibility in the K-Band
- Available clocks for comparison
- High demands of the VEGA launcher for an elliptical SSO orbit.
- Performance of FEEPs for slew manoeuvres to acquire the sun. Low thrust implies a lengthy commissioning phase.

FPE-A issues mainly relate to clock comparison through telemetry and an elliptical orbit. No major obstacles are seen for accommodating the hardware (even though specific technological development on the payload side would be required). On this basis, re-use of the LPF-SCM is considered to be a feasible option. Mass, power and data rate are not a concern.

The design drivers for FPE-B are:
- Accommodation of a cryostat within a small space (LPF central cylinder constraints allow only 6 month cryostat lifetime).
- Commissioning phase alone could be 4 months (LPF), leaving only two for science measurements. Although the STEP accelerometer could need only 20 days [30] for performing the actual calibration, such a period of time is considered as marginal.
- **Assuming a mission lifetime of 1 year, the cryostat needs to be enlarged to scales nearer STEP and GP-B (around 18 months lifetime). Penalties will experienced through cryostat size requiring structural changes.**
- Drag free control from continuously thrusting FEEPs. Their endurance under these conditions is not demonstrated yet.
- FEEP noise performance is very close to the requirements of the accelerometer.

FPE-B issues mainly relate to cryostat accommodation and FEEP noise and endurance performance in LEO. Although the LPF-SCM structure would need to be modified to host a larger cryostat, significant heritage still exists, with specific emphasis on overall system design, units reuse and DFACS. Mass, power and data rate are not a concern.

The design drivers for FPE-C are:
- High level of thermal stability
- Minimum number of eclipses
- SSO for thermal stability
- Thermal control relating to the lasers
- Strict control of the magnetic environment

In general FPE-C appears to be the least demanding on the LPF platform. Only small issues relate to accommodation. It also has the advantage of the development of the QUANTUS experiment to be used in the ZARM drop tower in Bremen [53] and [57] providing some heritage.

Advantages of platform re-use/adaptation:
- Procurement is easier. FPE-A being easier to adapt than FPE-B
- Project team continuity would be possible from LPF and other fundamental physics missions from both industry and ESA.
- In some areas the risk is lower. Notably in terms of platform, AIV/T and re-use of existing Ground Support Equipment.

The following areas would require additional analysis:
- Dedicated design activity for the cryostat unit.
- Assessment of the performance of the thermal control system in LEO. Thermal dissipation in new environmental conditions both inside the spacecraft (cryogenic, laser systems and/or added electronics) and externally due to eclipsing orbits (even in SSO).
- Mass impacts on structural modifications and the design of these themselves
- FEEP performances in LEO, with particular emphasis on providing less than 0.1 μN noise and endurance.
- Analysis of the calibration requirements especially for FPE-B as this will impact on mission lifetime requirements (available cryogen)

PART 5

CONCLUSION

11   The Way Forward

11.1   FPE Preliminary Development Plan

In order to implement a successful mission dedicated to fundamental physics, identification of the key technological drivers and corresponding planning of the required developments are required. As the technology to achieve the science goals is demanding, especially on the payload side, a clear and decisive approach is required to address all the development needs.

The first focus and the most definitely the priority is to develop the payloads in question. There is a high level of complexity involved for both FPE-A, B and C. A set of dedicated instrument assessment studies are required to identify the corresponding technology developments.

The preliminary development plan for the **FPE-A** payload could be, in order of priority:

- **Payload Trade Study** – Finalise baseline instrumentation when traded against science objectives (an initial trade can be found in Section (3.3))
- **Selection of Neutral or Single Ion Trap** – A study should be done to determine the basic clock type. This would weigh SNR of a single ion against the complexity of neutral atoms and the trapping a containment of neutral charge atoms.
- **Selection of Clock Transition –** A trade study is required to determine the atomic transition with which to base the OAC. This will be based on the areas highlighted in Section (3.4.2). Some areas to be traded are;
  - o   Resulting Accuracy
  - o   Instability
  - o   Number of lasers (dependant on transition structure)
  - o   Frequency (implications for fibres)

  This will enable the laser required for the comb and the ORs to be defined.
- **Space Qualified Lasers –** Following the selection of the laser wavelength, development must begin for space qualification of these units.
- **Trap Chamber Design –** A dedicated activity is required on the design of the UHVIC, specifically for space.
- **Transportable Frequency Comb (FC) –** development of a space qualified version is required.
- **Space Qualified FC Femto-Second Laser** – This unit is needed for the frequency comb.
- **Transportable OAC Development** – A design shall be established and an Engineering Model built. Ideally the transportable design will be representative of the type of clock to be flown and used as a breadboard.
- **Space OAC Prototype** – In preparation for the final design, an Engineering Model of the flight OAC unit shall be developed. This unit could potentially be used as a flight spare and used to assist in the characterisation the final space clock.
- **Space Qualified FC –** To be used with both the flight OAC and the prototype.
- **OR Design –** The potential flight version of the optical resonators needs to be studied, trading size against stability (larger sizes are more susceptible to vibration Equation (3.7)). The chosen clock frequency is important here, as if the beat between the OAC and LO is to

be in the GHz domain, the laser choice for the cavities depends on this, which determines the size. A final choice of material is required to maximise thermal stability.
- **Optical Resonator Bench Design –** This activity will ensure the accommodation of the cavities on the spacecraft.

The preliminary development plan for the **FPE-B** payload could be in order of priority:

- **Differential Accelerometer Concept Trade –** SQUIDs have been chosen based upon accuracy and heritage, however the other solution should not be discounted. Both SQUID sensing and atomic interferometry should be considered. An early decision should be made to determine the best solution.
- **Test Mass Pair Selection –** The DA development is dependant on a firm decision for material type. Extensive studies have been done [49]. The first key trade to finalise, nevertheless, is this.
- **Accelerometer Development –** A breadboard of the complete DA unit is required with which to determine cryostat requirements. A key aspect of this is the caging mechanism, as it shown an increase in mass will improve the performance of the accelerometer. However mass increases have the penalty of complexity in the caging.
- **Mutual TM CoM Offset –** This has to be determined to within the resultant gravity gradient for the final orbital (around 2×10^{-14} ms^{-2} for an offset of 1×10^{-8} m).
- **Cryostat Design –** The dual cryogen development should begin in earnest, not just for FPE-B but as an option for other future missions. However a cheaper cryostat should not be discounted as LPF could be modified.
- **Cryostat Venting** - This will become an external disturbance to the payload if done during measurement phases. The issue of how to deal with the vented gases must be addressed.
- **Atomic Interferometer (AIF)** – This study will should be run in parallel with OAC and DA development studies. Benefits from the OAC will come in the form of traps and lasers. In the case of AI, it is presently unclear as to exactly how two test species could be tested around a common centre of mass.

The preliminary development plan for the **FPE-C** payload could be, in order of priority:
- **BEC Vessel development –** The design and implementation of a prototype unit for UV desorption of materials from coatings. No current breadboard available. A design of the Zerodur chamber and the bonded fibre couplers would be required. Reinforcement and launch survival analysis required.
- **Material Coatings** – An assessment of the feasibility of coating the atomic samples on the vessel, rather than using a dispenser system.
- **Smearing Effects –** The potential of material attaching of the chamber, especially around the laser access points. An analysis would be needed to determine the severity of the effect and if too severe a solution has to be developed.

The spacecraft development plan should include the following (with reference to LPF re-use):

- **DFACS –** This subsystem needs to be assessed with respect to the use of new inertial sensors as the LTP has been removed. The re-design of the control system needs to confirm the viability of using the DA (FPE-B) as the IS and the new ONERA IS (FPE-A).

- **Cryostat Accommodation –** The best approach to cryostat accommodation needs to be established. Key factors to consider are complexity of changes, structural implications, mass, launch vehicle accommodation.
- **Approach Decision –** The AIF and DA decision would be dependant on the status of each's development. Adapting LPF for a cryostat against pursuing AIF needs to be traded.
- **Mission Profile –** Final orbit selection is required to determine magnitude of external disturbances and thermal instability. Controlling the magnetic moment of the spacecraft will allow more margins on FEEP performance. A full analysis of eclipses is required to determine the optimum launch date to maximise eclipse free periods.
- **FEEP Performance –** The FEEPs performance in LEO needs to be simulated. This needs to take into account the new inertial sensor and the need for extra propellant.
- **Definition of Changes –** An agreed plan based upon the choices above is required to determine the necessary changes to LPF.
- **LPF Re-Use Final Decision –** From the definition of required changes, adaptation of LPF can be pursued or not.

Table 11.1 summarises the required technology development.

FPE-A	Tests of SR and GR
	Frequency combs for space
	High Frequency Lasers for Space –
	Development of Optical Trap Lasers
	Space Qualified Optical Trap
	High Finesse Cavities
	Fibres
FPE-B	Tests of the WEP
	Dual Cryogen Cryostat
	Differential Accelerometer
	Caging Mechanism
FPE-C	Tests of BECs
	Zerodur Chamber
	Atomic Coatings for UV desorption
	Development of combined package.
Spacecraft	LPF Adaptation (depending A/B/C)
	DFACS
	Cryostat Accommodation, new structural design
	Thermal control in LEO
	FEEP Performance

Table 11.1 – Required Payload Technology Development for the Fundamental Physics Explorer

11.2   *Applicability to Cosmic Vision 2015-2025*

The work performed in the context of the FPE study is closely related to some of the proposals for potential fundamental physics missions, received within the Cosmic Vision exercise. The response from the scientific community demonstrated the existing interest for this science discipline.

Based on the work performed, it has become clear as substantial effort must be made in the area of payload technology development, in order to reduce the overall programme risk and enable the effective implementation of such missions.

An overview of the Cosmic Vision 2015-2025 proposals can be found in [50].

12   Conclusion

The work conducted on the Fundamental Physics Explorer (FPE) has allowed us to achieve a number of important objectives:

- improve our understanding of the scientific objectives of fundamental physics missions;
- establish the main technical requirements associated with the science requirements, with specific reference to the verification of the Equivalence Principle, of General Relativity and of the behaviour of Bose-Einstein Condensates;
- define preliminary concept designs of reference payloads, in each FPE domain;
- determine the technical challenges associated with the instruments development and prepare a list of high priority technology developments;
- address issues related to mission design and orbit selection;
- explore the accommodation of FPE instruments onboard the spacecraft, identifying the key design drivers;
- perform a preliminary assessment of the potential for re-use of the science module of the LISA Pathfinder (LPF).

The work performed showed the following main results:

- the complexity of the reference payload, due to the sensitivity level required;
- the low technology readiness level of key payload units and the corresponding need for substantial development work;
- the relative simplicity of the mission design, with Earth centered orbits (SSO), accessible with small, launchers such as Rockot and Vega;
- the overall compatibility of the science module of the LISA Pathfinder with the FPE needs, with potential advantages in terms of reduced development effort and risk;
- the need to further investigate a number of critical issues, with emphasis on payload design and DFACS.

Although the technical challenges associated with the development of a Fundamental Physics Explorer mission should not be under-estimated, the overall mission (LEO, small launcher vehicle) and spacecraft (LPF heritage) design are within reach, thus in principle opening the way to relatively inexpensive fundamental physics missions. On the other hand, the main development challenge is represented by the complex scientific instruments and the associated technology demands, which are presently beyond reach and need dedicated development and flight qualification effort.

13   References

13.1   Literature References

These are published works explicitly cited in the document.

[1]   **Reinhard, R.,** *"Ten Years of Fundamental Physics in ESAs Space Science Programme"* ESA Bulletin No. 98, June 1999

[2]   **Bignami, G.; Cargill, P.; Schutz, B. and Turon, C.,** *"Cosmic Vision – Space Science for Europe 2015-2025"* ESA BR-247, 2005

[3]   **Parmley, R. T.; Bell, G. A.; Murray, D. O. and Whelan, R. A.,** *"Performance of the Relativity Mission [GP-B] Superfluid Flight Dewar"*, Adv Space Research, Vol 32, Vol.7, p1407-1416, 2003

[4]   **Fichtner, W and Johan, U,** *"HYPER Industrial Feasibility Study – Executive Summary / Final Report",* HYP-9-04 Astrium GmbH, June 2003

[5]   **Blaser, J-P et al,** *"STEP- The Report on the Phase A Study"* ESA SCI(96)5, March 1996

[6]   **Mester, J., Torii, R., Worden, P., Lockerbie, N., Vitale, S., Everitt, C .W. F,** *"The STEP Mission: Principles and Baseline Design."* Classical and Quantum Gravity, 18 2475-2486, 2001

[7]   **PHARAO Project Team,** *"PHARAO Synthesis Document",* ESA/CNES, PH-DS.0.161.CNS, Edition 4, 15/05/05

[8]   **Touboul, P and Rodrigues, M.** *"The MICROSCOPE Space Mission."* Classical and Quantum Gravity, Vol. 18 p2487-2498, 2001

[9]   **Lammerzahl, C., Dittus, H., Peters, A. and Schiller, S.,** *"OPTIS: A Satellite-Based Test of Special and General Relativity."* Classical and Quantum Gravity, 18, 2499-2508, 2001

[10]   **Nobili et al;** *"Galileo Galilei (GG) Phase A Study Report."* Universita di Pisa and Agenzia Spaztiale Italiana, November 2000

[11]   **Nobili et al;** *"Galileo Galilei –GG: Design, requirements, error budget, and significance of the ground prototype".* Physics Letters A, 318, p172-183, 2003

[12]   **NASA,** *"NASA Facts – Gravity Probe B"* (www document) http://einstein.stanford.edu/content/fact_sheet/GPB_FactSheet-0405.pdf (Accessed 7/11/06)

[13]   **Braxmeier, C., Muller, H., Pradl, O., Mlynek, J., Peters, A. and Schiller S.,** *"Tests of Relativity Using a Cryogenic Optical Resonator."* Physical Review Letters, Vol. 88, No. 1, 2002

[14]   **Lammerzahl, C. and Dittus, H.,** *"Fundamental Physics in Space: A Guide to Present Projects"* Annalen der Physik, vol. 11, Issue 2, pp.95-150, 2002

[15]   **Cygnus Research,** *"Power Spectral Density"*
       http://www.cygres.com/OcnPageE/Glosry/Spec.html (www document accessed 9/11/07)

[16]   **Audoin, C.; Guinot, B. and Lyle, S.,** *"The Measurement of Time - Time, Frequency and the Atomic Clock",* Cambridge University Press, ISBN 0-521-00397-0, 2001

[17]   **Allan, D. W.; Ashby, N. and Hodge, C. C.,** *"The Science of Timekeeping"*, Hewlett Packard Application Note 1289, 1997.

[18]   **Eisberg, R and Resnick R.,** *"Quantum Physics of Atoms, Molecules, Solids, Nuclei and Particles"*, John Wiley & Sons, ISBN 0-471-87373-X, 1985

[19]   **Prestage, J. D.; Tjoelker, L. and Maleki, L.,** *"Atomic Clocks and Variations of the Fine Structure Constant",* Physical Review Letters, Vol. 74, No. 18, 1st May, 1995

[20]   **Everitt, C. W. F.; Damour, T.; Nordtvedt, K. and Reinhard, R.** *"Historical Perspectives on Testing the Equivalence Principle."* Advances in Space Research, Vol. 32, No. 7, p1297-1300, 2003

[21]   **DeBra, D. B.,** *"Drag-free Spacecraft as Platforms for Space Missions and Fundamental Physics",* Classical and Quantum Gravity, 14, 1549-1555, 2001

[22]   **Black, E. D.,** *"An Introduction to the Pound-Drever-Hall Laser Frequency Stabilisation."* American Journal of Physics, p-69-79, 2001

[23]   **Hollberg, L.; Oates, C. W.; Wilpers, G.; Hoyt, C. W.; Barber, Z. W.; Diddams, S. A.; Oksay W. H. and Bergquist, J. C.,** *"Optical Frequency/Wavelength References"* Journal of Physics B: Atomic, Molecular and Optical Physics, Vol 38, S469-S495, 2005

[24]   **Diddams, S.A; Udem, Th; Vogel, K. R; Oates, C. W.; Curtis, E. A.; Windeler, R. S.; A. Bartels, A; Bergquist, J. C. and Hollberg, L,** *"A Compact Femtosecond-Laser-Based Optical Clockwork,"* Proceedings of SPIE, Laser Frequency Stabilization, Standards, Measurement, and Applications, J. L. Hall, J. Ye, eds., vol. 4269, pp. 77-83 (2001).

[25]   **Oskay, W. H.; Diddams, S. A.; Donley, E. A.; Fortier, T. M.; Heavner, T. P.; Hollberg, L.; Itano, W. M.; Jefferts, S. R.; Delaney, M. J.; Kim, K.; Levi, F.; Parker, T. E. and Bergquist, J. C.,** *"Single-Atom Optical Clock with High Accuracy"* Physical Review Letters, Vol. 97, 2006

[26]   **Jones, D. J.; Diddams, S. A.; Ranka, J. K.; Stentz, A.; Winderler, R. S.; Hall, J. L. and Cundif, S. T.,** *"Carrier-Envelope Phase Control of Femtosecond Mode-Locked Lasers and Direct Optical Frequency Synthesis.",* Science, Vol 288, 28th April, 2000

[27]   **Bize, S.; Diddams, S. A.; Tanaka, U.; Oskay, W. H.; Drullinger, R. E.; Parker, T. E.; Heavner, T. P.; Jefferts, S. R.; Hollberg, L.; Itano, W. M.; and Bergquist, J. C.,** *"Testing the Stability of Fundamental Constants with the $^{199}Hg^+$ Single-Ion Optical Clock",* Physical Review Letters, Vol. 90, No. 15, 2003

[28] **Shulz, K-J.,** *"ESA Tracking Stations (ESTRACK) Facilities Manual (EFM)",* ESA Technical Description, DOPS-ESTR-OPS-MAN-1001-OPS-ONN, 17/07/2006

[29] **Swanson, P. N.,** *"Mini-STEP: A Minimal Satellite Test of the Equivalence Principle Experiment."* Classical and Quantum Gravity, Vol. 13, pA143-A147, 1996

[30] **Paik, H. J.; Blaser, J-P. and Vitale, S.,** *"Principle of the STEP Accelerometer Design."* Advances in Space Research, Vol. 32, No. 7, p1325-1333, 2003

[31] **Touboul, P; Foulon, B, Lafargue, L and Metris, G,** *"The Microscope Mission"*, Acta Astronautica, Volume 50, Issue 7,P-433-443, April 2002

[32] **Landragin, A and Bouyer,P.,** *"Atom Interferometry and Coherent Matter Waves"*, ESA SP-588, Trends in Space Science and Cosmic Vision 2020, Proceedings of the 39th ESLAB Symposium, 19-21 April 2005 Noordwijk, The Netherlands, p-43-52

[33] **Dittus, H.; Vodel, W.; Gregor, R.; Lochmann, St.; Mehls, C.; Koch, H.; Nietzcshe, S.; and Zameck-Glyscinski, J. v.** *"Drop Tower Tests of the Weak Equivalence Principle – One Step to Space Missions for Gravitational Physics."* Advances in Space Research, Vol. 32, No. 7, p1301-1305, 2003

[34] **Nordtvedt, K.,** *"Testing the Equivalence Principle with Laser Ranging to the Moon"*, Advances in Space Research, Vol. 32, No. 7, p1311-1320, 2003

[35] **Vitale, S.,** *"Mini-STEP"* ESA SP-420, Fundamental Physics in Space, Proceedings of the Alpach Summer School, Alpach, Austria, 22-31 July 1997, p-213-228, 1997

[36] **Nobili, A. M.; Bramanti, D.; Polacco, E.; Catastini, G.; Anselmi, A.; Portigliotti, S.; Lenti, A. and Severi, A.** *"The Galileo Galilei (GG) Project: Testing the Equivalence Principle in Space and on Earth."* Advances in Space Research, Volume 25, Issue 6, p. 1231-1235, 2000

[37] **STEP,** *Stanford University,* http://einstein.stanford.edu/STEP/ *(www document, accessed 2/4/07)*

[38] **Kent, B. et al,** *"STEP Payload Feasibility Report"* ESA Contract No. 15437/01/NL/HB, Final Report, July 2002

[39] **Gibbs, W. W.,** *"Ultimate Clocks",* Scientific American, September 2002

[40] **ECSS,** *"Space Engineering – Space Environment,"* ECSS-E-10-04A, 21/01, 2000

[41] **Arianespace, "***VEGA Users Manual"*, Issue 3, March 2006

[42] **Eurockot GmbH, "***Rockot User Manual",* EHB-0003, Issue 3, Review 1, April 2001

[43] **Seibersdorf Research**, *"Indium FEEP Microthruster. LISA Pathfinder Representative Micropropulsion Subsystem Endurance Test with 8-Emitter Cluster."* ARC Seibersdorf Research, FEEP Info – November 8th 2006

[44] **LISA Pathfinder Science Working Team,** *"The Science Case for LISA Pathfinder",* ESA-SCI (2007)1, ESA-ESTEC, Noordwijk, NL, 2007

[45] http://hpcc.engin.umich.edu/CFD/research/NGPD/ElectricPropulsion/feep/
(accessed 11/10/07)

[46] **Genovese, A.; Tajmar, M.; Buldrini, N. and Steiger, W.,** *"Extended Endurance Test of the Indium FEEP Microthruster",* AIAA 2002-3688, 38th AIAA/ASME/SAE/ASEE Joint Propulsion Conference and Exhibit, Indianapolis, Indiana, USA, 7-10 July, 2002

[47] **Marcuccio, S.; Gianelli, S. and Andrenucci, M.**, *"Attitude and Orbit Control of Small Satellites and Constellations with FEEP Thrusters"*, IEPC-97-188, Proceedings of the 25th Electric Propulsion Conference, Cleveland, OH, pp. 1152-1159, 1997

[48] **Landgraf, M.; Hechler, M. and Kemble, S.,** *"Mission Design for LISA Pathfinder",* Classical and Quantum Gravity, 22, S487-492, 2005

[49] **Kent, B. et al,** *"STEP Payload Feasibility Report"* ESA Contract No. 15437/01/NL/HB, Final Report, July 2002

[50] **ESA Science and Technology,** *"Cosmic Vision 2015-2025 Proposals"* **http://sci.esa.int/science-e/www/object/index.cfm?fobjectid=41177** *(www document, accessed 21/11/07)*

[51] **Cornell, E.,** *"Very Cold Indeed: The Nanokelvin Physics of Bose Einstein Condensation",* Journal of Research of the National Institute of Standards and Technology, Vol. 101, No. 4, August 1996.

[52] **Ketterle, W.,** *"Experimental Studies of Bose-Einstein Condensation",* Physics Today, p30-35, December 1999

[53] **Peters, A.,** *"QUANTUS – Quantum Gases Under Microgravity",* Presentation for Workshop on Advances in Precision Tests and Experimental Gravitation, Galileo Galilei Institute for Theoretical Physics, Arcetri, Firenze, 28th September 2006, (www document, accessed 23/11/07)

[54] **Zwierleinm, M. W.; Stan, C. A.; Schunck, C. H.; Raupach, S.M. F.; Gupta, S.; Hadzibabic, Z. and Ketterle, W.,** *"Observation of Bose Einstein Condensates of Molecules",* Physical Review Letters, Vol. 91, No. 25, 2003

[55] **Anderson, M. H.; Ensher, J. R.; Matthews, M. R.; Wieman, C. E.* and Cornell, E. A.,** *"Observation of Bose Einstein Condensation in a Dilute Atomic Vapour",* Science, Vol. 269, p-198-201, 14th July 1995

[56] **Klempt, C., van Zoest, T.; Henninger, T.; Topic, O.; Rasel, E.; Ertmer, W. and Arlt, J.,** *"Ultraviolet light-induced atom desorption for large rubidium and potassium magneto-optical traps",* Physical Review Letters A, 73, 2006

[57] **Vogel, A., Schmidt, M., K. Sengstock, K., et al,** *"Bose-Einstein Condensates in Microgravity",* Applied Physics B, Vol. 84, No. 4, p-663-671, 2006

13.2 Internal Technical Notes

These are the internal technical notes that this report is based upon.

[TN1] **Cacciapuoti, L.,** *"Fundamental Physics Explorer – Science Requirements"* ESA Technical Note, ESTEC, Noordwijk, NL, unpublished

[TN2] **Binns, D.,** *"Fundamental Physics Explorer - FPE-A – Payload Definition Document."* ESA Technical Note, ESTEC, Noordwijk, NL, Draft, unpublished

[TN3] **Binns, D.,** *"Fundamental Physics Explorer - FPE-B – Payload Definition Document."* ESA Technical Note, ESTEC, Noordwijk, NL, Draft, unpublished

[TN4] **Binns, D.,** *"Fundamental Physics Explorer – Mission Analysis and Design"* ESA Technical Note, ESTEC, Noordwijk, NL, Draft, unpublished

[TN5] **Binns, D.,** *"Fundamental Physics Explorer – Adaptability of the LISA Pathfinder Spacecraft for Re-Use"* ESA Technical Note, ESTEC, Noordwijk, NL, Draft, unpublished

[TN6] **Binns, D.** *"Fundamental Physics Previous Missions Review"* ESA Technical Note, ESTEC, Noordwijk, NL, Draft, unpublished

[TN7] **McNamara, P.,** *"LISA Pathfinder Presentation"* ESA-ESTEC, Noordwijk, NL, March 2007, unpublished

[TN8] **Di Cara, D.** *"Proba 3 Study – Propulsion Subsystem",* ESA Internal Memo, ESTEC, Noordwijk, NL, unpublished, 8 Nov 2005.